JOURNAL of ANALYTICAL and APPLIED PYROLYSIS

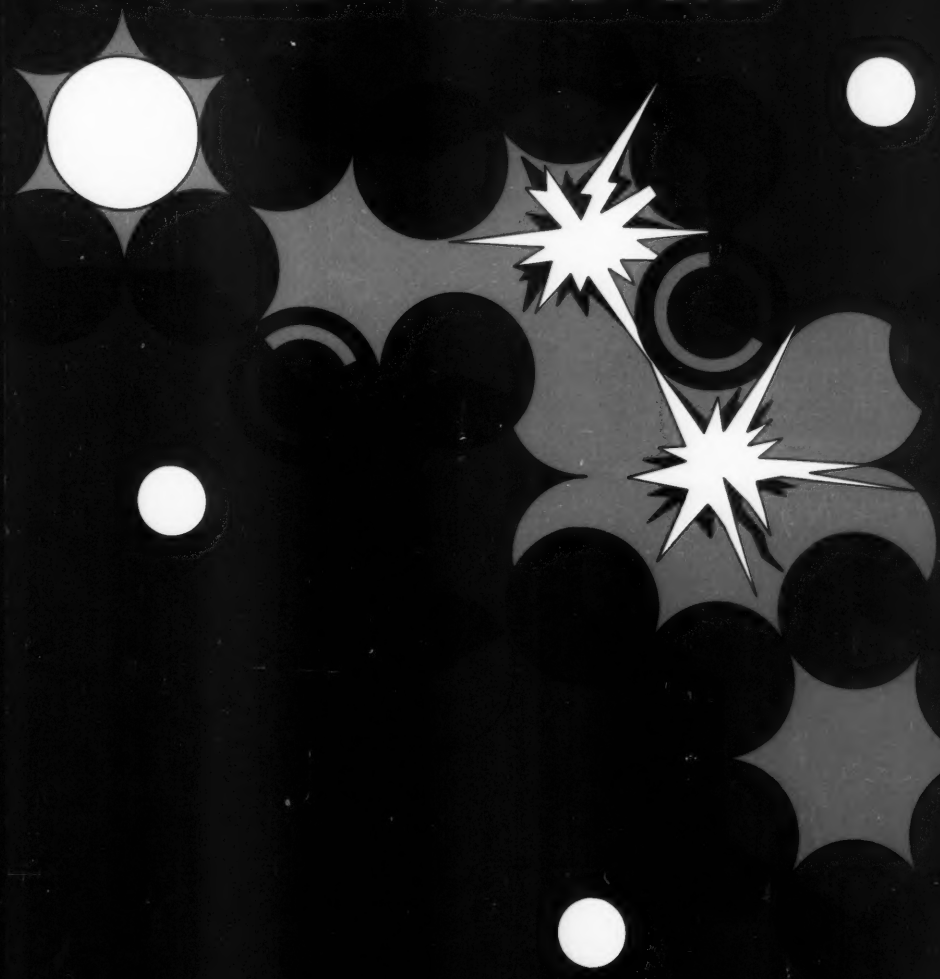

elsevier

JOURNAL OF ANALYTICAL AND APPLIED PYROLYSIS

The international *Journal of Analytical and Applied Pyrolysis* is devoted to the publication of qualitative and quantitative results relating to:

- Controlled thermal degradation and pyrolysis of technical and biological macromolecules;
- Environmental, geochemical, biological and medical applications of analytical pyrolysis;
- Basic studies in high temperature chemistry, reaction kinetics and pyrolysis mechanisms;
- Pyrolysis investigations of energy related problems, fingerprinting of fossil and synthetic fuels, coal extraction and liquefaction products.

The scope of the journal includes items such as the following:

1. Fundamental investigations of pyrolysis processes by chemical, physical and physicochemical methods.
2. Structural analysis and fingerprinting of synthetic and natural polymers or products of high molecular weight, including biopolymers, microorganisms, cells, tissues, humic materials, geopolymers and sediments.
3. Technical developments and new instrumentation for pyrolysis techniques in combination with such chromatographic or spectrometric methods as GLC, TLC, MS, UV, IR, NMR or combined GC/MS. Special attention will be paid to automation, optimization and standardization.
4. Computer handling and processing of pyrolysis data, including library filing and retrieval techniques, as well as computer matching and advanced pattern recognition techniques.

EDITOR

H.-R. Schulten
Fachhochschule Fresenius,
Department of Trace Analysis,
Dambachtal 20,
6200 Wiesbaden, F.R.G.

ASSOCIATE EDITOR

R.P. Lattimer
The BFGoodrich Company,
Research and Development Center,
9921 Brecksville Road,
Brecksville, OH 44141, U.S.A.

EDITORIAL ADVISORY BOARD

M.J. Antal, Honolulu, HI
J.J. Boon, Amsterdam
J.M. Bracewell, Aberdeen
J.W. de Leeuw, Delft
H. Dieu, Liège
M.A. Grayson, St. Louis, MO
C.S. Gutteridge, Reading
O. Hutzinger, Bayreuth
C.E.R. Jones, Redhill
S.R. Larter, Oslo
R.S. Lehrle, Birmingham
I. Lüderwald, Biberach
H.L.C. Meuzelaar, Salt Lake City, UT
G. Montaudo, Catania
G. Schaden, Marburg
T. Székely, Budapest
S. Tsuge, Nagoya
K.J. Voorhees, Golden, CO
B.B. Wheals, London
Zou Renjun, Shijiazhuang

Publication

The *Journal of Analytical and Applied Pyrolysis* has two volumes (Vols. 15 and 16) in 1989. The subscription price for 1989 is Dfl. 714.00 (ca. US $357.00), including postage. Back volumes are available at Dfl. 315.00 (ca. US $157.50) including postage. Subscribers in the U.S.A., Canada, Australia, New Zealand, P.R. China, India, Israel, South Africa, Malaysia, Thailand, Singapore, South Korea, Taiwan, Pakistan, Hong Kong, Brazil, Argentina and Mexico receive their copies by air delivery. Claims for missing issues will be honoured, free of charge, within three months after publication of the issue. Customers in the U.S.A. and Canada wishing additional bibliographic information on this and other Elsevier journals, should contact Elsevier Science Publishing Company Inc., Journal Information Center, 655 Avenue of the Americas, New York, NY 10010. Tel. (212) 633-3750.

Subscription orders may be sent to: ELSEVIER SCIENCE PUBLISHERS B.V., P.O. Box 211, 1000 AE Amsterdam, The Netherlands, tel (20) 5803911, telex 18582 ESPA NL.

See inside back cover for General Information.

Pyrofoil
Curie Point Pyrolyzer

Model JHP-3S

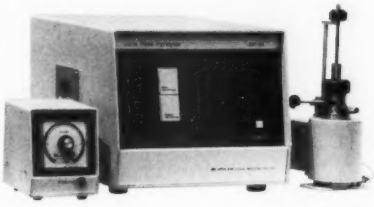

Innovation in polymer analysis:
from IR to JHP-3S

Effective for range of detection method:
i.e. GC, GC-MS and GC-FTIR.

No sample preparation is necessary:
run complex liquid or solid samples directly.

Generates highly reproducible pyrograms.

Analysis of acetylcholine

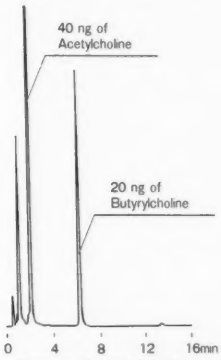

Pyrogram of Acetylcholine Iodide

Pyrolyzer : model JHP-3S
Pyrolysis temp. : 255°C, 6sec
GC : model GC 14ATFSC / Shimadzu
Column : CBP1-S25-050(methylsilicone)
i.d. 0.33mm × 25m
Column temp. : 80°C isotherm
Detector : model SID / Shimadzu
Surface Ionization Detector
Split ratio : 1 / 10

Representatives & Phone No.

India : Precision Analytical Instruments, New Delhi 11-5713373
Indonesia : P.T. New Module Int. Jakarta-Pusat 357-751
Korea : Sunil Developed Eng. 02-553-5721
Kuwait : Abdul Aziz-Yousuf Al-Essa & Co. Safat 4832229
Malaysia : Hisco (Malaysia) SDN. BHD. Selangor 03-7334236
Pakistan : Makkays, Islambad 828831
Taiwan : Pan-Co & Ivorist Association Co. Taipei 02-321-6011
Thailand : Eng. & Sci. Associates Co. Bangkok 4246005
U. K. : Applied Chromatography Systems Macclesfield 0625-34575
U.S.A. : Seamark Company, 1-800-826-3954
W.Germany : Zinsser Analytic Gmbh Frankfurt 069-789-1060

—The future of polymer analysis what we make it—

JAI Japan Analytical Industry Co.Ltd.
208 Musashi, Mizuho, Nishitama,
Tokyo 190-12 Japan Telex : 2842 234 JAI J
Phone : 0425 57 2331 Fax : 0425 57 1892

CURIE POINT PYROLYZER
for PY-GC-IR and MS

- attachable to any G.C.
- 'shock'-heating-up within milliseconds
- wide temperature range by ferromagnetic filaments or tubes in the range of 300 - 1000° C
- automatic sampler

FISCHER LABOR- UND VERFAHRENSTECHNIK

D-5309 Meckenheim bei Bonn • West Germany • Industriepark Kottenforst
Tel. (0 22 25) 40 44 u. 40 45 • Fax: 2225-4047 • Teletex: 2225-410

232A

JOURNAL OF ANALYTICAL AND APPLIED PYROLYSIS

VOLUME 16, 1989

JOURNAL of ANALYTICAL and APPLIED PYROLYSIS

EDITOR

H.-R. Schulten, Wiesbaden, F.R.G.

ASSOCIATE EDITOR

R.P. Lattimer, Brecksville, OH, U.S.A.

EDITORIAL ADVISORY BOARD

M.J. Antal, Honolulu, HI, U.S.A.
J.J. Boon, Amsterdam, The Netherlands
J.M. Bracewell, Aberdeen, Great Britain
J.W. de Leeuw, Delft, The Netherlands
H. Dieu, Liège, Belgium
M.A. Grayson, St. Louis, MO, U.S.A.
C.S. Gutteridge, Reading, Great Britain
O. Hutzinger, Bayreuth, F.R.G.
C.E.R. Jones, Redhill, Great Britain
S.R. Larter, Oslo, Norway
R.S. Lehrle, Birmingham, Great Britain
I. Lüderwald, Biberach, F.R.G.
H.L.C. Meuzelaar, Salt Lake City, UT, U.S.A.
G. Montaudo, Catania, Italy
G. Schaden, Marburg, F.R.G.
T. Székely, Budapest, Hungary
S. Tsuge, Nagoya, Japan
K.J. Voorhees, Golden, CO, U.S.A.
B.B. Wheals, London, Great Britain
Zou Renjun, Shijiazhuang, China

Volume 16, 1989

ELSEVIER, AMSTERDAM—OXFORD—NEW YORK—TOKYO

© ELSEVIER SCIENCE PUBLISHERS B.V. (1989)

0165-2370/89/$03.50

All rights reserved. No part of this publication may be reproduced, stored in a retrieval system, or transmitted, in any form or by any means, electronic, mechanical, photocopying, recording, or otherwise, without the prior written permission of the publisher, Elsevier Science Publishers B.V., P.O. Box 330, 1000 AH Amsterdam, The Netherlands.
Upon acceptance of an article by the journal, the author(s) will be asked to transfer copyright of the article to the publisher. The transfer will ensure the widest possible dissemination of information.
Submission of an article for publication implies the transfer of the copyright from the author(s) to the publisher and entails the author(s) irrevocable and exclusive authorization of the publisher to collect any sums or considerations for copying or reproduction payable by third parties (as mentioned in article 17 paragraph 2 of the Dutch Copyright Act of 1912 and in the Royal Decree of June 20, 1974 (S. 351) pursuant to article 16b of the Dutch Copyright Act of 1912) and/or to act in or out of Court in connection therewith.
Special regulations for readers in the U.S.A. This journal has been registered with the Copyright Clearance Center, Inc. Consent is given for copying of articles for personal or internal use, or for the personal use of specific clients.
This consent is given on the condition that the copier pays through the Center the per-copy fee stated in the code on the first page of each article for copying beyond that permitted by Sections 107 or 108 of the U.S. Copyright Law. The appropriate fee should be forwarded with a copy of the first page of the article to the Copyright Clearance Center, Inc., 27 Congress Street, Salem, MA 01970, U.S.A. If no code appears in an article, the author has not given broad consent to copy and permission to copy must be obtained directly from the author. All articles published prior to 1980 may be copied for a per-copy fee of US $2.25, also payable through the Center. This consent does not extend to other kinds of copying, such as for general distribution, resale, advertising and promotion purposes, or for creating new collective works. Special written permission must be obtained from the publisher for such copying.
No responsibility is assumed by the Publisher for any injury and/or damage to persons or property as a matter of products liability, negligence or otherwise, or from any use or operation of any methods, products, instructions or ideas contained in the material herein.
Although all advertising material is expected to conform to ethical (medical) standards, inclusion in this publication does not constitute a guarantee or endorsement of the quality or value of such product or of the claims made of it by its manufacturer.

Printed in The Netherlands

Journal of Analytical and Applied Pyrolysis, 16 (1989) 1–3
Elsevier Science Publishers B.V., Amsterdam – Printed in The Netherlands

EDITORIAL

OVERSEAS TRAVEL FOR AMERICANS – THE IMAGE AND THE EXPENSE

Early last year I received a letter from Colin Gutteridge, a respected British analytical chemist and organizer of the international symposium "Pyrolysis 86" in Reading, U.K. His letter was in response to my report "Comments on Conferences" [*J. Anal. Appl. Pyrolysis,* 12 (1987) 189–191]. Colin pointed out that while 30% of the attendees at the 1987 Gordon Research Conference on Analytical Pyrolysis (Plymouth, U.S.A.) were from outside the United States, only 15% of the attendees of the Pyrolysis 86 conference were from the U.S. Colin asked the question: why is it that many North Americans don't travel to conferences in Europe (and other parts of the world)? This issue has been raised before, but to my knowledge no satisfactory answer has been given. Thus I decided to take an informal survey of members of the analytical pyrolysis community in the United States and Canada to see what the main reasons for this phenomenon are. A survey form was sent to 175 North American "pyrolysis people", and 80 forms (a very pleasing 46%) were returned.

The average respondent said that he/she had attended 24.1 technical conferences/symposia/workshops in the past ten years. Of these meetings, 3.0 (12%) per respondent were held outside of the North American continent. There was a good mix of academic (31%), industrial (43%), and government (26%) respondents. Most of the questionnaires (78%) were from people who considered themselves "senior-level" scientists, engineers or professors. Only 11% of the forms were from "junior-level" professionals, and another 11% were from managers or directors. Thus the survey results largely reflect the views of more experienced scientists and engineers. Fourteen possible reasons for non-attendance of conferences outside the North American continent were listed on the questionnaires, and the respondents were asked to rate each in one of three categories: "important factor", "a factor", or "not a factor". The fourteen factors and the overall results are given in Table 1.

It is clear that the major non-attendance factors were high travel expenses (factor 1) and difficulty of obtaining employer approval (factor 3). It is unquestionably true that for Americans in the past few years, the devalued dollar has made overseas travel much more expensive than it was even four or five years ago. The image and expense of overseas travel is obviously a difficulty with many employers and granting agencies, as evidenced by the high ratings for factors 3, 4 and 5. The time involved in overseas travel

TABLE 1

Fourteen factors for non-attendance at conferences outside the North American continent

	Important factor	A factor	Not a factor
1. Travel expenses are too high	45%	35%	20%
2. Too much time away from work or family is involved	10	31	59
3. It is too hard to get approval from my employer	50	15	35
4. My employer or grant agency does not permit foreign travel	19	14	67
5. My employer looks at foreign travel as a luxury or vacation	19	25	56
6. I do not like or feel comfortable with foreign travel	1	9	90
7. I do not like to travel long distances or in airplanes	4	14	82
8. It is too much trouble to get a passport or visa	2	10	88
9. Language or cultural barriers are difficult for me to overcome	2	9	89
10. All important work in my field is covered in American conferences	9	22	69
11. Since foreigners come here, there is no need for me to travel	2	21	77
12. Foreign conferences are generally not well organized	0	4	96
13. The scientific program is of lower quality in foreign conferences	2	4	94
14. I can only attend one or two meetings a year, and foreign conferences are not first choices	19	20	61

(factor 2) is also important to many conferees. That is, it is often convenient to attend just one or two days of a domestic conference, while traveling overseas usually requires a full week (or more) commitment of time. Finally, for whatever reason, many respondents indicated (factor 14) that overseas conferences are generally not their first choices when they can attend only a limited number of meetings per year.

Interestingly, the responses varied somewhat among academic, industrial, and government respondents. Academic people attended an average of 31.1 conferences over the ten-year period, of which 6.6 (21%) were overseas. Only 8% had never attended a foreign conference. The overwhelming reason for non-attendance was travel expense (factor 1); this was cited by 80% of the respondents as "a factor" or an "important factor". Lesser factors also frequently cited were factors 2 and 14. One factor mentioned by some academic people (but hardly at all by industrial or government scientists) is that the timing of foreign conferences is often not favorable with respect to the typical American academic year.

Industrial people attended an average of 19.0 conferences over the ten-year period, of which only 1.5 (8%) were overseas. Thus, in general industrial scientists attend fewer conferences than their academic colleagues. One-half

of the industrial respondents had never attended a foreign conference. The industrial respondents cited factors 1 (travel expense) and 3 (employer approval) as the two major reasons for non-attendance at foreign conferences; both of these factors were cited by 79% of the respondents. Of lesser importance, but still frequently cited, were factors 5 and 14. A major difference between academic and industrial scientists is that the image of foreign travel appears to be more favorable in an academic than an industrial environment. It is unfortunately true that many industrial employers view foreign travel as an unnecessary luxury for most technical employees. Foreign travel is sometimes granted more as a "reward" for good performance than as something beneficial from a technical viewpoint.

Government people attended an average of 24.0 conferences over the ten-year period, of which only 1.1 (5%) were foreign. Over half (57%) of these respondents had never attended a foreign conference. The principal non-attendance factors cited were factors 3 (employer approval, cited by 90% of respondents) and 1 (travel expense, cited by 81% of the respondents). Lesser factors also frequently cited were factors 4 and 5 (which are both employer related). The government employee responses are similar to those of industrial scientists. Employer approval appears to be even more difficult for many government employees, however; several people mentioned specifically that they have to apply for a foreign conference a year or so in advance, and that approval may be granted only a few days in advance of the travel date! This obviously makes planning ahead very difficult and discouraging.

Overall, the survey results are interesting and I think instructive in some respects. It appears that most North American scientists (at least in the "analytical pyrolysis" community) would like to attend more overseas conferences. They apparently feel that the scientific content and technical interchange in foreign conferences is at least as good as that in American conferences. The major hurdles to overcome, however, are travel expense and employer approval. It would be interesting to hear the perspective from the other side (i.e. from Europeans and other non-Americans).

ROBERT P. LATTIMER
Associate Editor

Journal of Analytical and Applied Pyrolysis, 16 (1989) 5–25
Elsevier Science Publishers B.V., Amsterdam – Printed in The Netherlands

PYROLYSIS–GAS CHROMATOGRAPHY / MASS SPECTROMETRY AND PYROLYSIS–GAS CHROMATOGRAPHY / FOURIER TRANSFORM INFRARED / FLAME IONIZATION DETECTION STUDIES OF PARTICLE SIZE FRACTIONS OF WOODY PEAT *

G.D. CALVERT

Department of Chemistry, University of South Carolina, Columbia, SC 29208 (U.S.A.)

J.S. ESTERLE

Department of Geological Sciences, University of Kentucky, Lexington, KY 40506-0059 (U.S.A.)

J.R. DURIG *

Department of Chemistry, University of South Carolina, Columbia, SC 29208 (U.S.A.)

(Received August 26th, 1988; accepted December 9th, 1988)

ABSTRACT

Peat types are categorized by botanical composition and degree of degradation. The more decomposed, or sapric peats, contain a higher percentage of finer particles than the least decomposed, or fibric peats. These finer particles represent the degradative remains of larger plant particles and, hence, possess a chemical composition indicative of increasing humification. Pyrolysis–gas chromatography/Fourier transform infrared/flame ionization detection (FID) and pyrolysis–gas chromatography/mass spectrometry studies have been conducted on woody peats from a deposit near Jambi, Sumatra, Indonesia, in an attempt to correlate particle size fractions to chemical composition. Fifty-seven compounds, classified according to their origins (e.g., eugenol, which is derived from guaiacyl type lignins), are quantitatively monitored by normalizing the FID response to 1 for each particle size fraction for each sample. The relative concentrations for each compound are then plotted versus three particle size fractions, and a classification scheme developed based upon those plots. The schemes classify the compounds as being either more concentrated in the finer size fractions, coarse size fractions, or as having no discernible particle size fraction trend. The fate of individual compounds and classes of compounds (e.g., hexoses) are presented, and the chemical composition of the various peat types are reconstructed from these data.

Flame ionization detection; Fourier transform infrared spectroscopy; gas chromatography; mass spectrometry; peat; pyrolysis.

* Taken in part from the thesis of G.D. Calvert which will be submitted to the Department of Chemistry in partial fulfillment of the Ph.D. degree.

0165-2370/89/$03.50 © 1989 Elsevier Science Publishers B.V.

INTRODUCTION

Modern peat deposits consists of physically and chemically heterogeneous organic material that can be categorized by botanical composition and degree of decomposition. One parameter commonly used to estimate the degree of decomposition is the distribution of particle size within a peat type [1]. Decreasing particle size has been correlated to increasing decomposition as measured by chemical techniques and has been shown to directly affect the suitability of peat as a fuel or agricultural additive [2].

Recently, studies have reported general chemical differences between different sized particles within peat samples [3–7]. In general, coarse particles (> 2 mm) contain more cellulose and lignocellulose-rich compounds than do smaller (> 0.25 mm), more decomposed particles. Specific chemical compounds characterizing these shifts have not, however, been closely monitored. This concept has not been tested for different size fractions between peak types at different levels of decomposition. Knowing the physical and chemical characteristics of peat enables one to better correlate observed chemical changes with corresponding humification patterns and with shifts in the types of plants making up the peat.

If specific chemical changes can be directly related to particle size fractions, then simple sieve techniques can be used to estimate decomposition and chemical composition. The objective of this study is to determine the different concentrations of specific chemical compounds between particles of different size fractions within a variety of peat types at different degrees of decomposition.

Previous studies of the chemical variability of peat have used powerful analytical techniques including magic angle spinning ^{13}C nuclear magnetic resonance spectroscopy (MAS ^{13}C NMR) [8,9], pyrolysis–mass spectroscopy (MS), pyrolysis–gas chromatography/mass spectrometry (GC/MS) [10–15], and Fourier transform infrared (FTIR) spectroscopy [7,16–18]. We chose to use pyrolysis–GC/ FTIR/flame ionization detection (FID) and pyrolysis–GC/MS because of their ability to monitor the chemical variability of peat on a molecular level [19]. This combination of techniques has proved to be valuable in providing both qualitative and quantitative estimates of specific components derived from the breakdown of peat.

It should be mentioned that the presence or absence of inorganic ash is of critical importance in pyrolysis. It has been shown that the catalytic activity of the inorganic constituents of ash shifts the distribution of products in pyrolytic studies [20,21]. Since the percentage of ash increases in the finer matrix particles [22], one must devise a way to selectively exclude the majority of this ash without chemically altering the remaining peat.

Many studies of peat employ alkaline extraction and acid hydrolysis procedures [23–29]. The organic samples obtained cannot, however, be assumed to be quantitatively extracted and, in addition, many contain

artifacts originating from the extraction and/or hydrolysis steps [4]. It was therefore decided that extraction procedures would not be performed on the samples during preparation. Instead, whole powdered peat samples were used.

EXPERIMENTAL

Sample collection

Peat samples were selected from cores collected at four sites located along a 20 km traverse across a peat deposit in Jambi, South Sumatra, Indonesia (Figs. 1a and b). This deposit was selected because it is thick (up to 7 meters), extensive (covering an area of at least 400 km^2), and consists of very woody peat. Vegetation at the surface of the deposit consists of a dense angiospermous peat forest except in the vicinity of core JE where tall grasses and palm-like vegetation occur (readers are referred to Cameron et al. [30] and Anderson [31] for a detailed species list). This deposit was interpreted to have begun as an abandoned channel fill followed by paludification to the northwest and the establishment of a dense peat forest as the coast line prograded.

Cores were collected in continuous 50 cm intervals down to the underlying clay substrate using an Eykelkamp Edelman auger. Peat cores were immediately placed in poly(vinyl chloride) (PVC) tubing and sealed with aluminum foil before air shipment to the laboratory where they were stored under refrigeration.

The physical properties of this peat have been previously described [32]. The field descriptions show that the more decomposed sapric peats occur at the top and bottom margins of the deposits, whereas the less decomposed hemic and fibric peats occur in the central portions of the deposit. All peat types contain various amounts of wood fragments.

Sample preparation

Initially 25 samples, representative of the various peat types, were selected from the cores for particle size analysis. Samples were first vacuum dried and then separated into three size fractions using a #10 (2 mm) and a #120 (0.25 mm) mesh sieve. The distribution, between peat types, of the particle size fractions is shown in Fig. 2. The coarse fraction (Size 1, > 2 mm) consisted of wood, bark fragments, and rootlets with some leaves present in the bottom of core JB; the medium fraction (Size 2, 0.25–2.0 mm) consisted of fragmented plants; and the fine fraction (Size 3, < 0.25 mm) consisted of particulate plant material difficult to distinguish as botanical entities. Of the 25 samples, 3 size fractions for each of 9 samples (total 27) were selected for

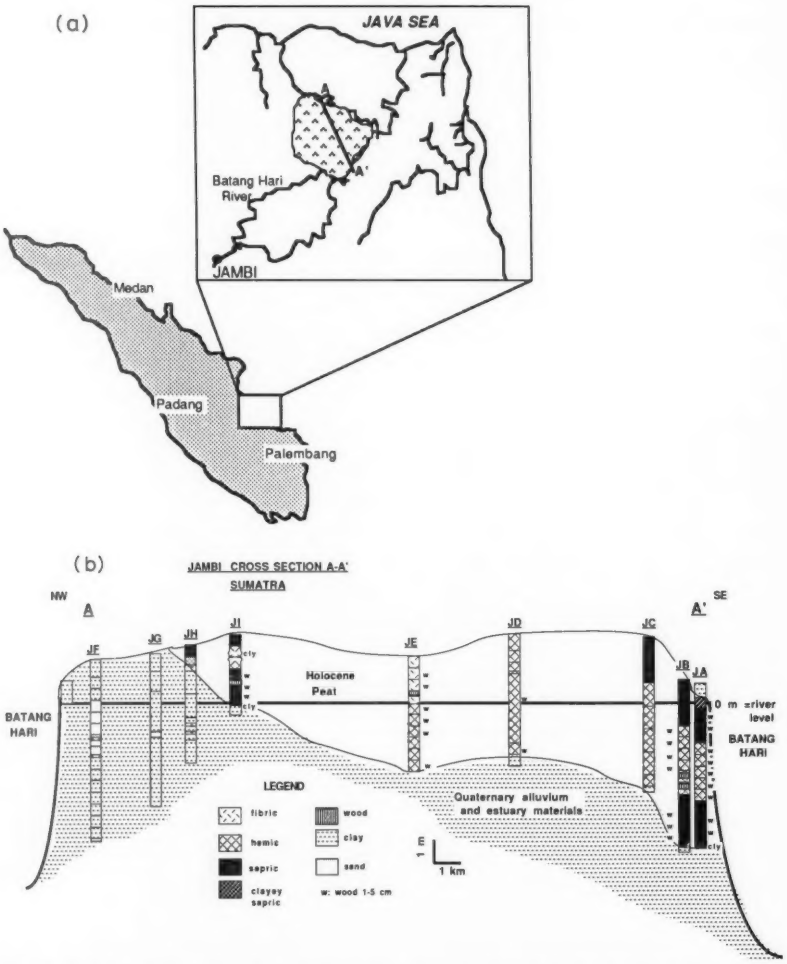

Fig. 1. (a) Map showing location of transect across peat deposit in Jambi province, Sumatra, Indonesia. (b) Cross section of peat deposit near Jambi showing the variability in the peat profile.

particle size	PEAT TYPE		
	fibric cs hemic	hemic	sapric clayey peat
>2.0 mm >25% <.25 mm <30%	7	4	0
>2.0 mm <25% <.25 mm <30%	1	8	2
>2.0 mm <25% <.25 mm >30%	0	1	2

Fig. 2. Distribution of particle size fractions between peat types in the Jambi deposit.

chemical analysis by pyrolysis–GC/FTIR/FID and pyrolysis–GC/MS. Samples came from two cores, JE and JI, and encompassed the variety of peat types occurring within the deposit.

CHEMICAL ANALYSIS

Pyrolysis–GC / FTIR / FID

Samples were analyzed using a Hewlett-Packard Model 5880A capillary gas chromatograph equipped with a flame ionization detector (FID), which was maintained at 300 °C. The apparatus and technique are described in detail in Durig et al. [19]. A Digilab Model FTS-14C Fourier transform interferometer was interfaced to the gas chromatograph using a Digilab lightpipe assembly (maintained at 250 °C) and a liquid nitrogen-cooled MCT (HgCdTe) detector. Spectra were obtained from 3200 to 700 cm^{-1} at 6 cm^{-1} resolution. FID signals were processed with a Hewlett-Packard Model 5880 series GC integrator. Total peak areas were integrated for each run, and a percentage of the total was reported for each eluting peak, thereby giving a normalized area for each compound.

A Chemical Data Systems Model 120 coil Pyroprobe equipped with 0.25 inch quartz sample cups was used to pyrolyze the 30 μg powdered peat samples at a set temperature of 555 °C for 5 seconds with an infinite ramp. The samples were loaded into the cups by statically charging a pulled glass rod, and then dipping the tip of the rod into the vials containing the powdered peat samples. By this method, we hoped to leave most of the heavier ash particles in the vial, while selectively removing the peat. An in-line rotary valve/liquid nitrogen cold trap interface introduced the pyrolysis vapors into the GC column head. Because the operation of this system has been previously described [19], it will not be discussed here other than to say that the primary purpose of this system is cryogenically to enhance the efficiency of the gas chromatograph. This, in turn, drastically reduces the time needed to separate over 200 pyrolysis products.

The GC column used was a J&W Scientific DB-1701 column (30 m × 0.32 mm I.D.), with 1 μm film thickness. The GC oven programme used was as follows: an initial oven temperature of 30 °C held for 2 min; a 20 °C/min ramp to 175 °C held for 0 min; and finally a 10 °C/min ramp to 240 °C held for 5 min. A post value of 280 °C for 5 min served to bake out the column after each run. A column flow-rate of 1.7 ml/min and a split flow of 3.0 ml/min were maintained.

Pyrolysis–GC / MS

Six of the Jambi samples were analyzed on a Finnigan 4021 gas chromatograph/quadrupole mass spectrometer equipped with a Finnigan 4521

TABLE 1

Complete list of identified compounds along with their MS scan numbers by combined pyrolysis–GC/FTIR/FID and pyrolysis–GC/MS studies

MS scan number	Compound
92	carbon oxydesulphide
100	2-butene
115	2-pentene
127	furan
138	2-propenal
144	2-propanone
152	2-methyl-1-pentene
161	2,5-dihydrofuran
169	propenoic acid
178	2-methylfuran
188	3-methylfuran
202	hexene
217	2-heptene
224	benzene
241	hydroxyacetaldehyde
245	pentan-3-one
251	2,5-dimethylfuran
259	2-butenal
261	dimethylfuran
271	pentenone
277	2-vinylfuran
283	2-ketobut-3-enal
292	2-octane
298	3-hydroxypropanal
304	toluene
308	2-propyn-1-ol
312	N-methylpyrrole
319	2-methyl-5-ethylfuran
324	pyridine
329	acetic acid
338	cyclopent-3-en-1-one
345	2,4-pentonedione
347	5-hexen-2-one
352	benzyl alcohol
355	2,4-(3H,5H)furanaline (T)
361	3-hydroxybutan-1-one
366	cyclopentanone
369	ethylbenzene
374	*o*-xylene
386	furan-3-one
394	*m* / *p*-xylene
398	ethenylbenzene
405	2-furaldehyde
413	2-*nor*-propylfuran
422	3-hydroxybutan-1-one
430	5-methylfuran-3-one

TABLE 1 (continued)

MS scan number	Compound
436	1,3-benzenediol
453	ethyl-methylbenzene
467	2-methyl-4-pyrimidinone
473	5-methyl-2-furanone
478	acetophenone
484	5-methyl-2-furaldehyde
490	unknown XYL
496	2-methyl-2-cylopenten-1-one
501	1-penten-3-one
514	4-hydroxy-5,6-dihydropyran-2-one
525	pyran-2,5-dione
528	2-hydroxy-3-methyl-2-cyclopenten-1-one
536	phenol
546	methyldihydrobenzofuran
550	guaiacol
555	methylindene
561	*o*-cresol
567	2-furfuryl-hydroxymethyl ketone
575	2-methyl-3-hydroxy-4H-pyran-4-one
578	*p*-cresol
584	guaiacylmethane (isomer)
590	4,7-dimethylbenzofuran
602	1,2-dimethoxybenzene
602	methylguaiacol
625	ethylguaiacol
627	ethenylguaiacol (isomer)
635	ethylguaiacol
639	C_2 phenol
646	ethylguaiacol
650	unknown PS (MW 116)
666	1,4 : 3,6-anhydro-α-D-glucopyranose
671	*m* / *p*-vinylphenol
678	vinylguaiacol
691	eugenol
695	5-(hydroxymethyl)-2-furancarboxyaldehyde
705	syringol
714	2-methoxy-6-(1-propenyl)phenol
723	*cis*-isoeugenol
731	syringol (isomer) (T)
735	3-ethanol-phenol (T)
743	1,4-dideoxy-D-glycero-hex-1-enopyranos-3-ulose
753	*trans*-isoeugenol
757	methylsyringol
771	vanillin
780	2,6-dimethyl-3(2H)-benzofuranone
786	unknown guaiacyl isomer (MW 162)
801	ethylsyringol
804	branched tetradecane

(Continued on p. 12)

TABLE 1 (continued)

MS scan number	Compound
813	4-hydroxy-3-methoxybenzoic acid
819	acetovanillone
824	guaiacylpropanaldehyde
837	ethenylsyringol
843	isomer of guaiacylpropanone
847	guaiacylpropan-2-one
852	4-hydroxyacetophenone
860	diethyl phthalate
869	isomer of guaiacylpropanaldehyde
878	3-hydroxy-1-(4-hydroxy-3-methoxy-phenyl)-1-propanone

EI source operated at 70 eV. A standard CDS GC interface (Model 3A01-0000) was connected to the injection port liner, and the GC column was fed up into the interface. The column used was a J&W Scientific DB-1701 column (25 m × 0.25 mm I.D.) with a 0.5 μm film thickness. The injection port and interface were maintained at 300 °C, and the oven and Pyroprobe temperature programmes were the same as in the pyrolysis–GC/FTIR/FID experiments.

RESULTS

Identification of the 107 compounds listed in Table 1 was accomplished by comparing the FTIR and mass spectra with EPA and NBS libraries, respectively, and by comparisons with literature references [8,10,28,33–39]. A typical FID chromatogram, that of a sample 100 cm deep, size fraction 1 in the JB hole, is shown in Fig. 3. For this study, it was decided to monitor only those compounds whose average normalized FID response was greater than 0.300%. This, we felt, would eliminate many of the non-linearities encountered by integrating peaks at or near baseline levels. With this as a criterion, we monitored the 57 compounds listed in Table 2 along with their respective GC/FTIR/FID retention times and origins, as determined from literature sources [13,20,27,33,35]. The total area of the 57 peaks ranged from 95 to 75% of the total FID area for these runs. The FID area for each compound was obtained by averaging the response of duplicate runs. Since the response of a FID is essentially linear over six orders of magnitude [36], it was assumed that linearity held for the range of concentrations involved in this study. In addition, because no quantitative determinations were being made between different compounds, the response factor of each compound could be neglected.

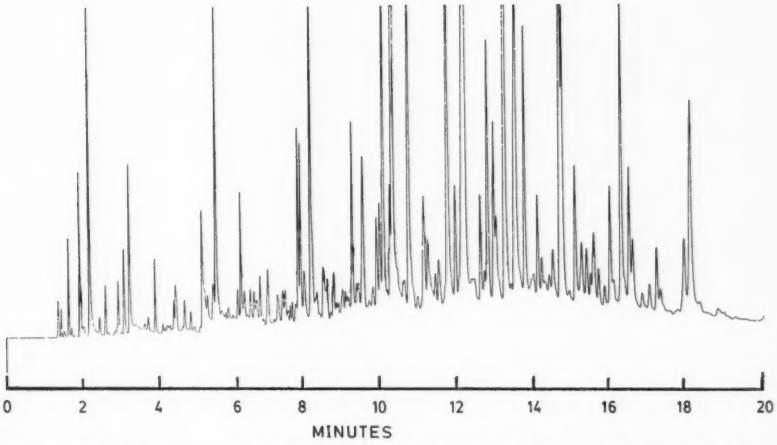

Fig. 3. FID chromatogram of a 100 cm deep, size fraction 1 peat sample from the JB hole.

In order to determine the differences in the pyrolysis products for each size fraction, each hole was initially considered separately. The normalized FID response for each compound was plotted for each size fraction in every sample. Based upon these plots, a classification scheme was devised which grouped those compounds with similar trends between particle size fractions. In Scheme 1, compounds were concentrated in the coarse size fractions, as represented by the particle size fraction plot of 5-methyl-2-furancarboxaldehyde in the JE hole, shown in Fig. 4. In Scheme 2, compounds showed no distinct or recognizable trends, as represented by the particle size

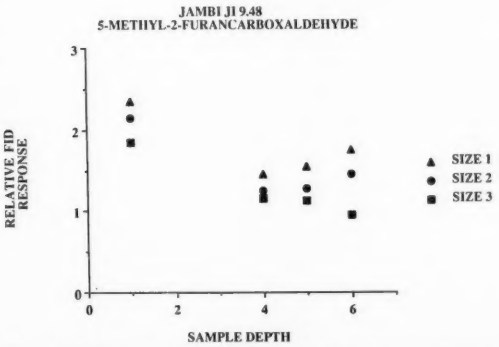

Fig. 4. Scheme 1, in which compounds are concentrated in the coarse size fraction, as represented by the particle size fraction plot of 5-methyl-2-furancarboxaldehyde in the JE hole. Sample depth is recorded in 0.5 meter increments.

TABLE 2

List of the 57 compounds and their origins which were monitored for particle size fraction concentration changes

FID ret. time	Compound	Origins *
1.16	2-butene	
1.71	furan	PS
2.20	2-propenal	
2.42	2-propanone	
2.64	2-methylpent-1-ene	
3.50	2-methylfuran	PS
4.19	benzene	LIG
5.01	toluene	LIG BIOD
5.15	N-methylpyrrole	EXT
5.32	pyridine	
5.47	acetic acid	XYL/PS
6.11	cyclopent-3-en-1-one	
6.83	ethylbenzene	LIG BIOD
7.72	furan-3-one	HEX
7.88	ethylbenzene	LIG BIOD
8.06	2-furaldehyde	PS
8.50	3-hydroxybutan-1-one	PS
8.68	5-methylfuran-3-one	HEX
8.92	1,3-benzenediol	PP
9.19	ethyl-methylbenzene	LIG BIOD
9.48	5-methyl-2-furancarboxaldehyde	PS
9.70	2-methyl-2-cyclopenten-1-one	PS
9.82	1-penten-3-one	PS
10.02	4-hydroxy-5,6-dihydro-(2H)-pyran-2-one	PENT
10.18	cyclopenten-1-one	HEX
10.25	phenol	LIG BIOD
10.60	methyldihydrobenzofuran	SPHAG
10.67	guaiacol	G LIG
11.10	2-methyl-3-hydroxy-(4H)-pyran-4-one	HEX
11.19	*p*-cresol	PP/LIG BIOD
11.30	isomer of guaiacylmethane	G LIG
11.38	4,7-dimethylbenzofuran	
11.73	1,2-dimethoxybenzene	PP/MOD LIG
11.77	guaiacylmethane	G LIG
11.90	ethylguaiacol (isomer)	G LIG
12.08	ethylguaiacol (isomer)	G LIG
12.59	ethylguaiacol (isomer)	G LIG
12.85	unknown PS peak (T)	PS
12.96	*m*/*p*-vinylphenol	LIG/MOD LIG
13.03	guaiacylethene	G LIG
13.24	eugenol	G LIG
13.55	5-hydroxymethyl-2-furancarboxaldehyde	PS
13.78	syringol	S LIG
13.99	2-methoxy-6-(1-propenyl)phenol	G LIG
14.12	*cis*-isoeugenol	G LIG
14.24	isomer of syringol (T)	S LIG

TABLE 2 (continued)

FID ret. time	Compound	Origins *
14.29	1,4-dideoxy-D-glycero-hex-1-enopyranos-3-ulose	HEX
14.71	*trans*-isoeugenol	G LIG
14.80	methylsyringol	S LIG
15.12	vanillin	LIG
15.29	2,6-dimethyl-3-(2H)-benzofuranone	
15.41	unknown guaiacyl isomer (MW 162)	G LIG
15.63	ethylsyringol	S LIG
15.74	branched tetradecane	
16.03	acetovanillone	LIG
16.13	isomer of guaiacylpropanaldehyde	G LIG
16.33	ethenylsyringol	S LIG
16.54	guaiacylpropan-2-one	G LIG
16.61	4-hydroxyacetophenol	LIG
17.92	1,2-propanediol	PS
18.10	glycerine	PS/HEX

* Abbreviations used: LIG BIOD, lignin biodegradation products; PS, polysaccharide; HEX, hexosan; XYL, xylan; PENT, pentosan; EXT, extensin; SPHAG, sphagnum, G LIG, guaiacyl-derived lignin; S LIG, syringyl-derived lignin; LIG, lignin; PP, polyphenol; MOD LIG, modified lignin; T, tentative assignment.

fraction plot of furan in the JI hole, shown in Fig. 5. In Scheme 3, compounds were concentrated in finer size fractions, as represented by the particle size fraction plot of ethyl benzene in the JI hole, shown in Fig. 6. These classification schemes helped to show changes in the chemical compositions from the coarse to the fine size fractions. In addition, each size

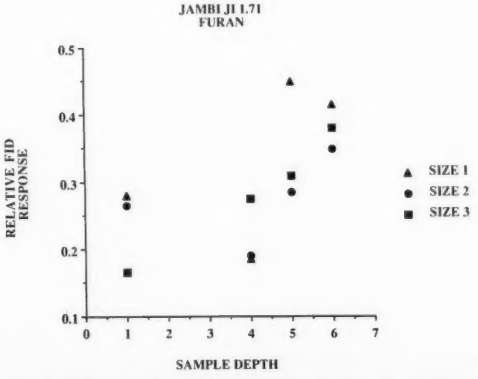

Fig. 5. Scheme 2, in which compounds show no distinct trends between particle size fractions, as represented by the particle size fraction plot of furan in the JI hole. Sample depth is recorded in 0.5 meter increments.

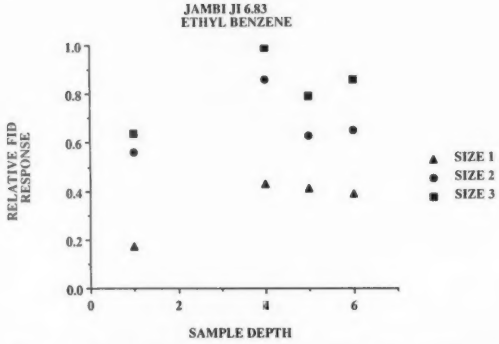

Fig. 6. Scheme 3, in which compounds are concentrated in the fine size fraction, as represented by the particle size fraction plot of ethylbenzene in the JI hole. Sample depth is recorded in 0.5 meter increments.

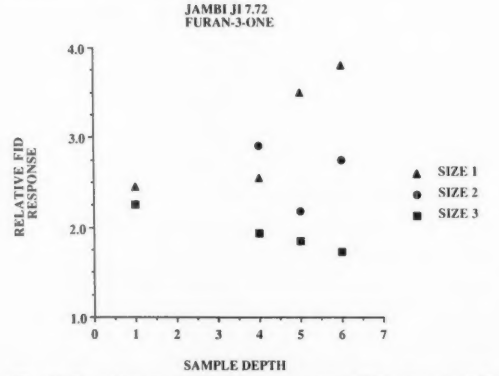

Fig. 7. Fanning open effect, as represented by the particle size fraction plot of furan-3-one in the JI hole. Sample depth is recorded in 0.5 meter increments.

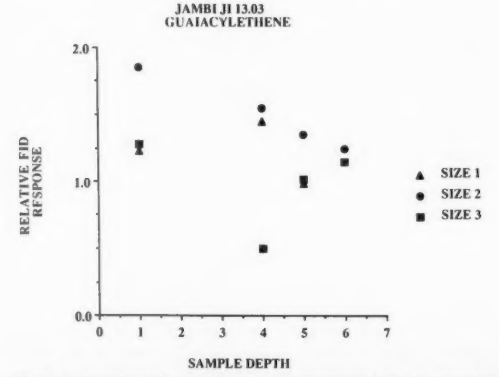

Fig. 8. Fanning close effect, as represented by the particle size fraction plot of guaiacylethene in the JI hole. Note: size fractions 2 and 3 have same value at sample depth 6. Sample depth is recorded in 0.5 meter increments.

fraction was plotted against depth to examine downhole trends. The downhole plots, such as Figs. 4 and 6, show that similar trends do occur within size fractions between samples of increasing decomposition.

Another interesting downhole trend is that of 'fanning open' or 'fanning closed'. This particular trend is characterized by increasing ('open') or decreasing ('closed') absolute differences between the size fraction concentrations with increasing depth. An example of the 'fanning open' effect is shown in Fig. 7, which is the particle size fraction plot of furan-3-one in the JI hole. The opposite effect, a 'fanning closed' phenomenon, is shown in Fig. 8, which is the size fraction plot of guaiacylethene in the JI hole.

DISCUSSION

Diagram 1 shows the breakdown of peat pyrolysis products which the authors used to trace the origins of the numerous pyrolysis products. In general, the lignin-derived products could be broken down into a guaiacyl-derived lignins, syringyl-derived lignins, lignin biodegradation products, and other miscellaneous lignin products. The cellulose derived products could be broken down into polysaccharides, hexoses, and other sugars. These classifications were then used to interpret size fraction trends within each category.

JE hole

The distribution of pyrolysis products among the three classification schemes for the JI hole are shown in Table 3. If one considers the origins of the pyrolysis products, some interesting trends become apparent. Of the lignin biodegradation products, most of the compounds with a phenolic substituent, i.e. phenol and vinylphenol, are more concentrated in the finer fractions, with only *p*-cresol more concentrated in the coarse size fractions. However, those compounds with a benzene substituent, i.e. toluene, ethylbenzene and ethyl-methylbenzene, are more concentrated in the coarse fractions. Only ethylbenzene is more concentrated in the finer size fractions. Benzene itself shows no clear trend, but this result could be affected by the fact that Pyroprobes appear to produce benzene during pyrolysis [37].

Of the guaiacyl-derived lignin products, the only clear trend occured in guaiacyl products with an alkyl side chain of propyl length, i.e. guaia-

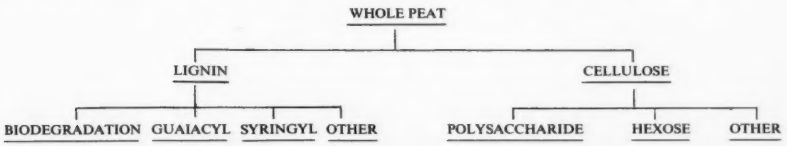

Diagram 1. Product distribution chart used to classify the origins of the pyrolysis products.

TABLE 3

Distribution of compounds in three classification schemes for the JE hole

1	2	3
Lignin biodegradation		
toluene	benzene	ethylbenzene
ethenylbenzene	ethyl-methylbenzene	phenol
p-cresol		*m* / *p*-vinylphenol
Guaiacyl lignin		
guaiacol	guaiacylmethane	vanillin
ethylguaiacol	ethylguaiacol (isomer)	acetovanillone
guaiacylethene	ethylguaiacol (isomer)	guaiacylpropanaldehyde
eugenol	2-methoxy-6-(1-propenyl)phenol	guaiacylpropan-2-one
trans-isoeugenol	*cis*-isoeugenol	
Syringyl lignin		
syringol	syringol (isomer)	ethylsyringol
methylsyringol	syringylethene	
Other lignin	1,2-dimethoxybenzene	4-hydroxyacetophenone
	1,3-benzenediol	
Polysaccharides		
2-furaldehyde	furan	acetic acid
5-methyl-2-furancarboxaldehyde	2-methylfuran	2-methyl-2-cyclopenten-1-one
unknown PS	3-hydroxybutan-1-one	
5-hydroxymethyl-2-furancarboxaldehyde	1-penten-3-one	
	1,2-propanediol	
	glycerine	
Hexoses		
furan-3-one	5-methylfuran-3-one	
2-hydroxy-3-methyl-2-cyclopenten-1-one		
2-methyl-3-hydroxy-(4H)-pyran-4-one		
1,4-dideoxy-D-glycerohex-1-enopyranos-3-ulose		
Other sugars		
N-methylpyrrole		
4-hydroxy-5,6-dihydro-(2H)-pyran-2-one		

cylpropanaldehyde and guaiacylpropan-2-one. These compounds were more concentrated in the finer size fractions, while those with an alkyl side chain of ethyl or less, i.e. guaiacylethane, guaiacol, and guaiacylethene, were more concentrated in the coarse size fractions. In addition, vanillin and acetovanillin were more concentrated in the finer size fractions. The syringyl-derived lignin products, syringol (isomer) and ethylsyringol, were more

concentrated in the finer size fractions, whereas syringol was more concentrated in the coarse size fractions.

From the remaining lignin-based products, 4-hydroxyacetophenone was more concentrated in the finer size fractions, whereas 1,2-dimethoxybenzene and 1,3-benzenediol had no evident trends.

The polysaccharide-derived products are generally more concentrated in the coarse size fractions. Among those polysaccharides, the pyrolysis products that have furancarboxaldehyde substituents, i.e. 5-methyl-2-furancarboxaldehyde and 5-hydroxymethyl-2-furancarboxaldehyde, are more concentrated in the coarse size fractions, whereas the simple furans, i.e. furan and 2-methylfuran, appear to have no trend with respect to the various size fractions.

All of the hexoses, including furan-3-one, 2-hydroxy-3-methyl-2-cyclopenten-1-one, 2-methyl-3-hydroxy-(4H)-pyran-4-one, and 1,4-dideoxy-D-glycerohex-1-enopyranose-3-ulose are more concentrated in the coarse size fractions. The extensin product, N-methylpyrrole, and the pentose product, 4-hydroxy-5,6dihydro-(2H)-pyran-2-one, are also more concentrated in the coarse size fractions.

JI hole

The distribution of pyrolysis products among the three classification schemes for the JI hole is shown in Table 4. Most of the lignin biodegradation products, such as toluene, ethylbenzene, ethylmethylbenzene and *p*-cresol are more concentrated in the coarse size fractions, whereas ethylbenzene, phenol, and *m/p*-vinylphenol are more concentrated in the finer size fractions.

The guaiacyl-derived lignin products were again evenly distributed throughout the three classification schemes, with the longer chained alkyl side groups being more concentrated in the finer size fractions. The syringyl-derived lignin products became more concentrated in the coarse size fractions, whereas the other lignin-derived products, 1,3-benzenediol and 4-hydroxyacetophenone had no distinguishable trend.

The polysaccharide products are more concentrated in the coarse size fractions with the same trends seen for the simple furans and furancarboxaldehydes as in the JE hole. The hexose-derived products are all more concentrated in the coarse size fractions, as was seen in the JE hole. The pentosan product, 4-hydroxy-5,6-dihydro-(2H)-pyran-2-one, became even more concentrated in the coarse size fractions, whereas the lone extensin product, N-methylpyrrole, had no apparent trend.

Overall

Between the two holes, excellent agreement was seen for almost all the compounds among the classification schemes. From the detailed comparison

TABLE 4

Distribution of compounds in three classification schemes for the JI hole

1	2	3
Lignin biodegradation		
toluene	benzene	ethylbenzene
ethenylbenzene		phenol
ethyl-methylbenzene		*m / p*-vinylphenol
p-cresol		
Guaiacyl lignin		
guaiacol	guaiacylmethane (isomer)	ethylguaiacol (isomer)
guaiacylmethane	2-methoxy-6-(1-propenyl)-phenol	acetovanillone
ethylguaiacol	*cis*-isoeugenol	guaiacylpropanaldehyde
ethylguaiacol (isomer)	vanillin	
guaiacylethene	guaiacylpropan-2-one	
eugenol		
trans-isoeugenol		
Syringyl lignin		
syringol	syringol (isomer)	ethylsyringol
methylsyringol	syringylethene	
Other lignin		
1,2-dimethoxybenzene	1,3-benzenediol	
	4-hydroxyacetophenone	
Polysaccharides		
2-furaldehyde	furan	acetic acid
5-methyl-2-furancarboxaldehyde	2-methylfuran	1,2-propanediol
	3-hydroxybutan-1-one	
unknown PS	2-methyl-2-cyclopenten-1-one	
5-hydroxymethyl-2-furancarboxaldehyde	1-penten-3-one	
glycerine		
Hexoses		
furan-3-one	5-methylfuran-3-one	
1,4-dideoxy-D-glycerohex-1-enopyranos-3-ulose	2-hydroxy-methyl-2-cyclopenten-1-one	
	2-methyl-3-hydroxy-(4H)-pyran-4-one	
Other sugars		
4-hydroxy-5,6-dihydro-(2H)-pyran-2-one	N-methylpyrrole	

of the data between the two holes, overall trends emerge between the coarse and finer size fractions. The lignin biodegradation products are slightly more concentrated in the coarse size fractions. Of the lignin biodegradation products, the benzene substituent products are more concentrated in the

coarse size fractions, whereas the phenol substituent based products are more concentrated in the finer size fractions.

The majority of the guaiacyl-derived lignin products were more concentrated in the coarse size fractions with an alkyl side chain length dependence. The propyl side chain guaiacyl products, guaiacylpropanaldehyde, and guaiacylpropan-2-one, were more concentrated in the finer size fractions, while the methyl and ethyl side chain guaiacyl products were slightly more concentrated in the coarse size fractions. While there was no overall syringyl-derived lignin trends, there was again a side chain dependence, with the longer chained ethyl-syringyl products being more concentrated in the finer size fractions, whereas the finer alkyl side chain syringyl products were more concentrated in the coarse size fractions.

The remaining lignin-derived products, e.g. vanillin, acetovanillone, and 4-hydroxyacetophenone, were more concentrated in the finer size fractions for both holes. At least two theories exist to explain why certain lignin pyrolysis products are more concentrated in the finer size fractions. As the lignocellulosic polymer is broken down into its component parts by degradation processes, some of the parts become biochemically altered. For example, vanillin, a lignin oxidation product, is residually concentrated in the finer size fractions. In the second theory, physically cleaved but chemically resistant components of the lignin cell polymer are concentrated in the fine size fractions. For example, those lignin products with a longer side chain, e.g. guaiacylpropan-2-one, might be more resistant to degradative processes than that of guaiacol. These theories deserve further investigation, and should be the subject of future publications from these authors. Altogether, the lignin-derived products, being aromatic in nature, showed a fairly even distribution throughout the size fractions, which is in agreement with Oades et al. [4], who saw a slight decrease in aromaticity in going from a particle size of 1.0 μm to a 1000 μm particle size.

The polysaccharide products are more concentrated in the coarse size fractions, as was seen by Ryan and her studies of the Florida Everglades, and Okefenokee Swamp peats [3], with acetic acid being the only exception. However, acetic acid could have a variety of origins [13,33] and, for this reason, should not be considered as being derived solely from polysaccharide. All of the hexoses are more concentrated in the coarse size fractions. Taken together, the polysaccharide and hexose results compare well with the study by Oades et al. [4], which reported a decreasing amount of carbohydrates in particles from 1000 to 1.0 μm with CPMAS ^{13}C NMR data of particle size fractions from an Urrbrae fine sandy loam. This could also be supported by the fact that these matrix particles are likely the product of degraded coarse plant fragments and, therefore, probably reflect a higher degree of humification than the coarse particle sizes from the same depth [38]. Since it is well known that cellulose is one of the first components degraded by microbial organisms [39–41], it is highly likely that very little cellulose would remain in these smaller particles.

TABLE 5

Special trends associated with compounds from both JE and JI hole

JE hole		JI hole	
Fanning open	Fanning close	Fanning open	Fanning close
2-ketobutan-1-ol	benzene	furan-3-one	2-methylpent-1-ene
p-cresol	ethylbenzene	2-furaldehyde	benzene
isomer of syringol	ethenylbenzene	phenol	N-methylpyrrole
branched tetradecane	ethyl-methylbenzene	guaiacol	3-hydroxybutan-1-one
glycerine	4-hydroxy-5,6-dihydro-(2H)-pyran-2-one	*p*-cresol	1,3-benzenediol
	2-methyl-3-hydroxy-(4H)-pyran-4-one		ethylguaiacol
	ethylsyringol		etheneguaiacol
	guaiacolpropanaldehyde		

The distribution of those compounds with no determined origin is shown in Table 5. For these compounds, several chemical trends are evident. Those compounds with an unsaturated C–C bond, such as 2-butene, cyclopent-3-ene-1-one and 2-methylpent-1-ene, were more concentrated in the larger size fractions at all depths for both holes. Finally, the benzofurans, such as 2,6-dimethyl-3(2H)-benzofuranone and 4,7-dimethylbenzofuranone, which have been identified as possible lignin biodegradation products, were evenly distributed between size fractions, and no trend was seen for either compound.

Fanning

Table 5 shows fanning open and fanning closed trends observed in the JE and JI holes. Two of the polysaccharide products, glycerine and 2-furaldehyde, fan open whereas 3-hydroxybutan-1-one fans open in the JE hole and fans close in the JI hole. The other cellulose-derived compounds, such as 4-hydroxy-5,6-dihydro-(2H)-pyran-2-one, 2-methyl-3-hydroxy-(4H)-pyran-4-one, and N-methylpyrrole, fan close. Of the sugars, only furan-3-one, a hexose-derived product, fans open.

The lignin biodegradation products with a benzene substituent, i.e. benzene, ethylbenzene, ethenylbenzene, and ethyl-methylbenzene, fan close. The lignin biodegradation products with a phenol substituent, i.e. *p*-cresol and phenol, fan open. The guaiacyl- and syringyl-lignin-derived products once again show an alkyl side chain length dependence. Those products with a longer side chain, i.e. guaiacylpropanaldehyde, ethylguaiacol, ethenylguaiacol, and ethylsyringol fan close. Those products with a shorter side chain, i.e. syringol (isomer) and guaiacol, fan open.

CONCLUSIONS

The application of pyrolysis–GC/FTIR/FID and pyrolysis–GC/MS can be a powerful technique for the analysis of particle size fractions of woody peats. By analyzing these particles separately, we gain a greater understanding of the degradation processes involved in the humification of these peats. The information yielded by these studies, combined with petrographic and downhole analysis by combined pyrolysis studies [42], should enable a more complete mapping of the geochemical processes of these highly acidic and anaerobic peat deposits.

Knowing that classes of compounds concentrate differently into the three size fractions should enable reconstructions of the chemistry of these particles and, hence, the peat types which are a combination of varying amounts of these particles.

The least decomposed fibric peats, dominated by coarser, well preserved plant parts (i.e., rootletss and wood fragments), retain much of their original lignocellulose character. The polysaccharide, hexose, pentose, and extensin character is well preserved, with a high furancarboxyaldehyde character in the polysaccharide fractions. Most of the lignin biodegradation products that are present have a benzene substituent, and usually possess a small alkyl side chain. The guaiacyl- and syringyl-based lignins are usually alcohols, and typically have either an ethyl or methyl alkyl side chain. There are little or no oxidized lignin products, and there is some unsaturated hydrocarbon character.

The hemic peats, which contain a mix of the fine, medium, and coarse particles, represent a transitory phase of peatification. The chemical composition of this peat therefore represents a stage between the fibric and sapric peats. The polysaccharide fraction is starting to degrade, and the hexose, pentose, and extensin character is rapidly disappearing. The lignin biodegradation products are a mix of phenolic- and benzene-based products, with some lignin oxidation products beginning to appear. The guaiacyl and syringyl lignins are a mix of methyl-, ethyl- and propyl-side chained lignins.

TABLE 6

Distribution of those compounds with no determined origin, for both JE and JI holes, in the three classification schemes

1	2	3
2-butene	2-propenal	2-propanone
2-methylpent-1-ene	2,6-dimethyl-(2H)-benzofuranone	
cyclopent-3-ene-1-one	4,7-dimethylbenzofuranone	
pyridine		
branched tetradecane		

The sapric, or more decomposed peats, contain a majority of the finer particles and, therefore, reflect a greater degree of decomposition. These peats have little remaining polysaccharide character, with even less hexose, pentose, and extensin character. The lignin biodegradation products are mostly phenolic, and there is a rapid increase in the concentration of oxidized lignins. Propyl and ethyl side chains dominate the guaiacyl- and syringyl-derived lignins. In addition, the syringyl-derived products are less concentrated, as a whole, than they were in the fibric peats.

ACKNOWLEDGEMENTS

The authors would like to thank Dr. Mike Walla for his assistance with the pyrolysis–GC/MS studies, and the South Carolina Energy Institute for funding this research. Field work was conducted under Dr. Cornelia Cameron of the U.S. Geological Survey–EMR Branch and Mr. Supardi of the Directorate of Mineral Resources–Indonesia, and was funded in part by a fellowship grant from Utah International, Inc.

REFERENCES

1 R.S. Farnham and H.R. Finney, Adv. Agron., 17 (1965) 115.
2 C.C. Cameron, Proc. 4th Int. Peat Congress, Helsinki, 1972.
3 N.J. Ryan, Ph.D. Thesis, The Chemical and Anatomical Compositions of Coal Precursers, Penn State University, 1985.
4 J.M. Oades, A.M. Vassallo, A.G. Waters and M.A. Wilson, Aust. J. Soil Res., 25 (1987) 71.
5 P.H. Given, C. Rhoades, P.C. Painter, W. Spackman, N.J. Ryan, R.J. Pugmire, L.B. Alemany and J.P. Boudon, Proc. 1983 Int. Conf. on Coal Sci., 1983, p. 389.
6 J.R. Bracewell, G.W. Robertson and B.L. Williams, J. Anal. Appl. Pyrolysis, 2 (1980) 53.
7 D.T. Durig, J.S. Esterle, T.J. Dickson and J.R. Durig, Appl. Spectrosc., 42 (1988) 1239.
8 C. Saiz-Jimenez, J.J. Boon, J.I. Hedges, J.K.C. Hessels and J.W. de Leeuw, J. Anal. Appl. Pyrolysis, 11 (1987) 437.
9 G.R. Hatfield, M. Sardashti and G.E. Maciel, Anal. Chem., 59 (1987) 1659.
10 S.A. Stout, J.J. Boon and W. Spackman, Geochim. Cosmochim. Acta, 52 (1988) 405.
11 R.K. Kotra and P.G. Hatcher, Fuel, submitted for publication.
12 P.G. Hatcher, H.E. Lerch, R.K. Kotra and T.V. Verheyen, Fuel, in press.
13 A.D. Pouwels, A. Tom, G.B. Eijkel and J.J. Boon, J. Anal. Appl. Pyrolysis, 11 (1987) 417.
14 F. Shafizadeh and V.L. Fu, Carbohydr. Res., 29 (1973) 113.
15 A. van der Kaaden, J.J. Boon and J. Haverkamp, Biomed. Mass Spectrosc., 11 (1984) 486.
16 A. Holmgren and B. Nordén, Appl. Spectrosc., 42 (1988) 255.
17 C.A. Rhoades, P.C. Painter and P.H. Given, Int. J. Coal Geol., 8 (1987) 69.
18 H.R. Ross and C. Byrne, Spectroscopy, 1 (1986) 40.
19 J.R. Durig, G.D. Calvert and J.S. Esterle, J. Anal. Appl. Pyrolysis, 14 (1989) 295.
20 Y.Z. Lai and F. Shafizadeh, Carbohydr. Res., 38 (1974) 177.
21 A. van der Kaaden, J. Haverkamp, J.J. Boon and J.W. de Leeuw, J. Anal. Appl. Pyrolysis, 5 (1983) 199.

22 D.J. Boron, E.W. Evans and J.M. Peterson, Int. J. Coal. Geol., 8 (1987) 1.
23 P. Pillon, J.M. Portal, B. Gerard, P. Jeanson and L. Jocteur-Monrozier, Org. Geochem., 9 (1986) 313.
24 M. Radke, R.G. Schaefer, D. Leythaeuser and M. Teichmüller, Geochim. Cosmochim. Acta, 44 (1980) 1787.
25 F. Finotello and R.B. Johns, Org. Geochem., 9 (1986) 265.
26 O. Faix, D. Meier and I. Grobe, J. Anal. Appl. Pyrolysis, 11 (1987) 403.
27 J.J. Boon, A.D. Pouwels and G.B. Eijkel, Biochem. Soc. Trans., 15 (1987) 170.
28 E. Alder, Wood Sci. Technol., 11 (1977) 169.
29 M. Ketola, E. Luomala, K. Pihlaja and T. Nyrönen, Fuel, 66 (1987) 600.
30 C.C. Cameron, S. Supardi, T.S. Malterer and J.S. Esterle, in Proc. International Peat Society Symposium on Tropical Peat and Peatlands for Development, 1987, Yogyakarta, Indonesia, in press.
31 J.A.R. Anderson, in Peat and Podzolic Soils and Their Potential for Agriculture in Indonesia, Proc. ATA Mid-term Seminar, 1976, pp. 45–55.
32 J.S. Esterle, S. Supardi and D.T. Durig, in Int. Peat Soc. Symposium on Tropical Peat and Peatland for Development, Yogyakarta, Indonesia, February, 1987, in press.
33 D.G. van Smeerdijk and J.J. Boon, J. Anal. Appl. Pyrolysis, 11 (1987) 377.
34 C. Saiz-Jimenez and J.W. de Leeuw, Org. Geochem., 10 (1986) 869.
35 R.J. Evans, T.A. Milne and M.N. Soltys, J. Anal. Appl. Pyrolysis, 9 (1986) 207.
36 C.F. Poole and S.A. Schuette, Contemporary Practice of Chromatography, Elsevier, Amsterdam, 1984.
37 J.J. Boon, personal communication.
38 M.A. Wilson, personal communication.
39 K. Ruel and F. Barnoud, in T. Higuchi (Editor), Biosynthesis and Biodegradation of Wood Components, Academic Press, New York, 1985, pp. 441–467.
40 K.-E. Eriksson and T.E. Wood, in T. Higuchi (Editor), Biosynthesis and Biodegradation of Wood Components, Academic Press, New York, 1985, pp. 469–503.
41 C.L. Chen and H.M. Chang, in T. Higuchi (Editor), Biosynthesis and Biodegradation of Wood Components, Academic Press, New York, 1985, pp. 535–556.
42 G.D. Calvert, J.R. Durig, J.S. Esterle and J.C. Ferm, Org. Geochem., submitted for publication.

Journal of Analytical and Applied Pyrolysis, 16 (1989) 27–35
Elsevier Science Publishers B.V., Amsterdam – Printed in The Netherlands

FLUIDIZED BED PYROLYSIS OF DIGESTED SEWAGE SLUDGE

W. KAMINSKY * and A.B. KUMMER

Institut für Technische und Makromolekulare Chemie, Universität Hamburg, Bundesstrasse 45, D-2000 Hamburg 13 (F.R.G.)

(Received October 16th, 1988; accepted October 20th, 1988)

ABSTRACT

Digested, thermally conditioned and dried sewage sludge has been pyrolyzed in an indirectly heated fluidized bed reactor at temperatures ranging from 620 °C to 750 °C. A quantity of up to 40 kg of sewage sludge per hour has been converted into pyrolysis gas, oil, product water and carbonaceous residues in a continuously working pilot plant.

The pyrolysis gas has a calorific value of approximately 23 MJ/m^3. The main constituents of the pyrolysis gas are hydrogen, methane, ethane, ethene and propene as well as carbon monoxide and carbon dioxide.

The oil fraction yielded contains up to 30% aromatic compounds. The heavy metals from the sewage sludge become to a large extent enriched in the solid residue on account of the reducing conditions of the pyrolysis process.

Fluidized beds; pyrolysis; sewage; sludges, sewage; waste water.

INTRODUCTION

More elaborate and refined purification methods in the treatment of communal and industrial crude waste water are leading to a continuous increase of the amount of sewage sludge to be processed. The expected annual amount of sludge is estimated to rise up to 320–430 mio m^3 in the EC in 1990 [1]. This demonstrates the whole problematic nature of the disposal and utilization of sewage sludge. At present, the sewage sludge is distributed as follows [2]:

- agriculture + decomposition 32%
- sanitary landfill 59%
- incineration 9%.

The utilization of sewage sludge as fertilizer seems to be reasonable, especially as the biological matter and its degradation products could be used as a new nutrient substrate. But, meanwhile, the use of agricultural

0165-2370/89/$03.50 © 1989 Elsevier Science Publishers B.V.

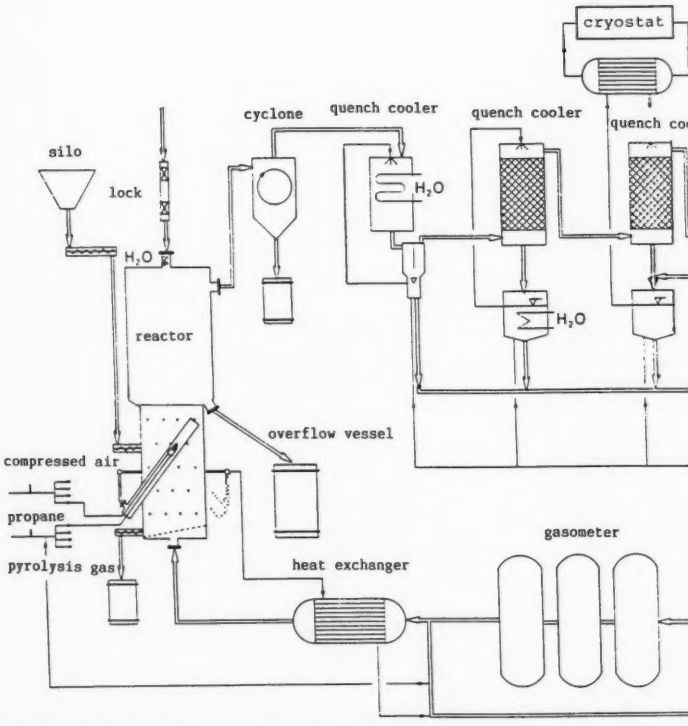

Fig. 1. Fundamental flow scheme of the pyrolysis pilot plant.

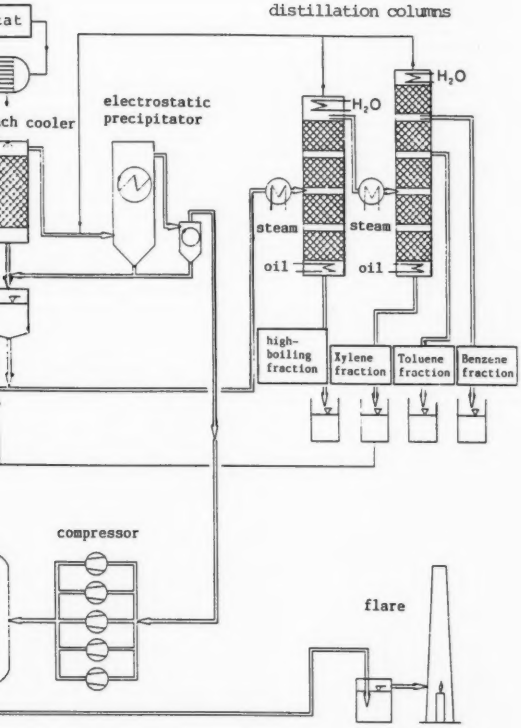
distillation columns
electrostatic
precipitator
H_2O
H_2O
steam
steam
oil
oil
high-
boiling
fraction
Xylene
fraction
Toluene
fraction
Benzene
fraction
compressor
flare

purposes has repeatedly been restricted because of the harmful components in the sewage sludge, such as heavy metals, polyaromatic hydrocarbons and polychlorinated biphenyls.

There are certain requirements to be met prior to the deposition of sewage sludge in landfills, such as dehydration, stabilization and deodorization having as their intent the avoidance of any kind of emission. In addition, neither the biological potential nor the chemical energy content are sufficiently exploited. In future, deposition of sewage sludge will be made more difficult as a result of a decreasing deposition capacity on the one hand and the increasing cost of deposition on the other.

Thermal conversion processes, such as combustion or pyrolysis, offer alternative waste disposal concepts. The combustion process yields a considerable amount of sulphur oxides and nitrogen oxides owing to the fact that sewage sludge contains sulphur and nitrogen compounds. Expensive precautions as regards flue gas purification have to be taken for the purpose of running combustion plants on an environmentally tolerable scale. In addition to that, problems arising from the increased elution capability of heavy metals out of the ashes produced from the oxidizing treatment have to be solved.

The pyrolysis of sewage sludge according to the Hamburg Process [3] seems to be advantageous as regards the minimization of emission due to a closed gas cycle in connection with an indirectly heated fluidized bed and the reduced volume of the depyrolyzed sewage sludge. The gain of gas and oil as well as the incorporation of heavy metals in the pyrolysis residue are facts in favour of the environmentally tolerable utilization [4,5] of the energy potential of sewage sludge.

APPARATUS AND RESULTS

The pilot plant

Fig. 1 shows the basic flow scheme of the fluidized bed pilot plant by means of which the pyrolysis of digested sewage sludge has been investigated.

The core of the plant is an indirectly heated fluidized bed, 450 mm in diameter. Right at the start of the pyrolysis, the fluidization material consists of quartz sand with particle sizes between 0.3 and 0.7 mm. In the course of the run the sand is gradually replaced by depyrolyzed sewage sludge. In order to ensure a constant height of the fluidized bed of approximately 650 mm during continuous input of sewage sludge an overflow vessel has been attached to the reactor.

Next to the reactor, a cyclone separates carbon and solid particles from the product gases. The cyclone is followed by three quench coolers where the

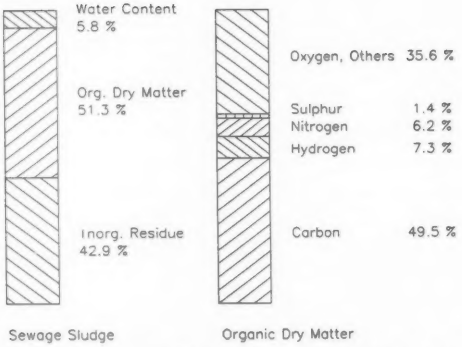

Fig. 2. Mean composition of the sewage sludge and the organic dry matter according to DIN 38.414 T3.

pyrolysis oils are subsequently quenched. At the end of the third cooler the temperature goes down to 0–5 °C. During the last condensation stage the product gas is freed from aerosols and entrained droplets in an electrostatic precipitator. The gas is then conveyed into five membrane compressors, connected in parallel, and stored in three gas tanks. One portion of the gas is used to fluidize the sand bed, whereas the rest of the gas may be used as fuel for the radiation heating tubes, thus allowing the plant to operate autothermally.

Feed stock

The feed stock for the pyrolysis experiments consisted of digested, thermally conditioned and dried sewage sludge originating from the Alfeld Community purification plant, Alfeld/Leine (F.R.G.). The water content of the sludge was very low, being 5–6% by mass, which was a result of the preceding thermal treatment [6]. This was the reason why the sludge was fed into the pyrolysis plant without any further drying steps. The size of the granules supplied ranged between 0.5 and 1.5 mm in diameter. Fig. 2 shows the mean composition of the sewage sludge as it was used for the pyrolysis experiments.

The pyrolysis experiments were carried out at temperatures of 620 °C, 690 °C and 750 °C. The sewage sludge was continuously and directly fed into the reactor from a silo via two screw conveyors. The conveying capacity was 25–40 kg/h and the whole charge of converted sludge amounted to more than 360 kg. The product fractions obtained consisted of gas, pyrolysis oil, product water, soot and pyrolysis residue. This solid residue contained the formed pyrolysis coke together with the inorganic fraction of the sludge.

TABLE 1

Product fractions of the pyrolysis of sewage sludge (% by mass of organic dry matter)

Temperature (° C)	620	690	750
Sludge mass (kg)	361.2	126.6	118.7
Organic dry matter (kg)	185.5	62.9	60.0
Product fractions (m%)			
Pyrolysis gas	22.7	30.7	40.8
Oil	40.1	34.3	21.1
Product waterli	12.6	10.8	8.0
Soot	0.8	0.8	1.9
Pyrolysis coke	20.0	19.2	22.3
Loss	3.8	4.2	6.8
Σ	100.0	100.0	100.0

Table 1 shows the composition of the organic pyrolysis products obtained at three different reaction temperatures. The water content of the sewage sludge was determined according to DIN 38.414 T2 and subtracted before calculating the product fractions.

The main contents of the pyrolysis gas are carbon monoxide, carbon dioxide, hydrogen as well as C_1–C_4 hydrocarbons. Small amounts of carbonyl sulphide and hydrogen sulphide are likely to be found. The calorific value of the pyrolysis gas amounts to 23 MJ/m^3, i.e. up to about 70% of the calorific value of natural gas.

The gaseous portion of the pyrolysis products increases with rising temperature from 620 °C to 750 °C from 22.7% to 40.8%. The chief constituents, the gas densities and the calorific values of the pyrolysis gases are listed in Table 2.

TABLE 2

Chief constituents of the pyrolysis gases

	Temperature (° C)		
	620	690	750
Compound (m%)			
Hydrogen	2.4	2.4	2.8
Methane	15.3	15.4	20.6
Ethane	4.9	3.4	4.3
Ethene	2.9	5.4	6.7
Propene	3.8	3.0	2.1
Carbon monoxide	33.0	39.9	44.3
Carbon dioxide	31.5	28.5	17.5
Σ other gases	6.2	2.0	1.7
Gas density (kg/m^3)	0.995	0.976	0.882
Calorific value (MJ/m^3)	22.8	21.7	22.8

TABLE 3

Composition of the pyrolysis oil

Compound (m%)	Temperature (°C)		
	620	690	750
C_5-Hydrocarbons	1.46	1.44	1.45
C_6-Hydrocarbons	2.21	2.53	1.51
C_7-Hydrocarbons	0.93	1.06	0.69
C_8-Hydrocarbons	0.35	0.37	0.23
C_9-Hydrocarbons	0.37	0.18	0.09
C_{10}-Hydrocarbons	0.32	0.16	0.04
C_{11}-Hydrocarbons	0.30	0.10	0.06
C_{12}-Hydrocarbons	0.21	0.18	0.06
Cyclopentadiene	0.23	0.40	0.22
Diels–Alder products	0.13	0.66	1.48
Σ Aliphatics/naphthenes	9.18	7.76	5.84
Benzene	1.81	3.62	9.32
Indene	0.30	0.68	1.58
Naphthalene	0.40	0.92	1.69
Biphenyl	0.21	0.38	0.46
Acenaphthylene	0.06	0.17	0.36
Fluorene	0.06	0.11	0.19
Phenanthrene	0.12	0.20	0.30
Anthracene	0.05	0.03	0.04
Fluoranthene	0.02	0.02	0.04
Pyrene	0.02	0.06	0.06
Chrysene/triphenylene	0.03	0.04	0.11
Σ Aromatics	8.70	15.32	29.54
Phenol	0.47	0.83	1.84
Cresols	0.67	1.37	1.88
Furan	0.02	0.01	0.01
Methylfuran	0.28	0.32	0.19
Methylbenzofurans	0.24	0.27	0.17
Dimethylbenzofurans	0.13	0.26	0.12
Σ O-containing compounds	1.85	3.08	4.25
Acetonitrile	1.36	0.69	2.39
Propionitrile	0.05	0.05	0.06
Acrylonitrile	0.03	0.05	0.21
Benzonitrile	0.08	0.06	0.13
Methylbenzonitriles	0.23	0.26	0.40
Naphthonitrile	0.08	0.28	0.32
Pyrrole	0.41	0.53	1.33
Methylpyrroles	0.26	0.07	0.09
Pyridine	0.09	0.04	0.08
Indole	0.30	0.45	0.80
Quinoline/isoquinoline	0.12	0.10	0.30
Methylquinolines	0.07	0.07	0.15
Carbazole	0.01	0.03	0.04

TABLE 3 (continued)

Compound (m%)	Temperature (°C)		
	620	690	750
Σ N-containing compounds	3.25	2.88	8.89
Σ other compounds	1.57	2.35	2.19
Tar/residue	75.45	68.61	49.29
Σ	100.00	100.00	100.00

The composition of the pyrolysis oils can be found in Table 3. The oil contains hydrocarbons and, in addition, some quantities of nitriles, phenols and heterocyclic compounds. With rising reaction temperature the oil yield decreases from 40.1% at 620°C to 21.1% at 750°C. The major portion of the pyrolysis oils is still tar, especially at low temperatures down to 620°C, amounting to 75.5%. This tar consists of substances which cannot be separated by distillation. The increase of pyrolysis temperature leads to a rising percentage of aromatic components due to progressive defunctionalization. The distillation residue contains the oil-insoluble substances as well as those parts of the pyrolysis coke that were included in the oil. A further cracking process and further utilization of these tars by means of recycling into the pyrolysis process and hydrogenation are under consideration.

The product water, which is obtained by decomposition of carbohydrates and carboxylic acids, contains a considerable amount of ammonia as well as organic water-soluble substances (Table 4).

A dominant part of chemical oxygen demand is caused by the considerable content of dissolved ammonia in the pyrolysis water. The extraction of

TABLE 4

Composition and analytical results of the product water

	Temperature (°C)		
	620	690	750
pH	9.9	9.8	9.5
NH_4^+ (g/l)	38.9	36.6	34.6
COD (mgO_2/l)	51500	47100	41300
Compound (m%)			
Methanol	0.13	0.05	0.07
Acetonitrile	1.05	0.76	0.60
Propionitrile	0.10	0.08	0.04
Pyrrole	0.13	0.09	0.06
Pyridine	0.09	0.06	0.08
Acetamide	0.02	0.21	0.37

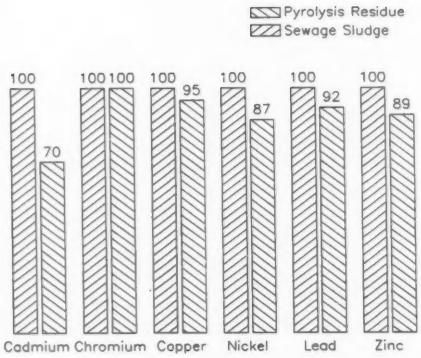

Fig. 3. Pyrolysis residue containing heavy metal fractions.

ammonia by stripping seems to be technically feasible. This may admittedly yield impure ammonia, still suitable enough for the catalytic removal of nitrogen oxides from flue gases of power plants as well as municipal solid waste incineration facilities.

Investigations of the pyrolysis residues, composed of the inorganic residue and the pyrolysis coke, show that the heavy metals originating from the sewage sludge are enriched in this fraction. This enrichment holds quantitatively true in the case of all relevant heavy metals except the volatile elements mercury and cadmium. For cadmium the pyrolysis temperature and the residence time are significant, whereas mercury is already volatile below 500 °C [7]. Fig. 3 shows the pyrolysis residue containing heavy metal fractions after pyrolysis at 620 °C.

Elution experiments with water according to DIN 38.414 T4 resulted in the finding that heavy metals are evidently more strongly incorporated in the matrix of pyrolysis residue than in the incineration ash, produced at 1200 °C, or in the sewage sludge itself. Table 5 shows that chromium, for

TABLE 5

Elutions according to DIN 38.414 T4

Element (μg/kg)	Sample		
	Sewage sludge	Incineration ash (1200 °C)	Pyrolysis residue (750 °C)
Cadmium	8	14	< 3
Chromium	100	7750	30
Copper	8150	100	50
Lead	350	55	50
Nickel	3860	125	25

instance, is more than 250-fold less liable to be eluted from pyrolysis residue than from incineration ash. Moreover, chromium is dissolved from ash essentially in the oxidation state(VI) as compared to chromium(III) from pyrolysis residues.

DISCUSSION

The investigations have shown that digested sewage sludge can be pyrolyzed according to the Hamburg Process without any pretreatment. The gas–oil ratio is adjustable to a great extent by varying the reaction temperature. With increasing temperature propagated cracking of the charged organic material with formation of small molecules and aromatic compounds can be observed. At the same time, it has been discovered that the spectrum of products can be simplified by extensive defunctionalization of the heteroatomic contents of the sludge. The resulting pyrolysis gases can be exploited for fuel purposes, thus allowing for an autothermal operating mode of the pyrolysis plant.

The use of the aromatic oils for petrochemical applications seems to be promising.

The reduction of volume and the strong incorporation of the heavy metals in the matrix of the pyrolysis residue eases the problem of sludge decomposition.

In summary, the pyrolysis of sewage sludge can be viewed as environmentally tolerable alternative to the conventional sewage sludge utilization.

REFERENCES

1 P. L'Hermite and H. Ott, in K.-J. Thomé-Kozmiensky (Editor), Recycling International, Freitag Verlag, Berlin, 1982, p. 342.
2 P.T. Blickwedel and W. Schenkel, Korrespondenz Abwasser, 33 (1986) 680.
3 W. Kaminsky, J. Anal. Appl. Pyrolysis, 8 (1985) 439.
4 T. Augustin, W. Kaminsky and M. Krüger-Betz, Chem.-Ing.-Tech., 56 (1984) 47.
5 W. Kaminsky, A.B. Kummer and U. Bellmann, in D. Gleisberg (Editor), Phosphatentfernung und Klärschlammnutzung, Hoechst Symposium, Frankfurt, 1987, p. 156.
6 D. Bahrs and H. Albers, Korrespondenz Abwasser, 31 (1984) 994.
7 R. Kistler, F. Widmer and P. Brunner, Swiss Chem., 8, 2a (1986) 45.

Journal of Analytical and Applied Pyrolysis, 16 (1989) 37–48
Elsevier Science Publishers B.V., Amsterdam – Printed in The Netherlands

THERMAL DECOMPOSITION STUDIES OF SOME ORGANOPHOSPHORUS COMPOUNDS *

J.R. DURIG, DAVID F. SMITH * and D.A. BARRON

Department of Chemistry, University of South Carolina, Columbia, SC 29208 (U.S.A.)

(Received December 8th, 1987; accepted October 14th, 1988)

ABSTRACT

The thermal decomposition of a series of six organophosphorus compounds has been carried out using vapor phase pyrolysis–gas chromatography/Fourier transform infrared spectroscopy. These studies have been made with the samples diluted with both helium and dry air using a previously described closed system. The relative decomposition rates under both atmospheres along with the observed decomposition products are discussed. A comparison is made with a previously reported decomposition mechanism.

Fourier transform infrared spectroscopy; gas chromatography; organophosphorus compounds; pyrolysis; thermal decomposition.

INTRODUCTION

The wide range of chemical reactivity of organophosphorus compounds has resulted in their use in a wide variety of applications. Some common forms are used commercially as pesticides while other forms have many industrial uses. Applications of this nature result in the broad dispersion of these compounds and has resulted in some concern about their environmental effects. One concern is a plan to decompose and detoxify such materials by exposure to heated surfaces. With the toxicity and relatively long lifetime of these compounds, failure to completely destroy or detoxify them could result in some serious problems. There have been little published thermal decomposition studies on these compounds and, therefore, it is of interest to investigate the thermal stability, possible decomposition mechanisms and the decomposition products of some of these materials. Therefore, we

* Taken in part from the thesis of David F. Smith which will be submitted to the Department of Chemistry in partial fulfillment of the Ph.D. degree.

0165-2370/89/$03.50 © 1989 Elsevier Science Publishers B.V.

initiated some studies on the vapor phase decomposition of a number of these organophosphorus compounds to evaluate relative decomposition rates and to obtain information on their possible thermal decomposition mechanisms. The study was designed to investigate compounds with functional groups and chemical properties which can be considered as simulants of compounds which are known to have adverse biological activity while avoiding working directly with the highly toxic materials.

We were specifically interested in the vapor phase decomposition properties of these compounds in two different atmospheres, dry air and helium, over a range of temperatures from 200 °C to 1000 °C. These requirements, combined with the handling problems associated with these air sensitive and highly volatile compounds, provided for a challenging project. The results of this study are reported herein.

EXPERIMENTAL

A total of six different organophosphorus compounds were used in this study. Four of these were obtained commercially. Ethylphosphonic dichloride, $CH_3CH_2P(O)Cl_2$, and methylphosphonic dichloride, $CH_3P(O)Cl_2$, were purchased from Alfa Inorganics, Inc. The ethyldichlorophosphine, $CH_3CH_2PCl_2$, and ethyldimethylphosphine, $CH_3CH_2P(CH_3)_2$, were purchased from Organometallics, Inc. The dimethoxymethylphosphonate, $(CH_3O)_2(CH_3)P(O)$, was prepared by the reaction of $NaCO_3$ with $CH_3P(O)Cl_2$. Ethylphosphonic difluoride, $CH_3CH_2P(O)F_2$, was synthesized from the corresponding dichloride by direct reaction with freshly sublimed antimony trifluoride (SbF_3). All of the above compounds were purified by vacuum distillation on a cold column prior to use.

The gas chromatograph utilized for these experiments was a Hewlett Packard Model 5880A gas chromatograph. This instrument has been optimized for operation with capillary gas chromatographic (GC) columns and is equipped with both a flame ionization detector (FID) and a Digilab Fourier transform infrared (FTIR) lightpipe interface accessory. The GC/FTIR data acquisition system consists of a Digilab Model FTS-14C infrared interferometer with a liquid nitrogen cooled MCT detector. The interferometer is connected to a Data General Nova/4 minicomputer. All GC/FTIR spectra were collected at 6 cm^{-1} resolution from 3200 to 700 cm^{-1} with the lightpipe heated to 280 °C. An uncoated fused silica capillary return line from the lightpipe to the flame ionization detector provided the ability to collect simultaneous Grahm–Schmidt (GS) and FID chromatograms for all samples. The pyrolysis apparatus was a Chemical Data Systems Model 120 Pyroprobe equipped with a coil probe and a modified quartz insert. The interface between the pyrolysis probe and the gas chromatograph was a specially designed device for these studies and is

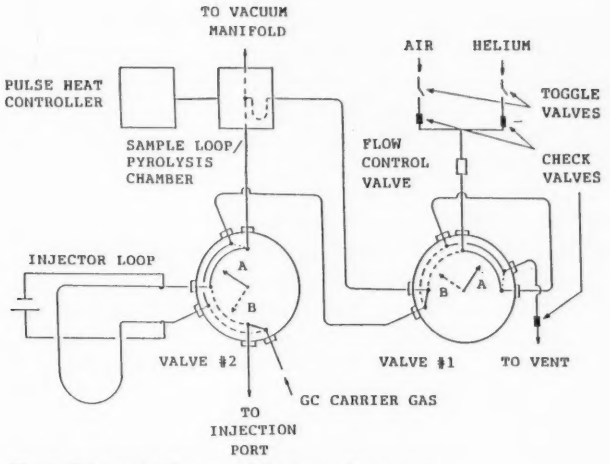

Fig. 1. Schematic diagram of the two valve system.

described in detail elsewhere [1]. This interface incorporates the Pyroprobe with a cold trap reinjection system, and allows reproducible offline sampling of volatile compounds through a vacuum manifold (Figs. 1 and 2). Pyrolysis of the compounds was by the procedure previously described. In all cases,

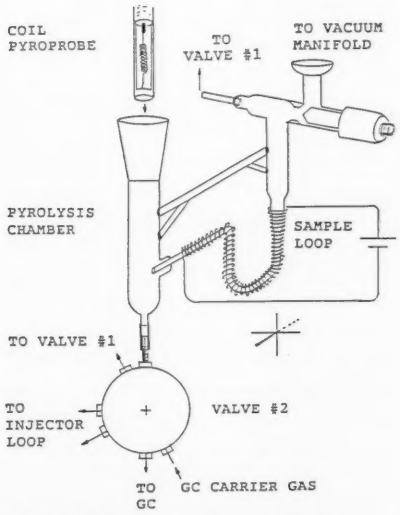

Fig. 2. Sample loop/pyrolysis chamber.

the dry air or helium carrier gas flow through the sample trap to the Pyroprobe was 10 ml/min. The probe was preheated to a preset temperature for 5 seconds prior to sample introduction and maintained at that temperature for a total of 20 seconds. Preset probe temperatures ranged from 200 to 1000 °C. Laminar flow through the Pyroprobe was assumed and the internal diameter of the quartz insert indicated a theoretical exposure time of approximately one second.

Oven conditions were the same for all of the compounds and are as follows: (1) hold 30 °C for 2 min; (2) ramp to 180 °C at 150 °C/min; (3) ramp to 240 °C at 25 °C/min; (4) hold for 5 min. The GC injection port was maintained at 300 °C and the pyrolysis interface was 175 °C. The GC split flow was 60 ml/min which created an injection flow velocity in the loop of approximately 120 cm/s. Helium was used as the carrier gas with a column flow velocity of 2.2 ml/min. Slower flow velocities were investigated but gave no significant increase in early peak resolution. The slower flows did, however, produce more peak tailing as a function of lightpipe volume, thus supporting the choice of the higher flow-rate.

A thick film non-polar column was used to perform the chromatographic separations (DB-1, 0.32 mm I.D., 5 μm film, J&W Scientific). More polar stationary phases suffered degradative damage from acidic pyrolysis products formed and the thick film helped resolve early eluting peaks at room temperature. Cryogenic cooling of the oven with liquid CO_2 was not possible since the large amounts of CO_2 required caused extreme baseline shifts in the GS chromatogram.

RESULTS AND DISCUSSION

Each of the compounds used in this study presented a unique set of problems in handling and sampling. Therefore, it is important to discuss our basic approach to sampling. In order to achieve comparable results, the experimental conditions such as flow-rate, exposure time and exposure temperature needed to be equivalent for each compound and reproducible for the series. Additionally, it was very important to introduce approximately equivalent sized samples into the Pyroprobe as it has been shown that large variations in sample size can result in poor reproducibility in terms of the type and relative amounts of pyrolysis products formed [2]. Although the vapor pressure of the different compounds varied significantly, it was still possible to collect samples consistently ranging from 50 to 150 μg. This was accomplished by varying the headspace over the sample into which the vapor phase was allowed to equilibrate, i.e. a compound with a low vapor pressure would be sampled in a large headspace volume and a compound with a higher vapor pressure would be sampled in a small headspace volume. Changes in headspace volume were controlled by open-

TABLE 1
Mean sample size as determined under non-pyrolysis conditions

Compound	Pyrolysis sample *		μg on column	Headspace ** volume (ml)	Sample size *** % R.S.D.
	μg	μmoles			
$CH_3P(O)Cl_2$	90	0.68	5.0	100	31.7
$CH_3CH_2P(O)Cl_2$	152	1.03	8.4	100	14.4
$CH_3CH_2P(O)F_2$	76.5	0.75	4.2	20	9.1
$(CH_3O)_2P(O)CH_3$	90.1	0.73	5.2	20	7.8
$CH_3CH_2P(CH_3)_2$	57.4	0.64	3.2	10	22.7
$CH_3CH_2PCl_2$	145	1.12	8.0	20	17.5

* Calculated from FID response.
** Estimated headspace volume.
*** Calculated from at least five standard sample runs.

ing and closing portions of a vacuum manifold. Sample sizes were monitored by FID response in non-pyrolysis runs. This sampling system follows the premise that, if a liquid sample size remains essentially constant along with temperature and internal pressure, then the equilibrium concentration of the vapor phase in a fixed headspace over the sample should also remain constant. Equilibrium sample temperatures below room temperature were maintained by placing the sample tube in a salt water and ice slush bath. It was expected that the vapor phase sample collection step would be rapid and quantitative. However, we found that this time varied considerably with sample vapor pressure.

In Table 1 is listed the average sample size introduced into the Pyroprobe as calculated from the FID response of non-pyrolysis experiments run periodically. The sizes are very similar ranging from 0.65 to 1.1 μmoles while the relative standard deviation runs from 8 to 32% which we believe is reasonable. These experiments under non-pyrolysis conditions were run intermittently during the data collection for each compound in order to ensure that consistent sample sizes were being delivered to the Pyroprobe.

The one exception to using the FID data for decomposition rate information was in the case of methylphosphonic dichloride in an air atmosphere. In this case, the pyrolysis products that were formed gave no FID response. The reduced FID response of the parent peak and the appearance of CO and CO_2 in the FTIR scans did indicate that decomposition was occurring. Therefore, for the decomposition under air of this one compound at 800 °C and 1000 °C, the ratio of the sum of total GS peak heights to the peak height of the pure compound was used to calculate the decomposition rate. While there is some precedent for this procedure [3], there is a potential major source on error which is due to the different absorptivities of the compounds (which effects peak height in the GS chromatogram). For methylphosphonic dichloride, however, this source of error is reduced since the primary decomposition product (CO_2) and the parent compound are

both strong infrared absorbers. The decomposition trends for this compound generated by the above method compare favorably with the rest of the data, but due to the nature of the technique we should consider data derived by it to be strictly qualitative and not quantitative.

No previous study on the gas phase pyrolysis of these organophosphorus compounds could be found. Work published by Bailey et al. [4] reports thermal decomposition data for trialkyl phosphine oxides. In this study the authors state that these compounds are generally extremely stable. Pyrolysis of ethyldimethylphosphine oxide at 600 °C shows only about a 50% decomposition while trimethylphosphine oxide shows almost no decomposition at 700 °C. The authors explain the difference in these two very similar compounds by the presence of a β-hydrogen on the ethyl side chain. From this series of compounds and a parallel study of the thermal decomposition of tertiary amine oxides [5] the authors speculate about a general decomposition mechanism:

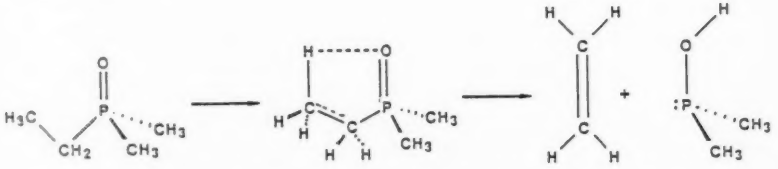

It is suggested that the decomposition takes place through elimination via a cyclic five-membered ring transition state. This would produce a trivalent phosphorus compound plus an unsaturated hydrocarbon.

The data presented in this study report qualitatively the relative stability of some 'similar' organophosphorus compounds and elaborate on the decomposition mechanism proposed by Bailey et al. [4], as it relates to this study.

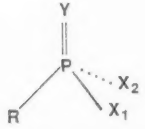

The series of compounds studied can be generally described by the above format where R = $-CH_3$ or $-CH_2CH_3$; Y = O or $2e^-$; X_n = –Cl, –F, or $-OCH_3$ with X_1 and X_2 not necessarily equal. In general, the decomposition mechanism suggested by Bailey et al. [4] seems valid for the compounds in this study containing a P–C bond. This can be seen by considering the major decomposition products of ethylphosphonic dichloride and ethylphosphonic difluoride. In each case the only significant hydrocarbon pyrolysis product is ethylene with a small amount of acetylene. Confirmation of the identity of these two products is provided by the FTIR spectrum (Fig. 3).

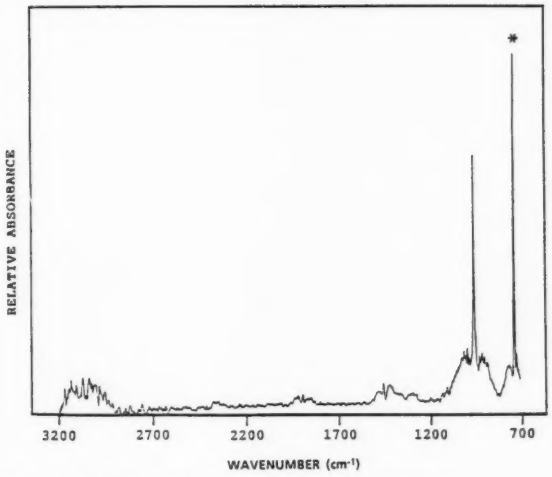

Fig. 3. Infrared spectrum of ethylene (* is acetylene).

These two products elute from the column almost simultaneously but the simplicity of their respective spectra allows their identification. In the case of dimethoxymethylphosphonate and methylphosphonic dichloride where R = $-CH_3$, both compounds were considerably more stable and would follow the postulated mechanism where the absence of β-hydrogens results in a more thermally stable structure.

Curiously, there are H atoms on the $-OCH_3$ group which could accommodate the 'β-hydrogen' decomposition theory. If it held for the methoxy group, the major product would be formaldehyde by:

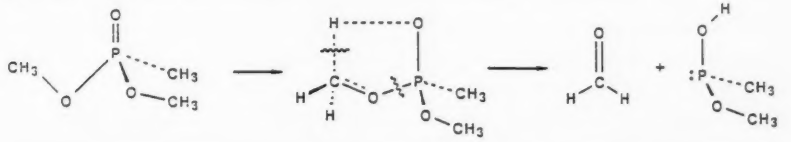

However, the major product is methanol, CH_3OH, indicating the cleavage of the P–O bond is through some other mechanism. This is further supported by the much higher thermal stability of the dimethoxymethylphosphonate molecule.

None of the phosphorus decomposition products were conclusively identified. Polymerization of the decomposition products was common with large deposits of high boiling liquids and solids evident in the glassware system. This would also follow from the suggested mechanism which predicts the formation of unstable phosphinic or phosphonic acids. These high boiling acidic compounds would not be analyzable by GC.

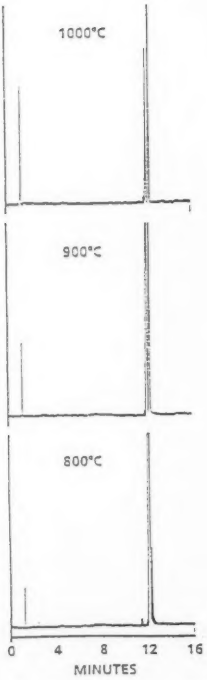

Fig. 4. GS pyrograms of ethylphosphonic dichloride at three different pyrolysis temperatures.

Representative GS and FID chromatograms for ethylphosphonic dichloride are shown in Figs. 4 and 5. Fig. 4 shows the growth of the decomposition product peaks (1.22 and 12.33 min) with increasing pyrolysis temperature. A comparison of FID (Figs. 5A and 5C) and GS (Figs. 5B and 5D) chromatograms is given in Fig. 5, for runs in which there was no pyrolysis (Figs. 5A and 5B) and a pyrolysis run at 1000 °C (Figs. 5C and 5D).

Ethylphosphonic dichloride was unusual in that it was the only compound studied that had a second major decomposition product directly related to the degree of decomposition. This decomposition product, whose spectrum is shown in Fig. 6, elutes at 12.33 min and probably does not contain any carbon as there are no analogous peaks in the FID trace (Figs. 5C and 5D). Unfortunately, we have been unable to identify this compound from its infrared spectra.

The compounds under investigation show some definite trends in thermal stability which can be related to the decomposition mechanism discussed as well as to the oxidation state of the phosphorus and the bond energies of the different side groups. Graphs are shown for each of the compounds studied (Figs. 7 and 8). Two lines are drawn on each, one for pyrolysis in helium and

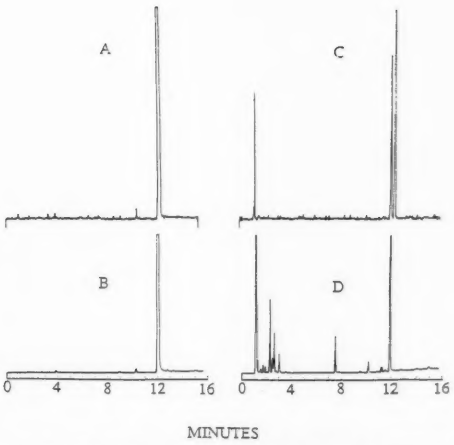

Fig. 5. FID (A and C) and GS (B and D) chromatograms of ethylphosphonic dichloride for runs: (A and B) with no pyrolysis and (C and D) with pyrolysis at 1000 °C.

one for decomposition in dry air. These plots depict the calculated percent of decomposition versus the Pyroprobe temperature used for each test. As previously described, the decomposition rate for each was calculated from the response of the flame ionization detector of the gas chromatograph

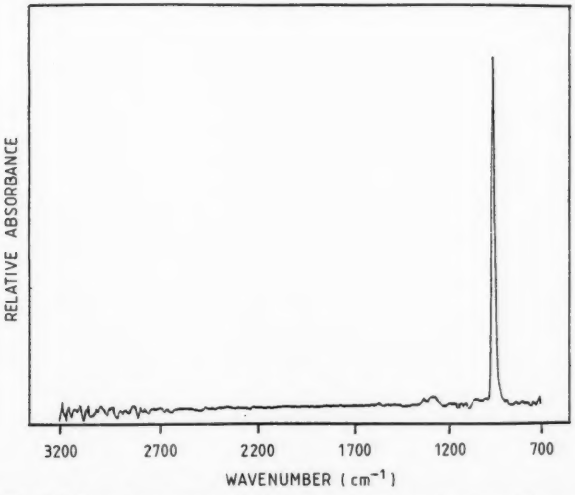

Fig. 6. Infrared spectrum of unknown phosphorus decomposition product from pyrolysis of ethylphosphonic dichloride.

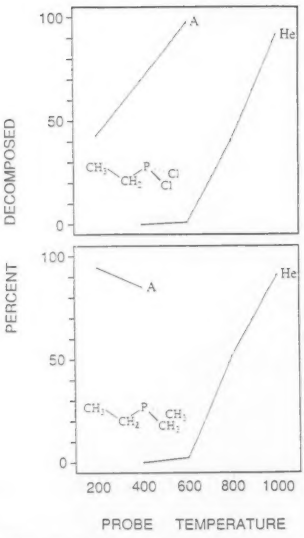

Fig. 7. Percent decomposition versus temperature of two trivalent phosphine compounds (A = decomposition under dry air; He = decomposition under helium).

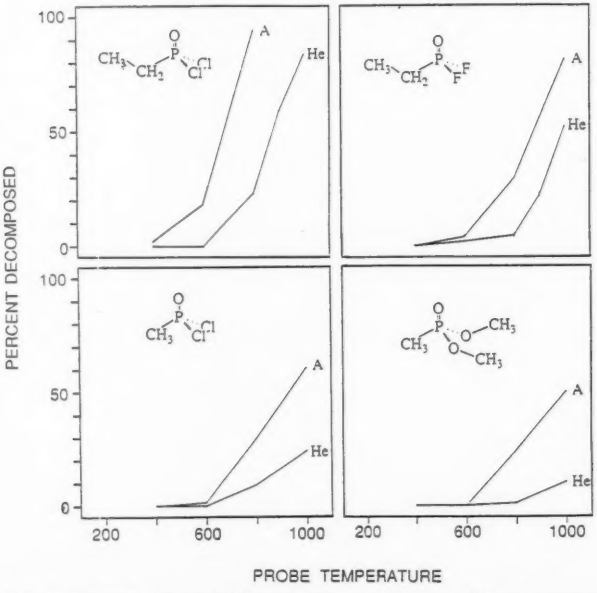

Fig. 8. Percent decomposition versus temperature of four pentavalent phosphine oxide compounds (A = decomposition under dry air; He = decomposition under helium).

TABLE 2

Bond energies of some phosphorus bonds *

Bond	Energy (kJ/mol)
P–F	490
P–Cl	326
P–C	264
P–O	335 (?)
P=O	544

* Taken from ref. 6.

except where noted. All of the data points were averaged for each temperature and the lines connect the mean values.

It is readily evident that the two compounds in which the phosphorus is in the oxidation state of three, ethyldichlorophosphine and ethyldimethylphosphine (Fig. 7), are less stable than the four pentavalent phosphine oxides (Fig. 8). However, both the these compounds exhibit reasonably high thermal stability under helium. Under air the ethyldichloride phosphine is the more stable of the two compounds. The higher degree of stability could be attributed to the greater bond strength of the P–Cl bond (Table 2). In both cases, the compounds are not actually decomposed, but rather are converted to their respective phosphine oxides.

The other compounds demonstrated extremely high relative stabilities both in dry air and helium. The plots seem to indicate higher degrees of stability than the trialkyl phosphine oxides reported by Bailey et al. [4]. None of the same compounds were tested because of the lack of volatility or availability so direct correlation is difficult.

The relative stability appears to be related to the presence of a P–C side chain containing a β-hydrogen as well as by the relative strength of the other side groups. This is demonstrated by both the ethylphosphonic dichloride and the ethylphosphonic difluoride where both are less stable than the remaining two compounds in both air and helium atmospheres. Between the two compounds, the difluoride is the more stable compound. A comparison of the relative bond strengths from Table 2 shows the P–F bond to be much stronger than the P–Cl bond which probably accounts for the difference in the stability of the two compounds.

The remaining two compounds, dimethylmethylphosphonate and methylphosphonic dichloride, demonstrated the highest degree of stability of the six compounds studied. Following the same reasoning, there are no multicarbon chains bonded directly to the phosphorus atom so no five-membered intermediate can be formed. Also, the two other substituents have either a P–Cl or a P–O bond with the same relative bond strengths. Within experimental error both compounds have about the same stability in air and helium and fit into the general trend of all of the compounds tested.

CONCLUSIONS

All of the compounds of interest in this study were somewhat air sensitive. Consequently, it was desirable to work with very small quantities of these materials in a closed system to avoid atmospheric decomposition. The system developed for use in this work was the best compromise to meet the requirements of the experiment with existing equipment. It is not suggested that this system simulated an industrial incinerator or hot manifold but, rather, was devised to provide basic decomposition data which would yield some insight into the overall stability of these materials and into problems which might be associated with handling and disposal of these types of compounds.

It can be concluded from this study that the pentavalent compounds exhibit high thermal stability under both dry air and inert atmospheres. The trivalent compounds also exhibit high stability in an inert atmosphere but are readily oxidized in air to their respective phosphine oxide.

Although no decomposition mechanism was apparent, some trends were observed. Of the compounds with alkyl side chains, those with more than one carbon appear to be less stable than those with only a methyl group and probably yield unsaturated hydrocarbon products under pyrolytic conditions. In the case of P–O–R moieties, the side chain product is more likely to be the respective alcohol. The fate of the phosphorus-containing moiety is unclear from the observed data although the formation of polyphosphorus compounds appears to be favored. Under oxidizing conditions, the formation of expected hydrocarbon combustion products such as CO_2, CO and H_2O was observed along with increased evidence of acids such as HCl and HF.

ACKNOWLEDGEMENTS

The authors gratefully acknowledge the financial support of this research by AVCO Lycoming, Inc.

REFERENCES

1 D.F. Smith and J.R. Durig, J. Anal. Appl. Pyrolysis, 13 (1988) 63.
2 I. Ericsson, J. Anal. Appl. Pyrolysis, 8 (1985) 73.
3 D.T. Sparks, R.B. Lam and T.L. Isenhour, Anal. Chem., 54 (1982) 1922.
4 W.J. Bailey, W.M. Nuir and F. Marktscheffel, J. Org. Chem., 27 (1962) 4404.
5 A.C. Cope, N.A. LaBel, H.H. Lee and W.R. Moore, J. Am. Chem. Soc., 79 (1957) 4720.
6 J. Huheey, Inorganic Chemistry, Principles of Structure and Reactivity, Harper & Row, New York, 1983.

Journal of Analytical and Applied Pyrolysis, 16 (1989) 49–55
Elsevier Science Publishers B.V., Amsterdam – Printed in The Netherlands

SIMULTANEOUS DETERMINATION OF NATURAL AND STYRENE–BUTADIENE RUBBER TIRE TREAD PARTICLES IN ATMOSPHERIC DUSTS BY PYROLYSIS–GAS CHROMATOGRAPHY

YONG-KEUN LEE * and MAN GOO KIM *

Department of Chemistry, College of Science, Yonsei University, Seoul 120-749 (Korea)

KYU-JA WHANG

Department of Manufacturing Pharmacy, College of Pharmacy, Sookmyung Women's University, Seoul 140-132 (Korea)

(Received August 26th, 1988; accepted November 16th, 1988)

ABSTRACT

A method for simultaneous determination of natural rubber (NR) and styrene–butadiene rubber (SBR) tire tread particles in atmospheric dust is described. Particulate rubbers are pyrolyzed at 740 °C for five seconds in a Curie-point pyrolyzer. The resulting pyrolyzates are separated and detected by a gas chromatograph equipped with dual flame ionization detectors. Among several pyrolysis products, isoprene and styrene are chosen as indicator compounds for NR and SBR, respectively. The method is applied to a suite of atmospheric dust samples collected in Seoul, Korea by an Andersen sampler and some analytical results are presented.

Atmospheric dust; gas chromatography; natural rubber; polymers; pyrolysis; styrene–butadiene rubber; tire tread.

INTRODUCTION

Pyrolysis–gas chromatography (Py–GC) has been successfully applied to the characterization of rubber components for many years [1–4]. Since Thompson et al. [5] reported evidence of tire-wear debris in the sweepings from tunnel and parking garages, several workers [6–8] have reported various analytical methods for determination of rubber particles in atmo-

* Present address: Department of Applied Chemistry, Faculty of Science and Technology, Keio University, Yokohama 223, Japan.

0165-2370/89/$03.50 © 1989 Elsevier Science Publishers B.V.

spheric dusts. The amount of rubber loss from automobile tires has been also estimated from the number of registered vehicles and tire sales to be about 90 mg/km due to vehicle motion [9]. According to Pierson and Brachaczek [10] and Brown et al. [11], less than 5% of the total tire wear becomes airborne, but this amount is equivalent to 20% of the total airborne particulate matter exhausted from internal combustion engines burning regular gasoline.

Penetration and deposition of the airborne particulates in man's respiratory tract is a subject of aerodynamics [12]. The toxicity of a particulate pollutant is thus determined not only by its concentration and chemical composition, but also by the particle size of the pollutant.

This paper presents details of an analytical procedure for the simultaneous determination of natural rubber (NR) and styrene–butadiene rubber (SBR) tire tread particles in atmospheric dusts by Py–GC. The performance of the procedure and its application to a suite of urban atmospheric dust samples are discussed. In addition, the measured concentrations of total rubber particles and those particles which are small enough to penetrate into the alveoli are presented.

EXPERIMENTAL

Atmospheric dust sampling

Atmospheric dust samples were collected from the street in front of Yonsei University Campus, Seoul, Korea using an Andersen sampler (Kanomax, Model 3351) which was run for 10 days for each sample. We chose polyester filters (diameter: 80 mm; thickness: 0.075 mm) which enabled us to remove the dusts from the filter easily and thus reduce the relative error when weighing the samples. The collected airborne dust was kept in a desiccator for at least two days, where relative humidity was maintained at 50% using calcium chloride solution. In order to remove organic contaminants originating from asphalt particles or vehicle exhaust, the samples were rinsed with benzene–ethanol (4 : 1, v/v) in an ultrasonic bath for 30 seconds. After being dried at room temperature, the samples were weighed on a semi-microbalance (Mettler Model HK60).

Analytical standards of NR and SBR tire tread rubbers were prepared following the recipes which are given in Table 1.

Pyrolysis–gas chromatographic conditions

A Curie-point pyrolyzer (Japan Analytical Industries, Model JHP-2) was directly coupled to a gas chromatograph (Hitachi Model 163) equipped with dual flame ionization detectors. Atmospheric dust samples (0.5–1.0 mg)

TABLE 1

Chemical composition of standard tire tread rubber [a]

Passenger car		Truck and bus	
SBR (OE) [b]	60 [c]	NR	80 [c]
BR (OE)	40	BR	20
ZnO	3	ZnO	3
Stearic acid	2	Stearic acid	2
Carbon black	70	Carbon black	50
Process oil	10	Process oil	8
Antioxidant 3C [d]	1.5	Antioxidant 6C [e]	1.7
Antioxidant RD [f]	1	Antioxidant RD [f]	0.8
Vulcanization		Vulcanization	
Accelerator CZ [g]	0.4	Accelerator MOR [h]	0.8
Accelerator TT [i]	0.8		
Sulphur	2	Sulphur	2

[a] Provided by Han Kook Tire Manufacturing Co., Seoul, Korea.
[b] Oil extended.
[c] Parts by weight.
[d] N-Isopropyl-N′-phenyl-*p*-phenylenediamine.
[e] N-(1,3-Dimethylbutyl)-N′-*p*-phenylenediamine.
[f] Poly(2,2,4-trimethyl-1,2-dihydroquinoline).
[g] Cyclohexylbenzothiazolylsulphenamide.
[h] N-Oxydiethylene-2-benzothiazolylsulphenamide.
[i] Tetramethylthiuram disulphide.

were pyrolyzed at 740 °C for five seconds. The temperatures of the pyrolyzer unit and the tube connecting pyrolyzer and gas chromatograph were maintained at 100 °C and 200 °C, respectively. The analytical column was a stainless steel tube (6 m × 3 mm I.D.) which was packed with 15% Apiezon grease L supported on 60–80 mesh Uniport B.

The column temperature was maintained at 55 °C for the first seven minutes and programmed to increase at a ramp rate of 20 °C/min up to 160 °C. The nitrogen carrier gas flow-rate was 20 ml/min (Table 2).

TABLE 2

Pyrolysis–gas chromatographic conditions

Column	:	Stainless steel, 6 m × 3 mm I.D.
Packing	:	15% Apiezon grease L on Uniport B, 60–80 mesh
Column temperature	:	Initial: 55 °C Final : 160 °C Rate : 0 °C for 8 min; 20 °C/min
Carrier gas	:	Nitrogen, 20 ml/minute
Detector	:	Flame ionization
Pyrolysis	:	740 °C for 5 seconds

RESULT AND DISCUSSION

Column selection

The column was selected in such a way that simultaneous quantification of the isoprene and styrene peak could be achieved. A non-polar packing material is needed for good separation of isoprene, while a high-temperature packing material is necessary for good separation of styrene. The packing materials tested in this work were Apiezon grease L, TCP, SE-30, OV-1, OV-17, DC-200, DC-550, PEG-20M and FFAP. Among them, a 6-m-long column containing 15% Apiezon grease L showed the best separation performance.

Pyrolysis temperature

Seven kinds of pyrofoils (358 °C, 445 °C, 590 °C, 670 °C, 740 °C, 920 °C and 1040 °C) were tested to observe the effect of temperature on the pyrolysis characteristics of standard tire tread rubbers. The functional relationships between the production yields of isoprene, styrene and dipentene and pyrolysis temperature are summarized in Fig. 1. At 358 °C, no pyrolyzates were produced. Yields of both isoprene and styrene were highest at 740 °C, while the maximum dipentene production was observed at 445 °C. Thus, only the 740 °C pyrofoil was used for routine sample analysis.

Quantification of tire tread rubbers

For quantitative determination of tire tread rubbers, the pyrograms of samples were compared with those of standard tire tread rubbers. Typical

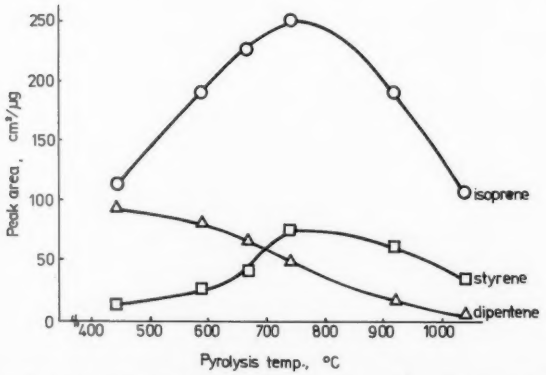

Fig. 1. Effect of pyrolysis temperature on pyrolysis products of the tire tread rubber.

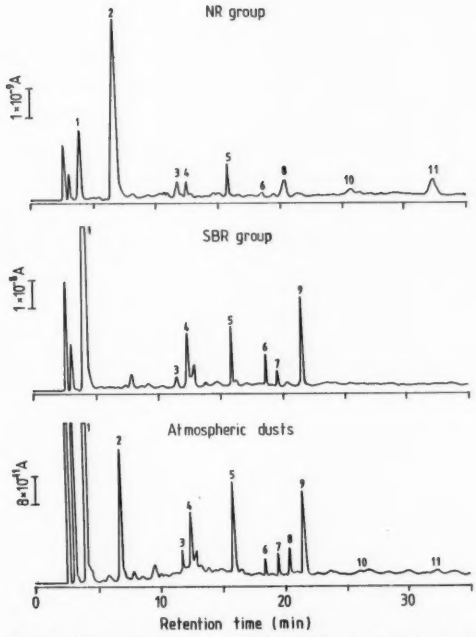

Fig. 2. Pyrograms of tire tread rubbers and atmospheric dusts. Peaks: 1 = 1,3-butadiene; 2 = isoprene; 3 = C_6H_{10}; 4 = benzene; 5 = toluene; 6 = vinylcyclohexene; 7 = ethylbenzene; 8 = xylene; 9 = styrene; 10 = $C_{10}H_{16}$; 11 = dipentene.

pyrograms of the SBR group and NR group tire treads, and atmospheric dusts trapped in the fourth stage of the Andersen sampler, are shown in Fig. 2. The styrene peak was used for the determination of SBR group tire rubber and the isoprene peak for the determination of NR group tire rubber. Theoretically, dipentene can also be used for NR group determination but, in this work, the amounts of NR group rubber in the dust samples were too small to produce sufficient dipentene. The reproducibility of the pyrolyzate formation was investigated by varying the particle size from 14 to 100 mesh.

TABLE 3

Reproducibility of the pyrolysis–gas chromatography *

Tire tread rubber	SBR (%)	NR (%)	R.S.D. (%) $n = 5$
Passenger car	31.5	0	9.7
Bus and track	0	47.6	8.3

* Based upon peak area integration.

TABLE 4

Size distributions of atmospheric dust and rubber components

Sampling period: January 13–22, 1987.

Stage number	Particle size range (μm)	Sample weight (mg)	Sample conc. ($\mu g/m^3$)	SBR ($\mu g/m^3$)	NR ($\mu g/m^3$)	Total rubber ($\mu g/m^3$)	Abundance ratio (%)
0	9.0–10	18.5	58.6	1.52	0.19	1.71	2.91
1	5.8– 9.0	2.24	7.09	0.11	0.01	0.12	1.69
2	4.7– 5.8	1.16	3.67	0.03	0.004	0.03	0.82
3	3.3– 4.7	4.89	15.5	0.12	0.01	0.13	0.84
4	2.1– 3.3	1.04	3.29	0.02	0.001	0.02	0.61
5	1.1– 2.1	5.77	18.3	0.10	0.01	0.11	0.60
6	0.7– 1.1	8.56	27.1	0.05	0.01	0.06	0.22
7	0.4– 0.7	7.59	24.0	0.03	0.004	0.03	0.13
Total		49.8	157.5	1.98	0.23	2.21	1.40

It appeared that the reproducibility was strongly related to the particle size. The best reproducibility was obtained when 50–100 mesh particles were used (Table 3). In the pyrograms SBR group (styrene peak) and NR group (isoprene peak) were 74 ± 5.2 area unit/μg and 380 ± 20.8 area unit/μg, respectively.

Particle size distribution of rubber components

Atmospheric dust samples were collected using the Andersen sampler which was operated continuously for 10 days in March 1987. The samples were analyzed for NR and SBR rubbers and weighed at each stage. As summarized in Table 4, it can be seen that the mass size distribution of rubber components is not bimodal, but unimodal. This implies that almost all of the rubber particulates were produced from automobile tire tread by mechanical abrasion.

It is generally known that atmospheric dusts trapped below the sixth stage of an Andersen sampler can penetrate into alveoli [13]. It appeared that 32.4% of the total atmospheric dust could penetrate into alveoli, of which the rubber components formed 0.2%. The concentrations of NR group and SBR group tire tread were 0.23 $\mu g/m^3$ and 1.98 $\mu g/m^3$, respectively.

ACKNOWLEDGEMENTS

This work was supported by a grant from the Korea Science and Engineering Foundation in 1986. Standard tire tread rubbers were provided by Han Kook Tire Manufacturing Company, for which the authors are grateful.

REFERENCES

1 A. Krishen, Anal. Chem., 44 (1972) 494.
2 A. Krishen and R.G. Tucker, Anal. Chem., 46 (1974) 29.
3 A. Krishen and R.G. Tucker, Rubber Chem. Technol., 48 (1975) 97.
4 L. Trojer and I. Ericsson, J. Chromatogr. Sci., 16 (1978) 345.
5 R.N. Thompson, C.A. Nau and C.H. Lawrence, Am. Ind. Hyg. Assoc. J., 27 (1966) 488.
6 J.A. Cardina, Rubber Chem. Technol., 46 (1973) 232.
7 S. Toyosama, Y. Umezawa, K. Ikoma, Y. Kameyama, T. Shirai and S. Yanagisawa, Bunseki Kagaku, 26 (1977) 38.
8 S. Higashi, H. Inoue, T. Shirai and S. Yanagisawa, Taiki Osen Gakkaishi, 16 (1981) 163.
9 M.L. Dannis, Rubber Chem. Technol., 47 (1974) 1011.
10 W.R. Pierson and W.W. Brachaczek, Rubber Chem. Technol., 47 (1974) 1275.
11 J.H. Brown, K.M. Cook, F.G. Ney and T. Hatch, Am. J. Public Health, 40 (1950) 450.
12 G.J. Harper and J.D. Morton, J. Hyg., 51 (1953) 372.
13 Andersen Sampler Manual (Model 3351, Mark II), Kanomax, Japan.

Journal of Analytical and Applied Pyrolysis, 16 (1989) 57–73
Elsevier Science Publishers B.V., Amsterdam – Printed in The Netherlands

MECHANISM AND KINETICS OF THERMOLYSIS OF ETHERS MODELLING THE OXYGEN–METHYLENE 'BRIDGE' BONDS IN COAL ORGANIC MATTER

V.Yu. KOROBKOV *, E.N. GRIGORIEVA, V.I. BYKOV and I.V. KALECHITZ

Institute of High Temperatures, Academy of Sciences of the USSR, Izhorskaya Street, 13/19, Moscow 127412 (U.S.S.R.)

(Received June 24th, 1988; accepted October 12th, 1988)

ABSTRACT

The kinetics of the thermolysis of 19 ethers under hydrogen pressure in excess tetralin have been studied. The data obtained make it possible to relate the reactivity and the mechanism of transformations of the 'bridge' bonds to the structure of the bridge itself and of the end groups and to the presence of substituents in these groups. For the first time it has been shown that correlation analysis can be used to predict the reactivity of the corresponding model compounds.

Coal organic matter; ethers, aromatic; kinetics, reaction; pyrolysis; thermolysis.

INTRODUCTION

At present it is widely accepted that coal organic matter (COM) consists of aromatic clusters connected by 'bridge' bonds in three dimensions [1,2]. The 'bridge' bonds contain methylene groups and can comprise heteroatoms, among which oxygen is the most widespread.

The study of the mechanism and kinetics of the thermolysis of oxygen–methylene 'bridges' for simple substances that model the structure of coal is of great interest. This is due to the fact that such 'bridges' are mostly reactive and, hence, any thermally induced transformation of COM most likely begins with the scission of the 'bridges'. In a recent paper [3] it was shown that the degree of liquefaction of 20 different coals is related to the intensity of the peaks in field ionization mass spectra corresponding to substances formed as a result of the destruction of the oxygen–methylene 'bridges'.

However, the study of the mechanism and kinetics of thermolysis of model ethers has so far not been systematic and has been confined to a

0165-2370/89/$03.50 © 1989 Elsevier Science Publishers B.V.

small number of compounds. Besides, the experimental conditions used were very often far from those of the liquefaction process (for instance, pyrolysis in sealed tubes [4–6]) and the reactivities of the compounds were compared on the basis of degrees of conversion [7–16]. However, a systematic comparison turned out to be impossible, since the conditions were not identical in different experiments.

Evidently, measurement of the kinetic constants under conditions that minimize secondary conversions might give the most reliable ideas about the dependence of the reactivity on the structure. However, the kinetics of thermolysis was studied only for several ethers (dibenzyl [6,17–21], benzylphenyl [15], and phenylethylphenyl [6,22]) under conditions that were not always comparable. Different experimental procedures resulted in different, sometimes quite opposed, interpretations of the mechanism. For instance, it was proposed that thermolysis of dibenzyl ether follows only the concerted mechanism (intramolecular rearrangement [21]), that the concerted [17] or chain radical [5,6] mechanism predominates, or that only the chain mechanism occurs [20].

The brief review given above shows that additional systematic investigations are required in order to draw reliable conclusions about the effect of the structure of oxygen–methylene 'bridges' on the mechanism and rate of thermolysis.

Up to the present time we have studied the kinetics of thermolysis of 19 compounds, the major part of which have been used for the first time as the subject of investigation. The measurement of the kinetic parameters of thermolysis of such a great number of compounds and the measurement of a concentration change of intermediates allowed us to study more thoroughly the effect of the structure of oxygen–methylene 'bridges' themselves, the structure of the end groups (clusters), and the presence of the substituents in them. It proved to be possible to calculate the rates of thermolysis of similar structures with the aid of the regularities found and hence to evaluate the thermolysis rates of the fragments of real COM.

EXPERIMENTAL

All the experiments were conducted in a specially designed autoclave, the introduction of the substrate occurring at the instant of time recording and sampling during the course of the experiment. Hydrogen pressure in the autoclave was 8.5 MPa and tetralin was used in a tenfold weight excess. The temperatures were chosen in such a way as to ensure the reliability of the kinetic measurements. For the sake of comparison the rate constants were recalculated for 350 °C (heating of the paste) and 410 °C (coal liquefaction) by the Arrhenius equation. Concentrations of all substances were determined by gas–liquid chromatography on an LXM-8MD-5 instrument

with a flame-ionization detector and temperature-programmed capillary columns (SE-30, 30 and 50 m). The reaction products were identified by chromatography/mass spectrometry on an LKB-2091 instrument. The details of the experiment are described in refs. 23 and 24.

RESULTS AND DISCUSSION

The effect of the 'bridge' structure in $C_6H_5(CH_2)_n - O-(CH_2)_m-C_6H_5$

The results are summarized in Table 1. Diphenyl ether is not included since it was stable at 410 °C. Thus, when $n = m = 0$ the 'bridge' is most stable, but introduction of one methylene group results in the highest reactivity. A further increase of the number of methylene groups decreases the reactivity.

The order of reactivity coincides mainly with a change in the C–O bond strength and only at 410 °C is dibenzyl ether ($n = 1$, $m = 1$) below benzylethylphenyl ether (Table 2). This may be due to the different mechanism, which is supported by the lowest activation energy of thermolysis of dibenzyl ether and a negative value of a change in activation entropy (Table 1). This confirms a possible intramolecular rearrangement proposed in refs. 17 and 21:

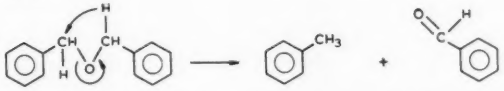

We have shown that conversions of dibenzyl ether and secondary conversions of benzaldehyde supported by the experiments with benzaldehyde [23] are best described by the following scheme:

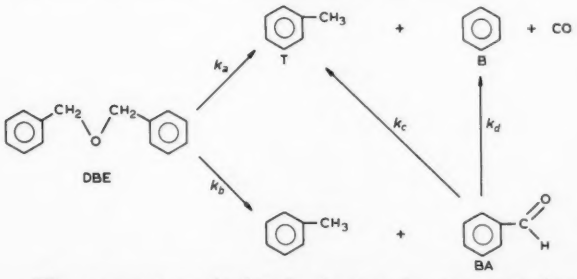

The computer-calculated changes in concentrations of dibenzyl ether (DBE), benzaldehyde (BA), toluene (T) and benzene (B) agree well with the experimental data and are plotted in Fig. 1. Mean square deviations of theoretical and experimental concentrations within the whole temperature range (350–410 °C) did not exceed ± 5%. Table 3 lists the reaction rate

TABLE 1

Kinetic parameters of thermolysis of ethers of the general formula $C_6H_5(CH_2)_n$

Compound	Rate constant k (min^{-1}) at T, °C				
	300	325	350	380	410
Benzylphenyl ether $n=0$; $m=1$	$(6.2\pm0.3)\times10^{-3}$	$(3.0\pm0.2)\times10^{-2}$	$(2.1\pm0.2)\times10^{-1}$	–	7.4 *
Phenylethyl-phenyl ether $n=0$; $m=2$	–	$(2.0\pm0.1)\times10^{-3}$	$(1.6\pm0.2)\times10^{-2}$	$(1.0\pm0.2)\times10^{-1}$	5.3×10
Dibenzyl ether $n=1$; $m=1$	–	–	$(7.7\pm0.6)\times10^{-3}$	$(1.8\pm0.3)\times10^{-2}$	$(5.8\pm1.$ $\times10^{-2}$
Benzylethyl-phenyl ether $n=1$; $m=2$	–	–	$(3.7\pm0.3)\times10^{-3}$	$(1.6\pm0.5)\times10^{-2}$	$(1.3\pm0.$ $\times10^{-1}$
Diethylphenyl ether $n=2$; $m=2$	–	–	$(7.6\pm0.4)\times10^{-4}$	$(4.4\pm0.4)\times10^{-3}$	$(2.4\pm0.$ $\times10^{-2}$

* Extrapolated by the Arrhenius equation.

$(CH_2)_n$–O–$(CH_2)_mC_6H_5$ (8.5 MPa, mass ratio of ether to tetralin = 1 : 10)

	Half-life (min) at T, °C		Activation parameter			
0	350	410	E_a (kcal/mol)	ΔS^* (e.u.)	ΔH^* (kcal/mol)	log A (min)
*	3.3	0.094	50.2	+15.6	49.0	16.93
3×10^{-1} *	43.3	1.3	50.2	+10.3	49.0	15.79
$8\pm1.0)\ 10^{-2}$	90.0	12.0	28.7	−25.8	27.4	7.94
$3\pm0.2)\ 10^{-1}$	187.3	5.3	50.5	+7.8	49.2	15.28
$4\pm0.6)\ 10^{-2}$	911.8	28.9	48.7	+1.8	47.4	13.97

TABLE 2

Bond strengths and reactivities of ethers

n and *m*	Half-life (min)		C–O bond energy (kJ/mol)
	350 °C	410 °C	
0 and 1	3.3	0.094	221 ± 20
0 and 2	43.2	1.3	220 ± 10
1 and 1	90.0	12.0	286 ± 10
1 and 2	187.3	5.3	310
2 and 2	911.8	28.9	330 ± 20
0 and 0	–	> 40 hours	

constants and the activation parameters for the second Scheme. High values of the activation energy and the change in the activation entropy for the reaction DBE → T + B indicate the probability of bond breaking and possibility of the radical mechanism. By contrast, low values of these parameters for the reaction DBE → T + BA support the idea that, in the course of conversions, no complete breaking of the chemical bonds occurs, i.e. intramolecular rearrangement following the concerted mechanism is more likely. The latter reaction is the main one for DBE transformation both at 350 and 410 °C. Since the activation energy of DBE is small, these facts determine the place of dibenzyl ether among the other ethers. Rearrangements similar to that described above are not observed in the case of other

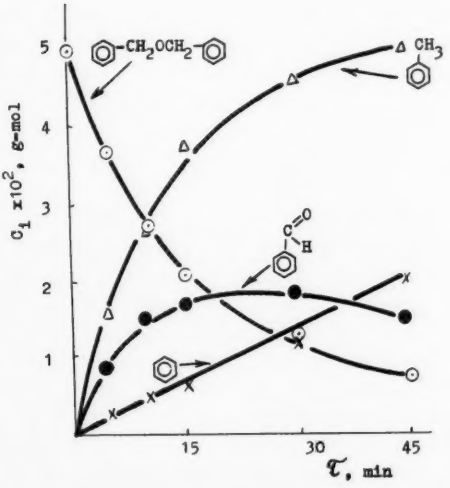

Fig. 1. Computed kinetic curves of dibenzyl ether thermolysis at 410 °C. The experimental data are shown by dots.

TABLE 3

Rate constants and activation parameters of the reactions in the second scheme (above)

	DBE → T + B	DBE → T + BA	BA → T	BA → B
$K_{350} \times 10^{-2}$ min^{-1}	0.084	0.730	1.030	0.007
$K_{380} \times 10^{-2}$ min^{-1}	0.448	1.375	1.380	0.065
$K_{410} \times 10^{-2}$ min^{-1}	1.900	3.980	1.500	1.300
E_a, kcal/mol	44.0	21.1	5.2	73.7
log A, min^{-1}	12.34	6.32	−0.16	21.7
$\Delta S^{\neq}$, e.u.	−5.6	−33.2	−62.8	+41.0

ethers. The reaction of benzylphenyl ether is accompanied by a partial rearrangement into benzylphenol:

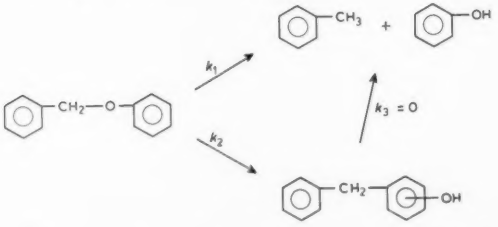

The calculations and the experiments with *o*-benzylphenol have shown that benzylphenols do not undergo transformations under the experimental conditions. The value of k_1 is 5.1×10^{-3}, 2.4×10^{-2}, and 1.6×10^{-1} at 300, 325, and 350 °C, respectively; the value of k_2 is 1.1×10^{-3}, 6.0×10^{-3}, and 5.5×10^{-2} for the same temperatures, i.e. k_2 is approximately 4 times smaller than k_1.

The activation energies of thermolysis of all ethers (except dibenzyl ether) are high and close to 48.7–50.5 kcal/mol, which points to direct homolysis of the C–O bond and to an insignificant role of the chain reactions in excess tetralin.

In addition to the rearrangement product, only toluene and phenol are formed in equimolar amounts from benzylphenyl ether (Fig. 2a); from phenylethylphenyl ether, ethylbenzene and phenol are obtained also in equimolar amount (Fig. 2b) with traces of styrene, the product of inner stabilization of the ethylphenyl radical. Thermolysis of benzylethylphenyl ether (Fig. 3a) yields toluene, ethylbenzene and benzene in a ratio of about 12 : 4 : 1. A predominant amount of toluene indicates that cleavage of the bond of oxygen with the benzyl radical is preferred and that decarbonylation of the $C_6H_5CH_2CH_2O\cdot$ radical occurs by analogy with the benzyloxy radical in the case of DBE. On the other hand, the formation of ethylbenzene and toluene in non-equimolar amounts show that $C_6H_5CH_2CH_2O\cdot$ radicals is partially reduced to ethylbenzene.

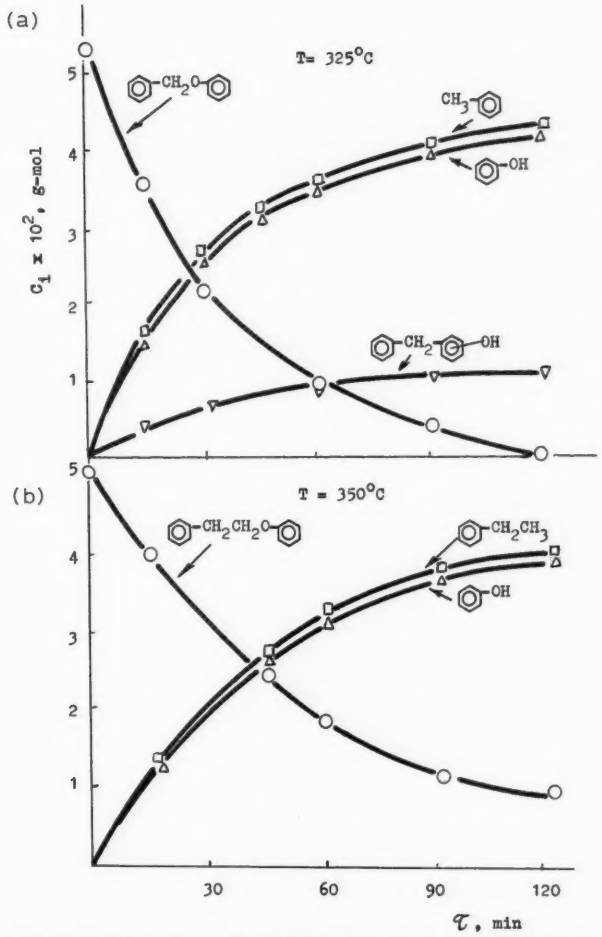

Fig. 2. Kinetic curves of thermolysis of (a) benzylphenyl and (b) phenylethylphenyl ethers.

Decarbonylation of $C_6H_5CH_2CH_2O\cdot$ is also confirmed by the composition of the products of diethylphenyl ether thermolysis (Fig. 3b): ethylbenzene and toluene are present almost in equimolar amounts.

The effect of the structure of the end groups in $ArCH_2OX$ and $ArCH_2OCH_2Ar'$ structures

The kinetic parameters are given in Table 4.

It can be seen from the table that the substitution of cyclohexyl for phenyl decreases the thermolysis rate by 4–7 times at 350–410 °C, i.e. the

TABLE 4

Kinetic parameters of thermolysis of ethers with different end groups (8.5 MPa, tetralin: substrat

Ether	Rate constant k (min^{-1}) at T, °C				
	200	225	250	275	300
Ar–CH_2–O–X structure					
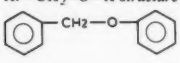	–	–	–	–	(6.2 ×10
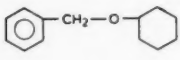	–	–	–	–	(2.1 ×10
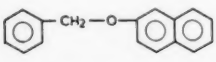	–	–	–	$(4.4 \pm 0.3) \times 10^{-3}$	(2.5 ×10
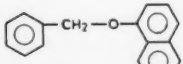	–	–	$(1.2 \pm 0.1) \times 10^{-2}$	$(6.3 \pm 0.2) \times 10^{-2}$	(2.6 ×10

ubstrate = 10 : 1)

				Half-life (min) at T, °C		E_a (kcal/mol)
300	325	350	410	350	410	
$(6.2 \pm 0.3) \times 10^{-3}$	$(3.0 \pm 0.2) \times 10^{-2}$	$(2.1 \pm 0.2) \times 10^{-1}$	7.4 *	3.3	0.094	50.2
$(2.1 \pm 0.3 \times 10^{-3}$	$(8.3 \pm 0.2) \times 10^{-2}$	$(4.8 \pm 0.2) \times 10^{-2}$	1.1	14.4	0.63	44.6
$(2.5 \pm 0.2) \times 10^{-2}$	$(1.1 \pm 0.1) \times 10^{-1}$	4.6×10^{-1} *	8.9 *	1.5	0.078	41.9
$(2.6 \pm 0.3) \times 10^{-1}$	–	3.4 *	45.4 *	0.2	0.015	36.6

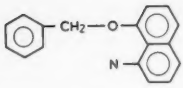	–	–	–	3.2×10^{-1} **	–
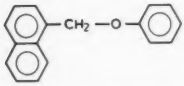	–	$(3.7\pm0.2)\times10^{-2}$	$(1.5\pm0.2)\times10^{-1}$	$(5.3\pm0.4)\times10^{-1}$	–
Ar–CH$_2$–O–CH$_2$–Ar′ structure					
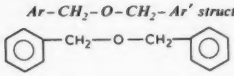	–	–	–	–	–
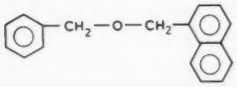	$(6.3\pm0.7)\times10^{-3}$	$(2.5\pm0.4)\times10^{-2}$	$(9.8\pm0.2)\times10^{-2}$	–	–

* Extrapolated by the Arrhenius equation.
** Rough estimation.

–	–	–	–	–	–	–
–	–	12.9 *	100.5 *	0.05	0.007	28.9
–	–	$(7.7 \pm 0.6) \times 10^{-3}$	$(5.8 \pm 1.0) \times 10^{-2}$	90	12	28.7
–	–	6.3 *	42.8 *	0.1	0.02	27.0

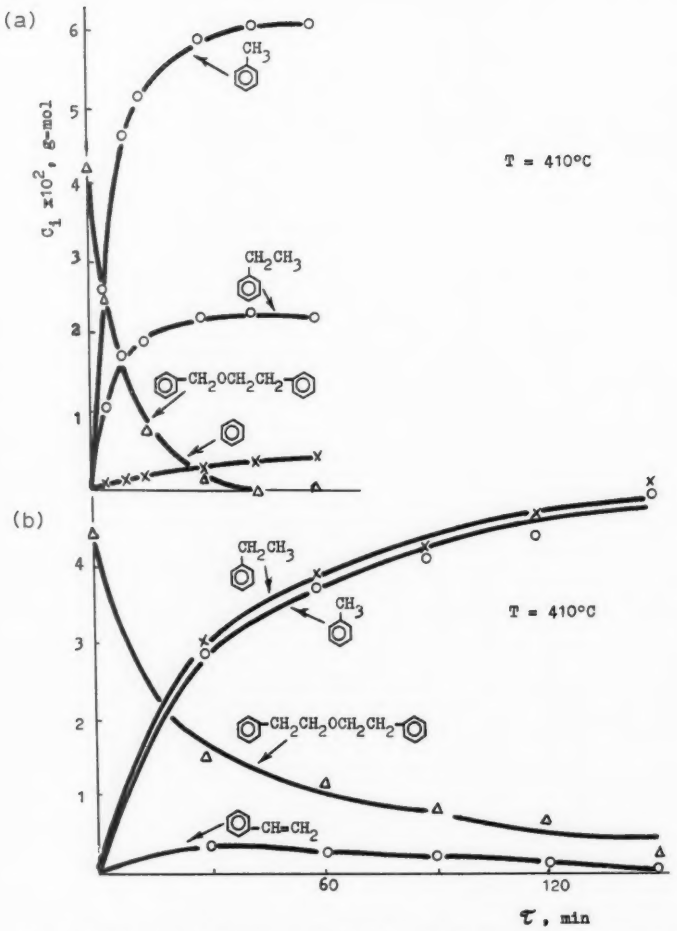

Fig. 3. Kinetic curves of thermolysis of (a) benzylethylphenyl and (b) diethylphenyl ethers.

effect is similar to that observed when a methylene group is introduced between oxygen and aryl (cf. benzylphenyl and dibenzyl ethers).

The substitution of a dicyclic end group for phenyl increases the thermolysis rate, the increase being much greater if this end group is bonded to the methylene group. For instance, ethers containing α-naphthyl form the following reactivity sequence:

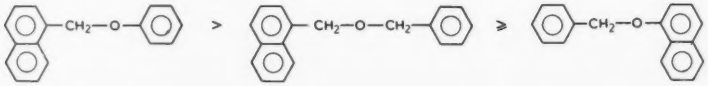

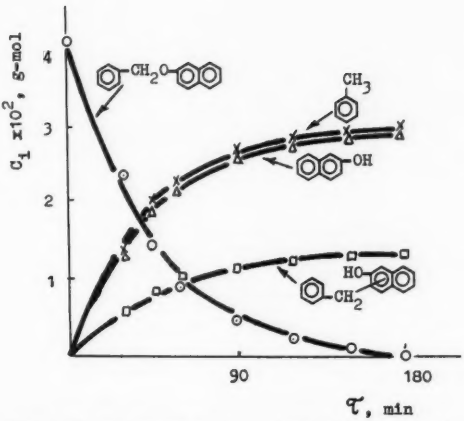

Fig. 4. Kinetic curves of thermolysis of β-benzylnaphthyl ethers.

Benzylnaphthyl ethers, similarly to benzylphenyl ether, yield benzylnaphthols as rearrangement products, together with toluene and the corresponding naphthol, which are the products of destruction (Fig. 4).

The condensation processes complicate thermolysis of phenyl-α-methylnaphthyl, benzyl-8-oxyquinolyl and benzyl-α-methylnaphthyl ethers.

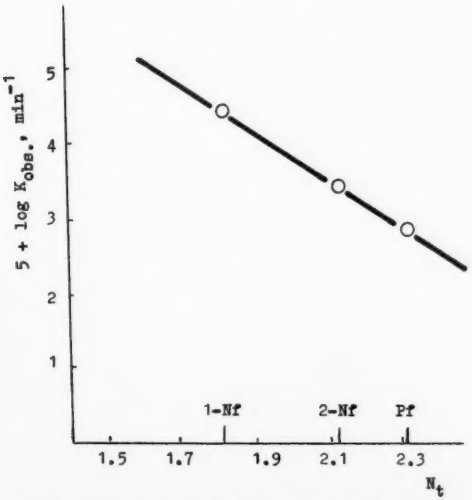

Fig. 5. The dependence log $k = f(N_t)$ for thermolysis of benzylaryl ethers $C_6H_5CH_2OAr$ at 300 °C. 1-Nf: Ar = 1-naphthyl; 2-Nf: Ar = 2-naphthyl; Pf: Ar = phenyl.

TABLE 5

The effect of the substituents in aryls on the rate of thermolysis of $Ar'-CH_2-O-A$ =10:1)

	Rate constant k (min^{-1}) at T, °C			
	225	250	275	300
$X-C_6H_4-CH_2-O-C_6H_4-Y$				
X = H, Y = H	–	–	–	$(6.2\pm0$ $\times10^{-3}$
X = H, Y = *m*-CH_3	–	–	(2.1 ± 0.3) $\times10^{-3}$	$(9.8\pm0$ $\times10^{-3}$
X = H, Y = *p*-CH_3	–	–	(4.9 ± 0.2) $\times10^{-3}$	$(2.0\pm0$ $\times10^{-2}$
X = H, Y = *p*-OH	–	–	(2.1 ± 0.2) $\times10^{-2}$	$(7.0\pm0$ $\times10^{-2}$
X = H, Y = *p*-CHO	–	–	–	$(3.7\pm0$ $\times10^{-3}$
X = *p*-CH_3, Y = H	–	–	(5.0 ± 0.5) $\times10^{-3}$	$(1.9\pm0$ $\times10^{-2}$
X = Y = *p*-CH_3	–	–	(1.7 ± 0.4) $\times10^{-2}$	$(5.8\pm0$ $\times10^{-2}$
$C_6H_5-CH_2-O-CH_2-C_6H_4-X$				
X = H	–	–	–	–
X = *p*-CH_3	(1.2 ± 0.1) $\times10^{-2}$	(3.8 ± 0.1) $\times10^{-2}$	(2.8 ± 0.3) $\times10^{-1}$	–

* Extrapolated by the Arrhenius equation.

–O–Ar′ and Ar–CH_2–O–CH_2–Ar′ ethers (8.5 MPa, tetralin : substrate

				Half-life (min) at T, °C		E_a (kcal/mol)
00	325	350	410	350	410	
.2±0.3) 10^{-3}	(3.0±0.2) $\times10^{-2}$	(2.1±0.2) $\times10^{-1}$	7.4 *	3.3	0.094	50.2
.8±0.2) 10^{-3}	(4.7±0.3) $\times10^{-2}$	1.8×10^{-1} *	3.2 *	3.85	0.22	40.5
.0±0.1) 10^{-2}	(8.9±0.4) $\times10^{-2}$	3.1×10^{-1} *	4.4 *	2.2	0.16	37.7
.0±0.5) 10^{-2}	(3.1±0.2) $\times10^{-1}$	1.0 *	12.9 *	0.69	0.057	35.5
.7±0.3) 10^{-3}	(1.8±0.1) $\times10^{-2}$	(3.8±0.2) $\times10^{-2}$	2.0 *	18.2	0.35	32.8
.9±0.2) 10^{-2}	(8.8±0.3) $\times10^{-2}$	3.1×10^{-1}	4.5 *	2.2	0.15	37.5
.8±0.2) 10^{-2}	(2.6±0.3) $\times10^{-1}$	7.6×10^{-1} *	10.1 *	0.9	0.07	36.4
	–	(7.7±0.6) $\times10^{-3}$	(5.8±1.0) $\times10^{-2}$	90	12	28.7
	–	1.5 *	8.0 *	0.5	0.09	23.8

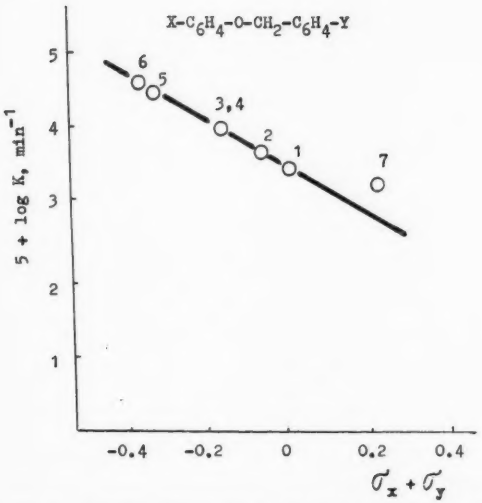

Fig. 6. The dependence log $k = f(\sigma_x + \sigma_y)$ for X–$C_6H_4OCH_2C_6H_4$–Y ethers. 1: X = H, Y = H; 2: X = *m*-CH_3, Y = H; 3: X = *p*-CH_3, Y = H; 4: X = H, Y = *p*-CH_3; 5: X = *p*-CH_3, Y = *p*-CH_3; 6: X = OH, Y = H; 7: X = *p*-CHO, Y = H.

Although the composition of the products obtained in the case of some ethers is complex, the products indicate that thermolysis of all structures proceeds along the C–O bond. One may then assume that the effect of the aryl group on the thermolysis rate is proportional to the reactivity index N_t of the postion at which the reacting grouping, i.e. the $-CH_2-O-$ group, is located. The calculation of N_t [25,26] has shown that logarithms of the thermolysis rate constants are directly proportional to the reactivity indices (Fig. 5. At 300 °C this dependence has the form:

$$\log K = -3.25\ N_t + 5.29$$

the correlation coefficients being 99.997%.

The correlation dependence so derived allows us to evaluate the thermolysis rate for any benzylaryl ethers of the type $C_6H_5CH_2OAr$.

The calculation of half-life periods (in min at 300 °C) has shown that, depending on Ar, the reactivity varies within a wide range from 0.044 (9-anthryl) to 114.36 minutes (3-biphenyl, phenyl).

The effect of the substituents in aryls

In real COM the ring-shaped clusters have a great number of substituents [1,2]. Stein [27] proposed that the presence of substituents decreases the activation energy E_a of COM destruction by at least 10 kcal/mole.

TABLE 6

Kinetic parameters of thermolysis of the $XC_6H_4-O-CH_2-C_6H_4Y$ ethers at 325 °C

Substituents X and Y in the ether		$\Sigma\sigma_x + \sigma_y$ *	$k_{observed}$ (min^{-1})
X	Y		
H	H	0	$(3.0\pm0.2)\times10^{-2}$
m-CH_3	H	−0.07	$(4.7\pm0.3)\times10^{-2}$
p-CH_3	H	−0.17	$(8.9\pm0.4)\times10^{-2}$
H	*p*-CH_3	−0.17	$(8.8\pm0.3)\times10^{-2}$
p-CH_3	*p*-CH_3	−0.34	$(2.6\pm0.3)\times10^{-1}$
p-OH	H	−0.37	$(3.1\pm0.2)\times10^{-1}$
p-CHO	H	+0.22	$(1.8\pm0.1)\times10^{-2}$

* The values of Hammett σ-constants are given, for instance, in ref. 25.

However, the effect of the substituents in $Ar-CH_2-O-Ar'$ and $Ar-CH_2-O-CH_2-Ar'$ structures has been virtually unstudied.

The data are listed in Table 5. As is seen from the values of the rate constants and half-life periods, electron-donor substituents such as *m*- and *p*-CH_3, and *p*-OH increase the thermolysis rate, whereas electron-acceptor substituents, such as *p*-CHO, decrease this rate. The activation energies decrease in all cases, which agrees with calculations performed by Stein [27].

The chemistry of the transformations of benzylaryl and methylbenzylaryl ethers is similar to that of the thermolysis of benzylphenyl ether: in all cases almost equimolar amounts of hydrocarbons and phenols * corresponding to the C–O bond homolysis are formed together with 20–25% of the rearrangement product.

Thus, the mechanism of thermolysis includes homolysis of the C–O bond, and hence the effect of the substituents manifests itself through the electron density of this bond. This means that the rate constants must depend on the Hammett σ-constants. Since the reaction rates of *p*-benzyloxytoluene and *p*-methylbenzylphenyl ether are almost equal, the introduction of the substituents into any ring of benzylphenyl ether results in the identical effect and in the case of introducing the substituents into both rings the effects must be additive. Table 6 lists the thermolysis rates for seven ethers at 325 °C and the corresponding sums of the Hammett σ-constants. The graph plotted by the data of Table 6 shows an excellent correlation $\log k/k_0 = -2.75 \times (\sigma_x + \sigma_y)$ with the exception of point 7 corresponding to the ether with an aldehyde group. The value of $\log k$ in this case is overestimated, since the aldehyde group is partially reduced to methyl in the course of the

* *p*-Benzyloxyphenol is an exception. Its thermolysis results in the formation of hydroquinone in an amount smaller than equimolar due to partial condensation.

experiment and the methyl substituent exerts quite an opposite effect and has a negative Hammett constant.

The introduction of the p-CH_3 substituent into dibenzyl ether accelerates thermolysis to a much greater extent than its introduction into benzylphenyl ether (130–190 times, i.e. more than by two orders of magnitude). This may be due to specific features of the mechanism of thermolysis of dibenzyl ether since it is the only ether in the structure of which, as was shown above, intramolecular rearrangement takes place with a very low activation energy. This rearrangement involves the transfer of a hydride ion.

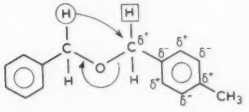

In the structure of p-methyldibenzyl ether the induction effect of the methyl group gives rise to redistribution of the electron density as a result of which the carbon atom of the methylene group adjacent to the substituted ring will have an additional charge promoting the hydride transfer (shown with a circle). The hydrogen atom closest to the substituted ring of the methylene group (shown with a square) has no such advantage. The experiment has confirmed the proposed mechanism: p-xylene and benzaldehyde are the main products of thermolysis and only when contact times were prolonged did a small amount of toluene form as a result of benzaldehyde reduction. A thorough analysis did not detect p-toluyl aldehyde in amounts exceeding the sensitivity limit of the chromatograph. Thus, the experiments with p-methyldibenzyl ether extend the regularity of the substituents' accelerating effect to the $-CH_2-O-CH_2-$ bridge as well as confirming the predominance (especially at low temperatures) of the molecular rearrangement mechanism proposed by Cronauer et al. [17] by the composition of the products and considerable acceleration of thermolysis.

SUMMARY

The constants of the rate of thermolysis of $Ar-(CH_2)_n-O-(CH_2)_m-Ar'$ ethers were measured under conditions close to those of coal liquefaction (hydrogen pressure of 8.5 MPa; temperature up to 410 °C) but minimizing secondary conversions (i.e. in excess tetralin). The ethers (when $Ar = Ar' =$ Ph) form the following reactivity series depending on the values of n and m: at 350 °C: [0; 1] > [0; 2] > [1; 1] > [1; 2] > [2; 2] ≫ [0; 0], and at 410 °C: [0; 1] > [0; 2] > [1; 2] > [1; 1] > [2; 2] ≫ [0; 0]. The substitution of a bicyclic end group for phenyl in the substrate increases the rate of thermolysis. The effect of the aryl group on the rate of thermolysis is proportional to the reactivity index of the position at which the reacting grouping is located.

Electron-donating substituents increase the rate of thermolysis while Electron-accepting substituents decrease it. The effect of substituents on the rate of thermolysis is described by the Hammett equation. The mechanism and pathways of ether conversions have been defined on the basis of the changing concentrations of the intermediate and final reaction products. In the case of benzylaryl and dibenzyl ethers the destruction was accompanied by intramolecular rearrangements.

CONCLUSION

It is likely that with progress of physicochemical methods of studying COM structure, information on the fraction of 'bridge' bonds and the structure of clusters will become available. The accumulation of kinetic data on the thermolysis of model compounds will allow calculation of the reactivity, since the calculation procedure can be applied to the variation of the structure of end groups as well as to a change in the number and structure of the substituents.

Hence, the data on kinetics of thermolysis of model compounds help not only in elucidation of the mechanisms of COM destruction but in evaluation of the reactivity as the structure of COM becomes clearer.

REFERENCES

1 D.W. van Krevelen, Coal, Elsevier, Amsterdam, 1980.
2 P.H. Given, in M.L. Gorbaty, J.W. Larsen and J. Wender (Editors), Coal Science, Academic Press, New York, Vol. 3, 1985, p. 65.
3 H.-R. Schulten and A. Marzec, in J.A. Moulijn, K.A. Nater and H.A. Chermin (Editors), Proceedings of the 1987 International Conference on Coal Science, Maastricht, The Netherlands, 26–30 October 1987, Elsevier, Amsterdam, 1987, p. 215; Fuel, 67 (1988) 619.
4 C.J. Collins, V.F. Raaen, B.M. Benjamin and G.W. Kabalka, Fuel, 56 (1977) 107.
5 K.E. Gilbert, J. Org. Chem., 49 (1984) 6.
6 K.E. Gilbert and J.J. Gajewski, J. Org. Chem., 47 (1982) 4899.
7 R. Brüker and G. Kölling, Brennst.-Chem., 46 (1965) 41.
8 Y. Takemura, H. Itoh and K. Ouchi, Fuel, 60 (1981) 379.
9 Y. Kamiya, Sh. Nagoe and S. Oikawa, Fuel, 62 (1983) 30.
10 J.W. Larsen and D. Lee, Fuel, 62 (1983) 463.
11 R.H. Schlosberg, P.F. Szajowsky, G.D. Dupre, J.A. Danic, A. Kurs, Y.R. Ashe and W.N. Olmstead, Fuel, 62 (1983) 690.
12 P.J. Cassidy, W.R. Jackson and F.P. Larkins, Fuel, 62 (1983) 1404.
13 G.A. Olah and A. Husain, Fuel, 63 (1984) 1427.
14 D.T. Allen and G.R. Gavalas, Fuel, 63 (1984) 586.
15 Y. Sato and Y. Yamakawa, Ind. Eng. Chem. Fundam., 24 (1985) 12.
16 R.K. Sharma, K.P. Raman and B. Miller, Fuel, 65 (1986) 738.
17 D.C. Cronauer, D.M. Jewell, Y.T. Shah and R.Y. Modi, Ind. Eng. Chem. Fundam., 18 (1979) 153.

18 R.H. Schlosberg, T.R. Ashe, R.J. Pancirov and M. Donaldson, Fuel, 60 (1981) 155.
19 S.V. Panvelker, Y.T. Shah and D.C. Cronauer, Ind. Eng. Chem. Fundam, 21 (1982) 236.
20 M.M. O'Malley and M.B. Simmons, Fuel, 64 (1985) 1027.
21 K. Kuranuki, M. Yukio and Y. Ogo, J. Chem. Soc. Jpn., Chem. Ind. Chem., No. 1 (1987) 60.
22 M.T. Klein and P.S. Virk, Ind. Eng. Chem. Fundam., 22 (1983) 35.
23 I.V. Kalechits, V.Yu. Korobkov, E.N. Grigor'eva and V.I. Bykov, Kinet. Katal., 28 (1987) 1014; Khimiya Tverd. Topl., No. 6 (1987) 46.
24 V.Yu. Korobkov, V.I. Bykov, E.N. Grigor'eva and I.V. Kalechits, Khimiya Tverd. Topl., No. 6 (1987) 63.
25 C.D. Johnson, The Hammett Equation, Cambridge University Press, 1973.
26 M.J.S. Dewar and R.C. Dougherty, The PMO Theory of Organic Chemistry, Plenum Press, New York, 1975.
27 S.E. Stein, in R.H. Schlosberg (Editor), Chemistry of Coal Conversion, Plenum Press, New York, 1985, p. 13.

Journal of Analytical and Applied Pyrolysis, 16 (1989) 75–85
Elsevier Science Publishers B.V., Amsterdam – Printed in The Netherlands

SLOW GAS-PHASE OXIDATION OF DIETHYLACETAL

J.A. GARCÍA DOMÍNGUEZ, M.J. MOLERA and J.M. SANTIUSTE *

Instituto Rocasolano C.S.I.C., c/Serrano 119, 28006-Madrid (Spain)

(Received May 30th, 1988; accepted October 10th, 1988)

ABSTRACT

The oxidation of diethylacetal at 170 °C has been studied using unlabelled and ^{14}C-labelled acetal. The reaction was followed by observing the pressure change and analysis of the products. The relative amounts of each product, if extrapolated to zero reaction time, show which are the primary reaction products. This feature, together with the reactivity results, enabled us to establish the stoichiometry of the reaction. Reaction enthalpies are calculated as well as relative values of the rate constants for the attack of the hydroxy radical to the different positions of the acetal molecule.

^{14}C labelling; diethylacetal; pyrolysis; radiochromatographic analysis; reaction mechanism; stoichiometry.

INTRODUCTION

The investigation of gas-phase oxidation reactions of a series of cyclic and linear acetals labelled with the radioactive isotope ^{14}C has been one of our goals over the last fifteen years [1–5]. The results published during that period strongly confirm the convenience of the use of this tracer in tackling such a complex reaction as oxidation.

Checking the ^{14}C distribution in the converted fuel, whenever possible, in other words, gathering information on the distribution of the radioactive products, helps to take account of a series of elementary reactions (which unfortunately occur in a great number) which no doubt would have been ignored or discarded at first. In many cases the method can allow the proposal of a reaction mechanism of a formidable complexity. There are not many techniques that yield so much information at such low cost as the use of tracers in oxidation.

The aim of this work is to contribute to the improvement of our knowledge of gas-phase oxidation reactions through the study of the slow combustion of unlabelled diethylacetal and of species labelled with ^{14}C in the two possible positions of the ethoxy group.

0165-2370/89/$03.50 © 1989 Elsevier Science Publishers B.V.

The explosion reactions and the cool flames produced in the oxidation under other experimental conditions have already been reported [6].

EXPERIMENTAL

The oxidation reaction of the unlabelled species of diethylacetal was carried out under static conditions [7] in a Pyrex glass cylindrical reactor of about 250 ml volume housed in an electric furnace kept at a constant temperature of $170 \pm 1°C$ by means of an electronic controller. Reaction mixtures were prepared in a mixing vessel at 80°C for a short period of 10–20 seconds before being charged to the reactor.

The reaction was followed by the change of the pressure with time and by quantitative analysis.

The species labelled with ^{14}C were oxidized in another vacuum line with some minor modifications concerning the sample storage and the radioactive material recovery system [2].

Materials

Diethylacetal (b.p. 103°C) pure quality (Fluka, Buchs, Switzerland) was treated by refluxing over extruded sodium with stirring followed by trap-to-trap distillation under vacuum with the aim of removing its major impurity, ethanol. Purity was checked by gas–liquid chromatography (GLC) and was found to be as high as 99.8%.

Dry oxygen from the Sociedad Española de Oxígeno was condensed from the bottle to a bulb held at liquid nitrogen temperature and then distilled under vacuum, using only the medium fraction of the distillate in the experiments. This fraction was expanded into a 4.5 l glass balloon before manipulation.

Methyl ethyl carbonate was synthesized [8] with ethyl chlorocarbonate and sodium methylate. [1-^{14}C]Ethanol and [2-^{14}C]ethanol were supplied by Amersham (Buckinghamshire, U.K.).

Other chemicals used for calibration or identification purposes were of commercial origin or synthesized by standard methods. Substances were purified when necessary.

Analyses

Identification of substances was performed by GLC and mass spectrometry. Quantitative analyses of products other than peroxides were carried out by gas chromatography.

Reaction products were fractionated at liquid nitrogen or solid carbon dioxide temperatures prior to their analyses.

The vacuum line sampling system consisted of three traps and a Toepler pump which could be connected to the reaction vessel. Fractionation was carried out by immersing the traps in freezing baths at liquid nitrogen temperature. In this way the uncondensable gases passed to the Toepler pump for storage after exhaustive pumping. By replacing liquid nitrogen by solid carbon dioxide in the baths, the gases which did not condense in solid carbon dioxide were distilled to a sampling device cooled with liquid nitrogen. Finally, those substances that were condensable in dry ice were distilled to another sampler cooled at the liquid nitrogen temperature. Traps and sampling devices were heated electrically to prevent condensation of the products.

The different parts of the system involved in the sampling and distillation process had been previously calibrated to determine their relative equivalent volumes, which were different depending on the freezing bath used.

Once the distillation operation had been adjusted to optimal conditions, the total amount of condensed products was transferred to a sampling device for analysis by GLC. Aliquot fractions of gaseous products stored in the Toepler pump were led to another sampler for GLC analysis.

All these calibrations were unnecessary for the labelled species, since we only measured relative amounts of substances in order to determine the relative activity of the peaks.

Analysis of peroxides

Total evaluation of peroxides was achieved by spectrophotometric analyses by the titanium sulphate method [3]. Measurements were carried out in a Beckman DU spectrophotometer. It had previously been determined that the complex absorbance was at a maximum at 410 nm. Samples condensed in a detachable trap at liquid nitrogen temperature were diluted with water and heated at 60 °C. The reagent was prepared by adding concentrated sulphuric acid (20 ml) to an 8% titanium sulphate solution (2.5 ml) followed by dilution to 100 ml with distilled water.

A calibration line was obtained by using 0.005 *N* hydrogen peroxide solutions, titrated against potassium permanganate immediately before use.

Hydrogen peroxide and organic peroxides were separately detected by thin-layer chromatography.

The samples were collected in the same way as described for spectrophotometry, but this time they were diluted with 0.5 ml of peroxide-free diethylacetal. Blank chromatograms of the diluent were made from time to time to ensure that it did not contain any peroxides.

Silica gel I.T.L.C. type SA strips from Gelman Inst. Co. were used after treatment [3] with a 5% solution of ethylene glycol in acetone. The moving phase was a 10% solution of *n*-butanol in light petroleum (b.p. 90–100 °C). The chromatograms were developed with N,N′-dimethyl-*p*-phenylenediamine dihydrochloride.

Radioactive diethylacetals

Labelled diethoxyethanes were prepared by reaction of acetaldehyde with the corresponding labelled ethanol. The reaction was performed in a 100-ml round-bottomed flask; 5.5 g of anhydrous calcium chloride, 18 ml of radioactive ethanol and 24 ml of acetaldehyde were mixed together, in that order. An azeotropic mixture of the acetal with ethanol was collected upon distillation at 102–104 °C. The same purification procedure as described above for unlabelled diethylacetal was repeated three times.

Degradation

Labelled diethylacetals were hydrolysed by adding two or three drops of a 10% sulphuric acid solution to 0.5 ml of the acetal. About 1 μl of the mixture was injected into the radiochromatographic system. A summary of the results corresponding to several injections is presented in Table 1.

The radiochromatographic system used to measure activity consisted of three parts: an analysis assembly, a combustion tube, and a proportional counter [4].

A PE 116 chromatograph coupled to an electronic integrator (PE D-26), a potentiometric recorder and a Kienzle D-21 printer were used.

The gases emerging from the chromatograph were passed through a copper oxide combustion tube (diameter 2.7 mm, stainless steel) and a magnesium perchloride desiccant tube of 7 mm diameter and 17 cm length. They were then mixed with methane and led to the counter tube, a 10-ml volume Berthold counter connected to a high voltage source, a preamplifier, a single channel analyser, a time scaler and a printing scaler, all supplied by Nuclear Chicago.

TABLE 1

Synthesis of labelled diethylacetals

	DEA (I) *	DEA (II) **
Active component	[^{14}C]ethan-1-ol	[^{14}C]ethan-2-ol
Activity (mCi)	0.75	0.75
Yield % (ethanol)	23	26
Chemical purity (%)	> 99.5	> 99.0
Specific activity (counts min^{-1} mol^{-6})	2332	2216
Degradation products (activity relative to DEA)		
Acetaldehyde	0	0
Ethanol	50.3 ± 1.8	50.5 ± 6

* DEA (I) = 1-ethoxy-[1-^{14}C]ethoxy-α-ethane.

** DEA (II) = 1-ethoxy-[1-^{14}C]ethoxy-β-ethane.

TABLE 2

Analytical results in the oxidation of diethoxyethane at 170 °C

Amounts of products expressed as Torr in the reaction vessel.

	Time (min)				
	2.5	5	7.5	10	15
CH_3CHO	8.5	7	17.8	20	23.5
$HCOOC_2H_5$	0.1	0.07	0.20	0.355	0.806
CH_3OH	0.4	1.77	0.9	2.95	5.28
C_2H_5OH	4.5	6.2	12	19	21
$CH_3COOC_2H_5$	1.3	3.33	6.4	8.64	9.2
$C_6H_{14}O_2$ (DEA)	58.2	56	45.8	39.3	36.4
H_2O	5.2	12	11.5	21	28.5
HCHO	0.12	0.25	0.4	0.39	0.46
CH_3COOH	6	8	15	17	20
HCOOH	0.06	0.14	0.2	0.21	0.36
$CO(OC_2H_5)_2$	0.04	0.09	0.11	0.13	0.17
CO	0.4	0.6	0.85	1	1.6
CO_2	0.4	1.2	2.8	4.6	9.4
O_2	122	115	104	92	76

Counts were fed to an SA 41 Intertechnique multichannel analyser provided with a printer. The efficiency of combustion to carbon dioxide and the total removal of water was checked.

The results in Table 2 were obtained under the following experimental conditions: 1875 V, 45 ml/min of helium and 22.5 ml/min of methane.

RESULTS

Reproducible results were obtained without difficulty, but from time to time we observed pressure increment–time of reaction curves that were lower than expected. In those cases the reaction vessel was cleaned several times with oxygen at 450 °C followed by degassing. Reproducibility was thereby restored.

The slow reaction

The pressure increase versus time plots in the oxidation of diethylacetal are sigmoid in shape. For 1 : 2 fuel-to-oxygen mixtures a proportionality was found between pressure rise and oxygen consumption in the first stages of the reaction between 150 and 200 Torr, with a proportionality constant independent of temperature over the 160–180 °C range. Runs carried out at 170 °C at constant oxygen pressure (133.3 Torr) and different acetal initial pressures showed that the maximum rate of pressure increase was proportional to the latter.

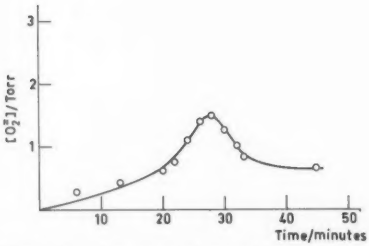

Fig. 1. Total amount of peroxides formed at 170 °C. Initial pressure, 200 Torr. Fuel : oxygen ratio, 1 : 2.

Analytical results

Experiments were carried out at 170 °C, 200 Torr initial pressure and acetal : oxygen ratio of 1 : 2. Analytical results corresponding to different reaction times are presented in Table 2.

Small amounts of the following substances were also detected: hydrogen, methane, ethylene, propylene, methyl ethyl carbonate and ethyl vinyl ether. Material balances of atomic carbon, hydrogen and oxygen, and pressure balances of the results shown in Table 2 were fitted with errors below 3%.

Total peroxides were determined by carrying out runs at different reaction times, other experimental conditions being as stated in Table 2. The maximum concentration of total peroxides (1.48 Torr) was reached at 28 min of reaction (see Fig. 1).

TABLE 3

Oxidation products of labelled diethylacetal

Reaction product	Pressure (Torr)	DEA (I)		DEA (II)	
		Number of runs	Activity (%)	Number of runs	Activity (%)
Acetaldehyde	23.5	8	0	7	32.3±4.5
Methanol	5.3	10	0	13	37.2±3.7
Ethanol	21	10	56.1±3	9	53 ±3.2
Ethyl acetate	9.2	9	54 ±2	8	50.7±4
Ethyl formate	0.8	–	–	4	56.9±3.8
Carbon monoxide	1.6	10	6.7±0.6	5	7.1±0.9
Carbon dioxide	9.4	6	12.6±1.3	7	10.7±1
Ethylene	0.03	–	–	3	25.1±1.3
Ethane	0.2	–	–	4	28 ±1.6
Formaldehyde	0.47	3	0	3	0
Acetic acid	12	5	7.2±0.5	2	24.8±1.2
Formic acid	0.36	5	0	–	–

Two spots were detected on the thin-layer plates, a first intense $R_F = 0.1$ spot attributed to hydrogen peroxide and another spot, $R_F = 0.8$ (also strong), which might probably correspond to an unresolved mixture of hydroperoxides derived from diethylacetal.

Radiochromatographic analyses

Oxidation experiments for 1-ethoxy-[1-^{14}C]ethoxy-α-ethane (DEA I) and 1-ethoxy-[1-^{14}C]ethoxy-β-ethane (DEA II) were carried out for reaction times of 15 min. Mean values of various runs are presented in Table 3, expressing activities as percentage of the activity of the corresponding parent acetal molecule.

DISCUSSION

The ratio of the amount of each reaction product to the diethoxyethane consumed has been calculated for different reaction times and plotted in Fig. 2. Extrapolation to zero reaction time shows that a few substances (carbon dioxide, methanol and ethyl formate) are not produced at the beginning of the reaction. They seem to be formed from primary reaction products. The remainder of the substances are produced in appreciable amounts at very short reaction times, and may be considered as primary

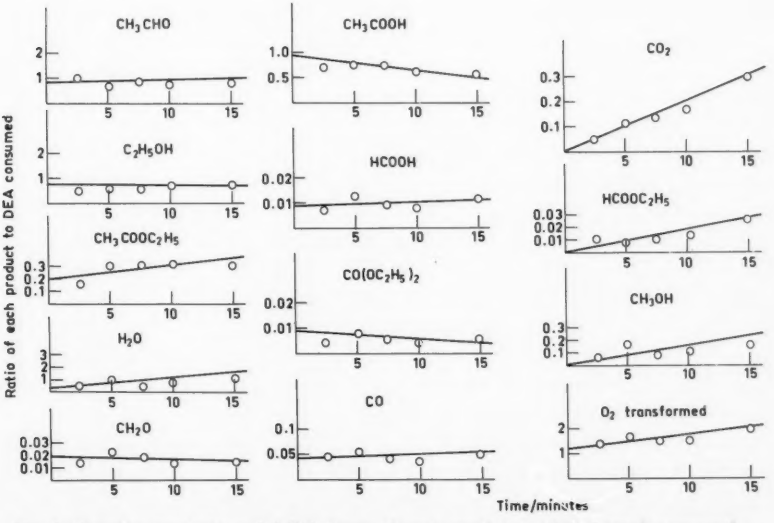

Fig. 2. Reaction products at 170 °C. Ratio of each product to diethylacetal consumed.

reaction products. The extrapolated values are consistent with the following stoichiometric equation:

$$1000\ DEA + 1159\ O_2 \rightarrow 781\ CH_3CHO + 766\ C_2H_5OH + 966\ CH_3COOH + 200\ CH_3COOC_2H_5 + 9\ CO(OC_2H_5)_2 + 9\ HCOOH + 20\ CH_2O + 40\ CO + 274\ H_2O$$

In this stoichiometric equation we have ignored the small quantities of peroxides. The equation may be divided into the following partial stoichiometric equations:

$$DEA + H_2O \rightarrow CH_3CHO + 2\ C_2H_5OH \quad (28.3\%) \quad (1)$$

$$DEA + 2\ O_2 \rightarrow CH_3CHO + 2\ CH_3COOH + H_2O \quad (49.8\%) \quad (2)$$

$$DEA + 0.5\ O_2 \rightarrow CH_3COOC_2H_5 + C_2H_5OH \quad (20\%) \quad (3)$$

$$DEA + 2\ O_2 \rightarrow CO(OC_2H_5)_2 + HCOOH + H_2O \quad (0.9\%) \quad (4)$$

$$DEA + 4.5\ O_2 \rightarrow 2\ CH_2O + 4\ CO + 5\ H_2O \quad (1\%) \quad (5)$$

Eqs. 1–3 account for 98% of the 1,1-diethoxyethane consumed at very short reaction times. These three reactions have been proposed on the basis of the radioactivity results and the results shown in Fig. 2. We have taken into consideration that the acetaldehyde produced in the oxidation of DEA (I) has zero activity, while that produced from DEA (II) has an activity of 32.3%. According to this result, no partial stoichiometric equation may simultaneously produce two acetaldehyde molecules, for in this case it will show activity, independently of its origin [DEA (I) or DEA (II)]. Furthermore, acetaldehyde may not be formed at the same time as ethyl acetate since it would then always present an activity of 50%, and even with the existence of reaction 1, some activity would always be observed. The fact that activities are measured at 15 min reaction time does not change the argument, since oxidation of acetaldehyde may change the amount found but never the activity of the molecule. The activity found in acetaldehyde shows that it is always formed from the carbon atom β of the ethoxy group and one of the carbon atoms of the CH_3CH group. Also, the fact that acetaldehyde formed from DEA (II) has an activity lower than 50% indicates that there is another reaction producing acetaldehyde of activity zero: reaction 1 must therefore be important at very short reaction times.

The relative amounts of acetaldehyde, ethanol, acetic acid and ethyl acetate (Fig. 2) have caused us to disregard other possible stoichiometric equations that could explain their formation. Eqs. 1–3, on the other hand, explain the activities found. Thus eqs. 1 and 3 would produce ethanol and ethyl acetate of 50% activity. Eq. 2 indicates that the activity of acetic acid would be 50% [DEA (I)] or 25% [DEA (II)]. At a reaction time of 15 min

part of the acetaldehyde has been oxidized to acetic acid, so the observed activity of the latter is considerably lower in the case of DEA (I) (activity of acetaldehyde = 0) and is not very different from that expected in the case of DEA (II) (activity of acetaldehyde = 32.3%).

Formaldehyde is a minor product having zero activity in all cases. It cannot be formed from the ethoxy groups of the acetal. Carbon monoxide presents an activity lower than might be expected on the basis of reaction 5 (25%) due to the fact that it is also formed by oxidation of reaction products with lower, or zero activity. Carbon dioxide is another product formed by the oxidation of some of the primary reaction products, thus its activity is low and does not allow us to draw any conclusions. Methanol is never formed from the α carbon atom of the ethoxy group. It is mainly formed from the terminal methyl groups of the ethoxy groups and, in part (about 25%), from the other methyl group of the molecule. In the case of the oxidation of dimethoxyethane it was found that methanol was mainly formed from the terminal methoxy groups [1].

Estimating enthalpies of formation of some of the species taking part in the stoichiometric eqs. 1–5, or using values taken from the literature [10], we have calculated that the stoichiometric eq. 1 (hydrolysis) is slightly endothermic by about 64 kJ mol^{-1}, while eqs. 2–5 are exothermic by 818, 222, 506 and 1302 kJ mol^{-1}, respectively.

Chain initiation and chain propagation reactions

It is generally accepted that chains are initiated by oxygen attack on the fuel molecule:

$$DEA + O_2 \rightarrow DEA^{\cdot} + HO_2^{\cdot}$$

$HO_2^{\cdot}$ radicals will eventually produce hydrogen peroxide and oxygen [11]:

$$2\ HO_2^{\cdot} \rightarrow H_2O_2 + O_2$$

A surface initiation process to form radicals may not be excluded at the temperature of the experiments. The radicals produced in the reaction system may act as chain propagation agents. Of the various radicals present, the most reactive is probably the hydroxyl radical, which will react with fuel molecules to produce water and the four $DEA^{\cdot}$ radicals below:

$$CH_3CH(OC_2H_5)_2 + HO^{\cdot} \rightarrow H_2O + CH_3\dot{C}(OC_2H_5)_2 \quad (6)$$

$$\rightarrow H_2O + CH_3CH(OC_2H_5)(O\dot{C}HCH_3) \quad (7)$$

$$\rightarrow H_2O + \dot{C}H_2CH(OC_2H_5)_2 \quad (8)$$

$$\rightarrow H_2O + CH_3CH(OC_2H_5)(OCH_2\dot{C}H_2) \quad (9)$$

We may accept that the frequency factor for the attack of the OH radical at any position of the molecule is about the same: Greiner [12] found a value

of A_{sec} for cyclohexane between 295 and 497 K of 1.96×10^{-12} molecule^{-1} s^{-1}. A value of A_{prim} of 2.94×10^{-12} molecule^{-1} s^{-1} may be deduced as an average of the literature values [12–16]. The value of A for the attack of OH radicals to the tertiary carbon atom of diethylacetal is unknown, but we may consider it to be of the same order as A_{sec} and A_{prim}. For the discussion that follows we may suppose that the value of A will not depend on the position of the hydrogen atom being abstracted. Activation energies for the attack of the OH radical on the different positions of the DEA molecule will be taken as follows: for the primary carbon atoms, the mean value of various determinations [12–16] for the case of ethane: i.e. 10.3 kJ mol^{-1}. For the case of secondary carbon atoms the activation energy will be lower than that corresponding to the attack on cyclohexane (2.65 kJ mol^{-1}) due to the proximity of the oxygen atom. For the case of the tertiary carbon atom we suppose it to be zero. Therefore, at 170 °C $k_6/k_8 = 5.46$, $k_6/k_9 = 2.73$, $k_6/k_7 = 0.25$ (For $E_7 = 0$), $k_6/k_7 = 0.5$ (For $E_7 = 2.65$ kJ mol^{-1}). We may suppose E_7 to be about 1.7 kJ mol^{-1} and consequently, we may say that $k_7 : k_6 : k_9 : k_8 \approx 14 : 5.5 : 2 : 1$.

The relative values of the rate constants can be estimated by Atkinson's procedure [16]. Using the parameters tabulated by this author, we have calculated the following values:

$k_6 = 37.8 \times 10^{-12}$ cm^3 molecule^{-1} s^{-1}

$k_7 = 14.2 \times 10^{-12}$ cm^3 molecule^{-1} s^{-1}

$k_8 = 0.5 \times 10^{-12}$ cm^3 molecule^{-1} s^{-1}

$k_9 = 1.1 \times 10^{-12}$ cm^3 molecule^{-1} s^{-1}

Therefore we may conclude that all four radicals formed according to reactions 6–9 take part in the chain propagation process although they are not all of equal importance. From the values estimated above it seems clear that reactions 6 and 7 predominate in the process.

It is unfortunate that, due to the lack of ^{14}C-labelled acetaldehyde, diethylacetal labelled in the acetaldehyde part of the molecule could not be synthesized, so the study of the mechanism could not be completed. Experiments carried out by oxidizing unlabelled DEA in the presence of ^{18}O could help us to understand some of the elementary reactions which lead to the reaction products.

ACKNOWLEDGEMENTS

We thank P.J. Navarrete for his help in carrying out some of the experimental work. We also are grateful to Dra. A. Couto for her valuable suggestions in revising the manuscript. J.M.S. is grateful to the Fundación

Juan March for a grant. Part of this research has been financed by the Comisión Asesora de Investigación Científica y técnica.

REFERENCES

1 M.J. Molera, J.A. García Domínguez, A. Rodríguez and J.M. Santiuste, J. Chem. Soc. Faraday Trans. 1, 73 (1977) 1900.
2 M.J. Molera, J.A. García Domínguez and A.U. Acuña, An. Quím., 70 (1974) 559.
3 M.J. Molera, J.A. García Domínguez and A.U. Acuña, J. Chem. Soc. B, (1971) 1919.
4 M.J. Molera, J.A. García Domínguez, J. Morales and J.M. Santiuste, An. Quím., 77 (1981) 25.
5 M.J. Molera, J.A. García Domínguez, J. Morales and J.M. Santiuste, An. Quím., 78 (1983) 284.
6 M.J. Molera, J.A. García Domínguez, A. Rodríguez and J.M. Santiuste, An. Quím., 73A (1977) 634.
7 M.J. Molera, J.A. García Domínguez and J.M. Santiuste, An. Quím., 70A (1974) 579.
8 K.F.W. Kohlrausch and A.Z. Pougratz, Z. Physik. Chem., (B)27 (1934) 195.
9 M.J. Molera, J.A. García Domínguez and A.U. Acuña, An. Quím., 70A (1974) 559.
10 S.W. Benson, Thermochemical Kinetics, Wiley, New York, 1976, p. 178.
11 B.A. Trush and G.S. Tyndall, J. Chem. Soc. Faraday Trans. 2, 78 (1982) 1469.
12 N.R. Greiner, J. Chem. Phys., 53 (1970) 1070.
13 L.G. Anderson and R.D. Stephens, 15th Informal Conference on Photochemistry, Stanford, CA, 1982, General Motor Research Laboratories, Warren, MI, 1982, Report GMR-4087, ENV 130.
14 C.A. Smith, L.T. Molina, J.J. Lamb and M.J. Molina, Int. J. Chem. Kinet., 16 (1984) 41.
15 R. Atkinson, Chem. Rev., 86 (1986) 69.
16 R. Atkinson, Int. J. Chem. Kinet., 18 (1986) 555.

Journal of Analytical and Applied Pyrolysis, 16 (1989) 87–97
Elsevier Science Publishers B.V., Amsterdam – Printed in The Netherlands

UNIMOLECULAR THERMAL REACTIONS OF C_5 TO C_8 ALKYNES

LOW TEMPERATURE MATRIX IR SPECTROSCOPIC AND MASS SPECTROMETRIC STUDIES

ULRICH ZIEGLER, GERHARD ZIMMERMANN * and BERND ONDRUSCHKA

G.D.R. Academy of Sciences, Central Institute of Organic Chemistry, Department for Basic Organic Materials, Permoserstr. 15, DDR-7050 Leipzig (G.D.R.)

LEONID E. GUSEL'NIKOV *, VERA V. VOLKOVA and LUDMILA V. SHEVELKOVA

U.S.S.R. Academy of Sciences, A.V. Topchiev Institute of Petrochemical Synthesis, Leninsky Prospekt 29, Moscow (U.S.S.R.)

(Received September 27th, 1988; accepted November 22nd, 1988)

ABSTRACT

The very low pressure pyrolysis of 1-alkynes in the C_5–C_8 range ($\leqslant$1450 K, 10^{-3} s, 10^{-2}–10^{-3} mbar) was investigated using two different detection set-ups: matrix isolation/IR and mass spectrometry. The results confirm that there are mainly three unimolecular reaction routes: (a) a retro-ene analogy leading to allene and the corresponding 1-alkenes, (b) a C–C bond rupture preferentially resulting in propargyl and alkyl radicals, and (c) a reaction course ending up in five-membered ring hydrocarbons. The last reaction seems to occur via an acetylene–vinylidene rearrangement followed by 1.5-C,H insertion of the intermediately formed alkylidene carbenes and consecutive reactions of the primary cyclization products.

Additionally, the formation of benzene from 1-octyne, which probably occurs via a four-step sequence inducing 3- and 4-methylenecyclopentene as key intermediates, was substantiated.

Alkynes, C_5–C_8; infrared spectroscopy; mass spectrometry; pyrolysis; reaction mechanism.

INTRODUCTION

The thermal conversion of alkyl acetylenes of length $\geqslant C_5$ has already been studied several times by means of techniques that facilitate unimolecular reaction steps exclusively or at least to a great extent (shock tube [1,2]

0165-2370/89/$03.50 © 1989 Elsevier Science Publishers B.V.

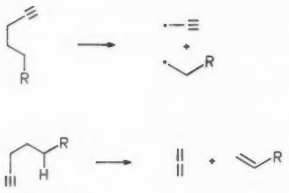

Scheme 1.

and very low pressure pyrolysis (VLPP)/mass spectrometric (MS) experiments [3–5] showing that there are two competitive mechanisms:

- a C–C bond homolysis originating in propargyl and alkyl radicals,
- an analogous retro-ene reaction resulting in a 1 : 1 mixture of allene and the corresponding olefine [6] (Scheme 1).

Very recently we observed that under unimolecular conditions, typical of VLPP experiments, five-membered ring species are formed to a remarkable extent from alkyl acetylenes of length $\geqslant C_5$ [7].

It has been proposed that the formation of e.g., cyclopentadiene and methylcyclopentadienes is started by a 1,2-shift of the acetylenic H atoms (acetylene–vinylidene isomerization [8]) followed by 1,5-C,H insertion of the alkylidene carbenes formed as intermediates, whereby 3-alkylated cyclopentenes should be formed as primary cyclization products. Only hydrocarbons with a cyclopentadiene structure were detected, rather than the correspond-

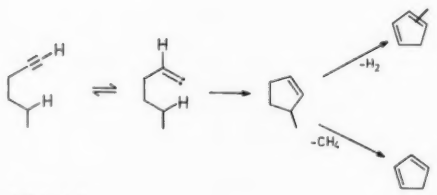

Scheme 2.

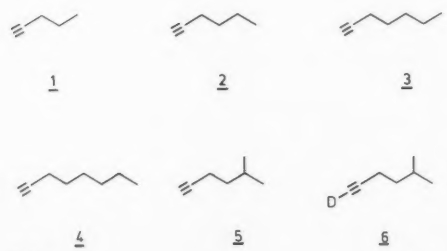

Scheme 3.

ing 3-alkyl cyclopentenes. Therefore we concluded that, under the conditions used in ref. 7, the primary products of cyclization are obviously not stable enough to survive, since they may undergo subsequent H_2 or formal CH_4 elimination (Scheme 2).

In order to get a better understanding of the complex reaction course we studied the thermal conversion of alkyl acetylenes in more detail. The unimolecular conversion of the alkyl acetylenes **1–6** (Scheme 3) investigated by means of VLPP using two different detection set-ups (matrix isolation/IR and MS) is described in the present paper.

EXPERIMENTAL

*Preparation of the parent alkynes **1–6***

Compounds **1–5** (Scheme 3) were prepared from sodium acetylide and the corresponding alkyl halides in liquid ammonia by the standard procedure described in ref. 9. [1-D_1]-5-Methyl-1-hexyne (**6**) was obtained by treatment of the sodium salt of **5** with D_2O in dibutyl ether [10] or by repeated H–D exchange of **6** with NaOD. The purity of the synthesized 1-alkynes was > 99% (determined by gas chromatography (GC) (25-m glass capillary, OV-1). The D content of **6** was determined by MS and ^{1}H-NMR (> 96%), the D position follows from the relevant ^{1}H-NMR spectra.

Preparation of model hydrocarbons

Cyclopentadiene (**7a**, Scheme 4) was produced from the dimer analogously to the procedure given in ref. 11. GC purity, 99.9%.

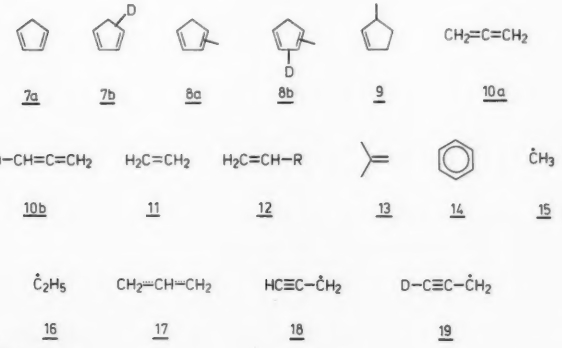

Scheme 4.

Methylcyclopentadiene (**8a**) was prepared from a dimer fraction of **8a** in a way similar to that described for **7a**. GC purity, 99.1%.

3-Methylcyclopentene (**9**) was synthesized from 3-chlorocyclopentene and methyl magnesium chloride [12,13]. GC purity, 98%.

Equipment

A set-up was used for VLPP matrix isolation/IR investigations ('A') which has already been described in ref. 14. The optical window was CsI. The reaction temperature was varied between 920 and 1250 K, the pressure of the samples between 6×10^{-2} and 4×10^{-3} mbar. The residence time amounted to about 10^{-3} s, the target temperature was 10–15 K. The matrix gas (nitrogen) was used in a five hundred-fold excess relative to the hydrocarbon studied. In some cases solid phase spectra were recorded either at 65 K (parent alkynes and reference compounds) or at 77 K (products of singled out pyrolysis runs). After recording the IR spectra, the pyrolysis products were transformed into the gas phase and analyzed by GC or (after recondensation at 77 K) by GC–MS (3-m stainless steel column, Al_2O_3).

For the VLPP/MS investigations a set-up ('B') was used that was suitable for observing the qualitative dependence of product concentrations on the reaction temperature. 'B' consisted of a quartz cell (130 mm × 6 mm I.D., diameter of the orifice: 3 mm) as VLPP reactor [15], which was firmly connected to the ion source of the mass spectrometer (Varian MAT CH6) used for on-line product analyses (see, for example, refs. 3–5). With respect to the reaction parameters (300–1450 K, 10^{-2}–10^{-3} s, 10^{-5} mbar and molecular masses of the parent alkynes studied between 80 and 100) the average numbers of substrate–wall collision amounted to nearly 400 whilst those of the substrate–substrate collisions tended to zero. The ionization energy used for recording the product spectra was normally 12 eV in order to diminish mass spectrometric fragmentations.

RESULTS AND DISCUSSION

Fig. 1a–d shows representative integral matrix/IR spectra of the reaction products from the parent alkynes **1**–**4**, while Fig. 2a, b gives the spectra of the pyrolysis products from **5** and **6**. These spectra contain the absorption bands of the unconverted parent alkynes (e.g., 620–650, 3330 cm^{-1}). The results of the product analyses performed by means of matrix isolation/IR were completed by VLPP/MS investigations of the parent alkynes **2**–**5**. The data obtained in this way are given in Fig. 3a–d as plots of relative MS intensities (I) versus reaction temperature. The molecular ion peaks of the unconverted parent alkynes could not be considered because of their low intensities [16]. Therefore, the degree of conversion of **2**–**5** was observed

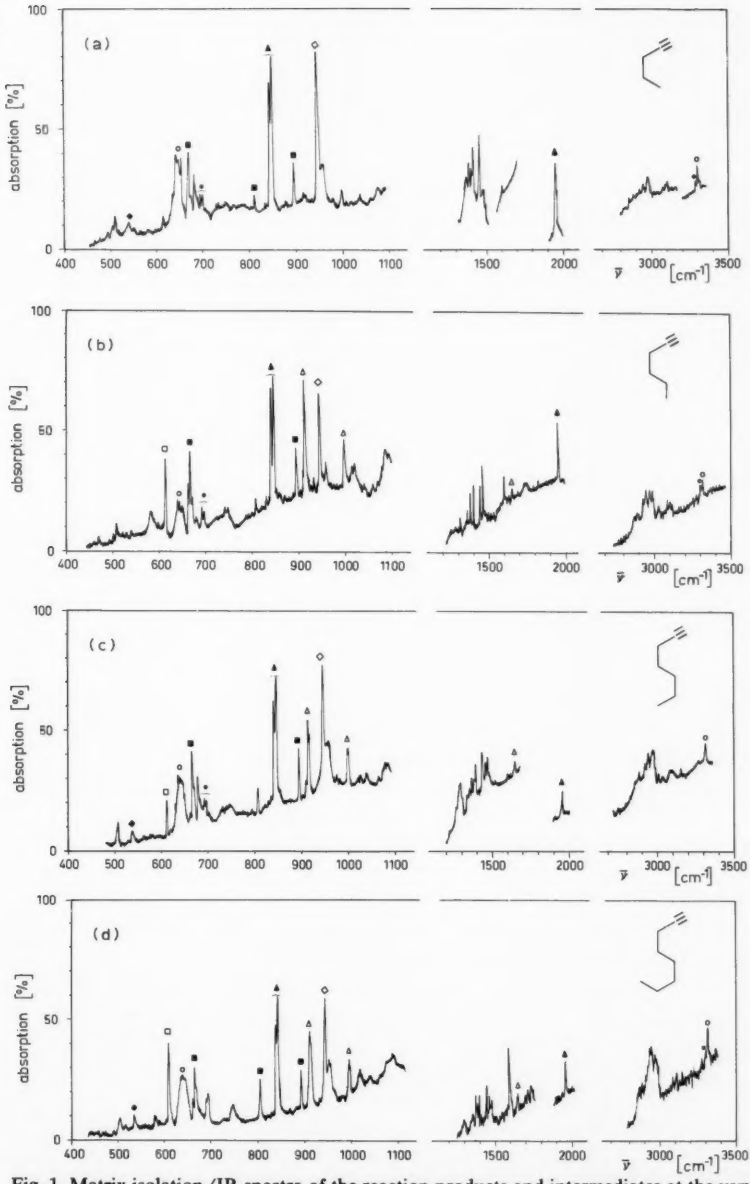

Fig. 1. Matrix isolation/IR spectra of the reaction products and intermediates at the very low pressure pyrolysis experiments [matrix gas: nitrogen (4×10^{-1} mbar)] of **1**–**4** (5×10^{-3} mbar) **1** (1190 K), **2** (1190 K), **3** (1110 K), and **4** (1040 K). Symbols: ○, parent alkynes; ●, propargyl radical; ◆, ethyl; □, methyl; ■, ethylene; △, 1-olefins (C_3–C_5); ▲, allene; ◇, cyclopentadiene and methylcyclopentadienes.

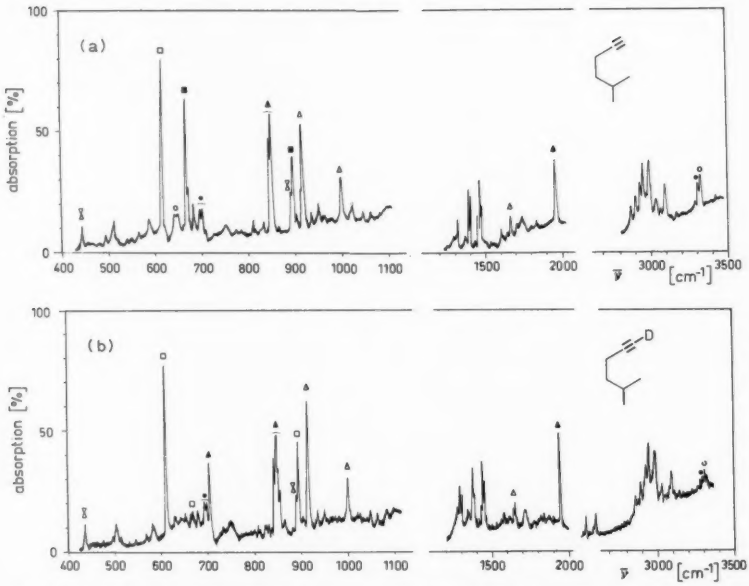

Fig. 2. Matrix isolation/IR spectra of the reaction products and intermediates at the very low pressure pyrolysis experiments [matrix gas: nitrogen (4×10^{-1} mbar)] of **5** and **6** (1220 K, 5×10^{-3} mbar). Symbols: see Fig. 1; ⧖, isobutene.

indirectly only in relation to the intensity of m/z 81, which was found to be formed in a significant quantity from **2**–**5**, and in similar manner. All results depicted in Fig. 3 are to be understood as qualitative (and at best semi-quantitative) findings [17]. Identified species and those to be expected as a result of VLPP of the alkynes **1**–**6** are compiled in Scheme 4.

For a better understanding of the formation of **7a** and **8a** from **1**–**5**, and of **7b** and **8b** from **6**, VLPP of **9** was additionally studied using the set-up 'A'. Besides IR bands originating from **7a** and **8a** there are, however, no spectral data which can exposure the existence of remnants of **9** in the matrices of its pyrolysis products [18].

Our results clearly confirm the suggestion expressed in the introduction that the unimolecular thermal conversion of 1-alkynes of length $\geqslant C_5$ occurs via three competitive reaction channels which are mainly characterized by

- a retro-ene analogous course [route (a)]
- a homolytic C–C bond rupture [route (b)] and
- a 1.2-H shift of the acetylenic hydrogen connected with the formation of alkylidene carbene intermediates [route (c)].

In all cases the thermal conversion became significant under VLPP conditions at temperatures from 900 to 1000 K only.

In agreement with refs. 1–5 (see also ref. 6) the main product formed is allene (**10a**) from **1–5** (846–850, 1960 cm^{-1}, m/z 40) and D_1-allene (**10b**) from **6** (707, 841–846, 1956 cm^{-1}, m/z 41), confirming the importance of the analogous retro-ene reaction course (Scheme 1). The formation of **10a** is

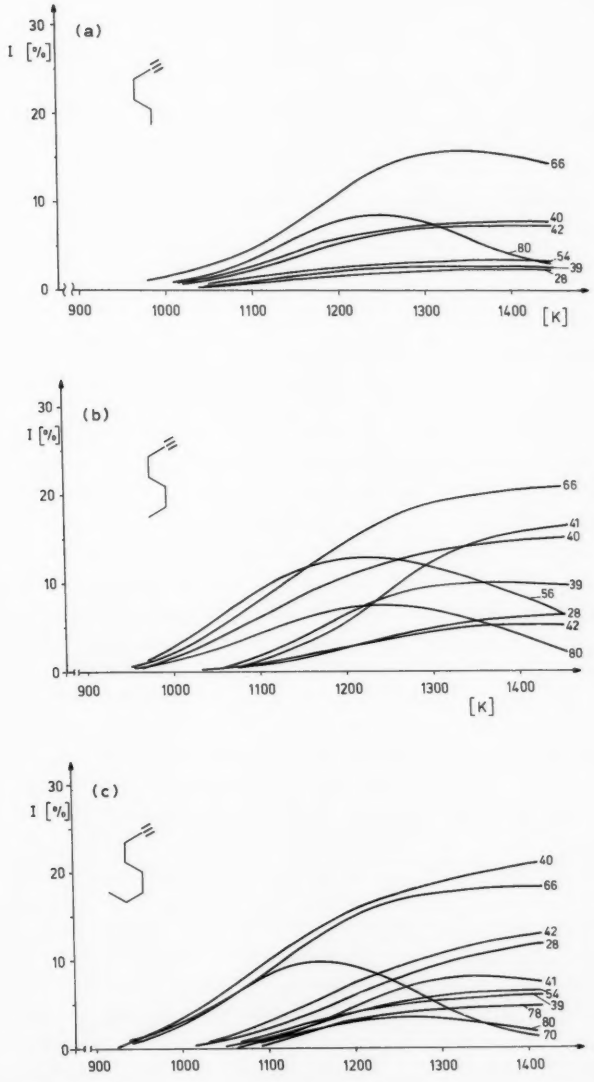

Fig. 3.

(Continued on p. 94)

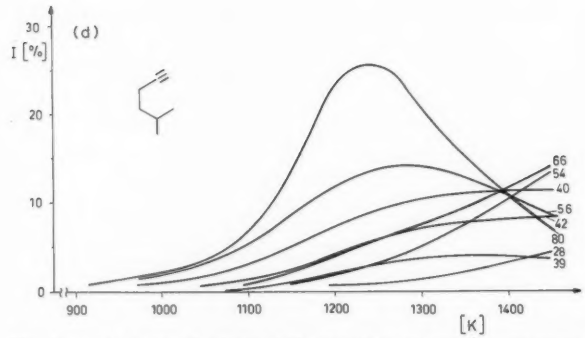

Fig. 3. m/z plots of relative MS intensities of reaction products and intermediates at the pyrolysis of **2**–**5** vs. reaction temperature.

accompanied by the corresponding 1-alkenes (**11** from **1**: 950 cm^{-1}; propylene from **2**: 915–919, 997 cm^{-1}, m/z 42; 1-butene from **3**: 915–919, 997 cm^{-1}, m/z 56; 1-pentene from **4**: 915–919, 997 cm^{-1}, m/z 70), that of **10b** from **6** by isobutene (887 cm^{-1}, m/z 56). Under the VLPP conditions used by us 1-butene and 1-pentene are less stable than **11** and propylene [18]. The former apparently decomposes by β(C–C) bond rupture, yielding the allyl radical **17** (m/z 41) and alkyl radicals (**15**: 613 cm^{-1}, **16**: 533 cm^{-1}) and hydrogen atoms [19]. The propargyl radical **18** (496, 688, 696, 701 3310 cm^{-1}, m/z 39 [20]) and **19** (568, 2545 cm^{-1}, m/z 40) are the main radical species. The homolytic bond rupture in the β-position to the triple bond of the parent alkynes is clearly favoured. The corresponding alkyl radicals $\geqslant C_3$ could not be detected. They obviously have no change of survival on the way to the target. Instead of these radicals ethylene and smaller radicals were detected. Besides the products whose formation is explainable by retro-ene analogous reactions we succeeded in proving the formation of some products which cannot immediately be interpreted. This concerns the products with m/z 54 and m/z 52, which may reasonably be thought to be butadienes and/or butynes (m/z 54) and vinylacetylene (m/z 52). These products had already been detected when pyrolyzing $> C_5$ alkynes in shock tube experiments [2] and in vacuum UV photolysis of 1-hexyne (**2**) [6] and identified as 1,2- and 1,3-butadiene, 1-butyne and vinylacetylene, respectively.

Another point worth noting is the formation of five-membered ring hydrocarbons. In principle, species with carbon numbers greater than or equal to those of the parent alkynes can be formed by cyclization of alkenyl radicals (see, for example, refs. 13 and 21). But such a cyclization is not compatible with the fact that bimolecular events are insignificant under our conditions of very low pressure pyrolysis. Therefore, the formation of cyclic hydrocarbons demands unimolecular processes obviously involving a 1.5-C,H

insertion of alkylidene carbene species, as has already been published partly [7] and which has meanwhile been recognized as an important reaction channel even under conditions favouring bimolecular steps [13]. Unfortunately, we failed to detect such hydrocarbons in the matrices as would be expected as primary cyclization products (e.g., cyclopentene from **1**, **9** from **2**, 3,3-dimethylcyclopentene from **5**). Instead of these products we found **7a** (668, 809, 912, 960 cm^{-1}) from **1**, **7a** and **8a** (680, 813, 890, 902 cm^{-1}, m/z 80) from **2**, **8a** from **5** and **8b** (653, 865, 1590 cm^{-1}) from **6**. We explain these results as being due to the fact that at high temperatures the expected primary cyclization products have scarcely any change of survival because they undergo rapid consecutive reactions such as 1,4-H_2 elimination or radical demethanization. Therefore, when **9** was subjected to the same pyrolysis conditions as **2** only **7a**, **8a** and **15** could be detected with certainty in the corresponding matrices. Starting from **2**, **3**, and **5** the MS plots of intensity vs. reaction temperature (see Fig. 3) show m/z 80 but only traces of m/z 78 could be observed. On the other hand the appropriate plot for the thermal conversion of **4** indicates the presence of m/z 78 and m/z 80 in a significant amount. Furthermore, the intensity of m/z 80 runs through a maximum at about 1200 K. At higher temperatures, **8a** obviously decomposes via a mechanism that is not explainable from the experimental results, since we failed to detect either the methylcyclopentadienyl (m/z 79) or the cyclopentadienyl radical (m/z 65). The result that **4** gives more m/z 78 than **2**, **3**, and **5** indicates a different behaviour in benzene formation. Therefore, the conversion of 3-*n*-propylcyclopentene **20** seems to occur by way of

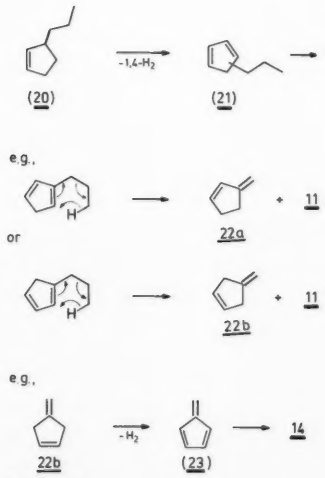

Scheme 5.

another mechanism, as discussed for **9**. Such an alternative might very probably involve 1,4-H_2 elimination of **20** leading to a mixture of the *n*-propylcyclopentadiene isomers (**21**) and retro-ene decomposition of **21** to 3- and 4-methylenecyclopentene (**22a** and **b**) followed by their dehydrogenation and finally resulting in pentafulvene (**23**) [23] (Scheme 5).

Although during the course of VLPP **20**–**23** are obviously not stable enough to accumulate in concentrations allowing their spectroscopic identification, **23** is a plausible intermediate that is known to isomerize into benzene (**14**) [23,24].

CONCLUSIONS

It has been demonstrated that during unimolecular thermal conversion of $\geqslant C_5$ 1-alkynes there is a third route (c) besides the well-known retro-ene analogous decomposition [route (a)] and the homolytic C–C bond rupture [route (b)]. At temperatures of the order of 1100 K, the ratio of these routes was already estimated to be (a) : (b) : (c) 50 : 35 : 15 [7] given in terms of the percentage of the converted parent alkyne. With regard to the formation of five-membered ring species our results are consistent with a mechanism involving a 1.2-shift of the acetylenic hydrogen and a 1.5-C,H insertion of intermediate alkylidene carbenes, leading to 3-alkyl cyclopentenes as primary products. These products could not be detected because of rapid consecutive reactions resulting in the preferential formation of cyclopentadiene and methylcyclopentadienes. Additionally a secondary process has been proposed, which is useful in interpreting the formation of m/z 78 (benzene) from 1-octyne.

REFERENCES

1 W. Tsang, Int. J. Chem. Kinet., 2 (1970) 23.
2 W. Tsang, Int. J. Chem. Kinet., 10 (1978) 687.
3 K.D. King, Int. J. Chem. Kinet., 13 (1981) 245.
4 T.T. Nguyen and K.D. King, J. Phys. Chem., 85 (1981) 3130.
5 K.D. King, Int. J. Chem. Kinet., 13 (1981) 273.
6 H. Deslauriers, G.J. Collin and B. Simard, J. Photochem., 21 (1983) 19.
7 L.E. Gusel'nikov, V.V. Volkova, U. Ziegler, L.V. Shevelkova, I.N. Shishkina, G. Zimmermann and B. Ondruschka, Izv. Akad. Nauk SSSR, Ser. Khim., (1986) 2829; C.A., 107 (1987) 175336.
8 R.P. Duran, V.T. Amborebieta and A.J. Colussi, J. Am. Chem. Soc., 109 (1987) 3154.
9 K.N. Campbell and B.K. Campbell, Org. Synth., 30 (1952) 15.
10 R.E. Dessy, S.H. Wotiz and C.A. Hollingworth, J. Am. Chem. Soc., 79 (1957) 338.
11 K. Ramhold, K.K. Moll, E. Roschka, G. Zimmermann, Th. Smola and L. Krukowka, J. Prakt. Chem., 326 (1984) 924.
12 G. Grane, C.E. Boord and A.L. Henne, J. Am. Chem. Soc., 67 (1945) 1237.

13 B. Ondruschka, G. Zimmermann, M. Remmler, U. Ziegler, F.-D. Kopinke, B. Olk and M. Findeisen, Chem. Ber., in press.
14 L.E. Gusel'nikov, V.V. Volkova, V.G. Avakyan and N.S. Nametkin, J. Organomet. Chem., 201 (1980) 137.
15 See, for example, D.M. Golden, G.N. Spokes and S.W. Benson, Angew. Chem. Int. Ed. Engl., 12 (1973) 534.
16 See, for example, Z. Dolejsek, V. Hanus and K. Vokac, Advances in Mass Spectrometry, Vol. 3, Institute of Petroleum, London, 1966, pp. 503–514.
17 Eight Peak Index of Mass Spectra, Mass Spectrometry Data Centre, Aldermaston, U.K., 1st ed., 1970.
18 M. Olzmann and K. Scherzer, Ber. Bunsenges. Phys. Chem., 92 (1988) 908.
19 (a) J. Pacansky, D.W. Brown and J.S. Chang, J. Phys. Chem., 85 (1981) 2562.
(b) J.C. Schultz, F.A. Houle and J.L. Beauchamp, J. Am. Chem. Soc., 106 (1984) 3917.
20 M.E. Jacox and D.E. Milligan, Chem. Phys., 4 (1974) 45.
21 B. Ondruschka, G. Zimmermann, U. Ziegler, F.-D. Kopinke and M. Teuber, J. Prakt. Chem. (Leipzig), in press.
22 M. Remmler, Thesis, Academy of Sciences, Berlin–Leipzig, 1989.
23 B.J. Gaynor, R.G. Gilbert, K.D. King and P.J. Marman, Austral. J. Chem., 34 (1981) 449.
24 G. Zimmermann, M. Remmler, B. Ondruschka, F.-D. Kopinke and B. Olk, Chem. Ber., 121 (1988) 1855.

Journal of Analytical and Applied Pyrolysis, 16 (1989) 99–100
Elsevier Science Publishers B.V., Amsterdam – Printed in The Netherlands

SYMPOSIUM REPORT

The Analytical Pyrolysis/Mass Spectrometry Symposium was convened during the XV Federation of Applied Chemistry and Spectroscopy Societies Conference in Boston, Massachusetts, 3 November 1988. Richard A. Yost (University of Florida), Mass Spectrometry Symposium coordinator, appointed A. Peter Snyder (U.S. Army Chemical Research, Development and Engineering Center) to organize and chair the Symposium. A series of four papers were presented that related the common theme of using analytical pyrolysis as the sample processing concept.

Professor Kent Voorhees (Colorado School of Mines) presented Curie-point wire pyrolysis (Py) interfaced to mass spectrometry (MS) and MS/MS analyzers. Microorganisms as well as microorganism/interferent mixtures were investigated; multivariate analysis as well as artificial intelligence (AI) augmenting a multivariate analysis of the Py–mass spectra of an organism mixture were necessary in order to provide meaningful detection and identification conclusions. The Py–MS–AI concept was used to separate closely related Py–mass spectra of *Xanthomonas* and *Pseudomonas* species. This is important because the former bacterium is pathogenic to citrus tree orchards. The organism in suspect leaf samples was misclassified as *Xanthomonas* by microbiological techniques but was later found to be the innocuous *Pseudomonas* species using Py–MS–AI.

Dr. A. Peter Snyder presented the quartz tube pyrolysis concept interfaced to an atmospheric pressure ionization MS/MS analyzer. This analytical interface was applied to the detection and identification of solid analytes in solid formulations. The explosive cyclotrimethylenetrinitramine (RDX) was observed in a polymeric-based munition and pharmaceuticals such as aspirin, caffeine, acetaminophen, pseudoephedrine and phenylpropanolamine were found, via MS and MS/MS analyses, in their respective over-the-counter cold remedy products such as Anacin, Bufferin, Tylenol, Sinutab, Exedrin and Contac. No preprocessing of the sample was required and operator ease of a typical analysis highlighted the experimental procedure.

Professor Henk Meuzelaar (University of Utah) presented Curie-point wire pyrolysis in conjunction with transfer/gas chromatography (GC) columns into ion trap mass spectrometry analyzers. The extraction of the high molecular weight lipid information from microorganisms was presented where they were either directly pyrolyzed or methylated with on-line derivatization (OLD). The latter procedure significantly reduced the time of

evolution of the methylated fatty acids. Furthermore, the OLD procedure produced identical results with that of the manual extraction/derivatization procedures, and only microgram amounts of bacteria need be used in comparison to the milligram levels required of the manual procedure.

Professor Stephen Morgan (University of South Carolina) presented evidence that quartz tube pyrolysis GC/MS is beneficial for the extraction of various key pyrolyzate compounds that are unique and/or important for differentiating various bacteria. Compounds such as acetamide, propionamide, 2-acetylamino-2-butenoic acid, furfuryl alcohol and the postulated cycloacetylalanine compound were influenced by the amount of peptidoglycan present. This is a function of whether the organism is a Gram positive or negative bacterium or fungus.

Financial contributions for the speakers of the Symposium were generously provided by Bristol-Myers Co., Wallingford, CT; Chemical Data Systems, Oxford, PA; Fischer America, Inc., Waukesha, WI and Somatogen, Broomfield, CO.

Mass spectrometry was shown to be a practical, invaluable tool in analyzing sample information from pyrolysis devices. Conversely, pyrolysis devices were shown to produce meaningful sample information in an experimentally expedient manner.

Professor Voorhees saw the current status of pyrolysis as similar to that of supercritical fluid technology in the early part of this decade. He further pointed out that a greater emphasis on concerted commercialism and industry support for the pyrolysis concept would be most welcomed by the scientists that use the technique. This would no doubt attract "fresh blood" to further expand the user base and hence create/enhance the applications of the technique.

The Gordon Conference on Analytical Pyrolysis and the International Symposium on Analytical and Applied Pyrolysis are important meetings that concentrate on the pyrolysis concept. The FACSS XV meeting, however, is believed to be the first multidiscipline, major scientific conference that sponsored a Symposium concentrating on the analytical pyrolysis technique. It is hoped that this scientific area will be incorporated more substantially in future FACSS and other major conferences.

A. PETER SNYDER
Research Chemist,
U.S. Army Chemical Research,
Development and Engineering Center,
SMCCR-RSL,
Aberdeen Proving Ground,
MD 21010-5423, U.S.A.

Journal of Analytical and Applied Pyrolysis, 16 (1989) 101–102
Elsevier Science Publishers B.V., Amsterdam – Printed in The Netherlands

Meeting Announcement

GORDON RESEARCH CONFERENCE ON ANALYTICAL PYROLYSIS

The Gordon Research Conference on Analytical Pyrolysis has been scheduled for June 19–23, 1989 at New Hampton School, New Hampton, New Hampshire, U.S.A. This time the conference will highlight two major items. The first part of the week will be focussed on fundamental aspects of flash-pyrolysis and thermal degradation, the second half will be dedicated to applications in natural product chemistry and in petroleum and coal geochemistry. For information: Dr. J.W. de Leeuw, Technical University Delft, Department of Chemical Engineering, Organic Geochemistry Unit, de Vries van Heystplantsoen 2, 2628 RZ Delft, The Netherlands, tel. (0)15-786325, telex butud 38151, fax (0)15-786522.

Programme

Monday morning

Fundamental Aspects of Thermal Analysis I

Chairman: H.-R. Schulten, Fresenius Inst., Wiesbaden, F.R.G.

1. R.S. Lehrle, University of Birmingham, U.K.: The future of pyrolysis: further progress in the subject demands the same approach as that for improving a molecule – strengthen the weak links in the chain!
2. J.R. MacCullum, University of St. Andrews, U.K.: The problems of pyrolysis: can theory help?

Monday evening

Fundamental Aspects of Thermal Analysis II

Chairman: S. Tsuge, Nagoya University, Japan.

3. J.J. Boon, FOM-Institute, Amsterdam, The Netherlands: Time resolved flash pyrolysis–EI/CI/PI–mass spectrometry of plant cell walls and cell wall polymers.
4. H.L.C. Meuzelaar, University of Utah, Salt Lake City, U.S.A.: Comparison of thermogravimetry, Curie-point pyrolysis and laser pyrolysis; some mechanistic and kinetic aspects.

Tuesday morning

Mechanisms of Pyrolysis

Chairman: R.P. Lattimer, B.F. Goodrich Co., Brecksville, U.S.A.

5. T.P. Wampler, Chemical Data Systems, Oxford, U.S.A.: An assessment of the proposed degradation mechanisms of poly(ethylene) with implications for geopolymers.
6. L.M. Stock, University of Chicago, U.S.A.: On the origins of the alkanes in coals and coal products.

Tuesday evening

Quantitation and Reproducibility in Thermal Analysis

Chairman: G. Eglinton, University of Bristol, U.K.

7. S. Larter, University of Oslo, Norway: Aspects of quantitation in slow and fast analytical and applied pyrolysis.
8. J. Sleeckx, Dow Chemical, Terneuzen, The Netherlands: Reproducibility in flash-pyrolysis.

Wednesday morning

Mass Spectrometric Detection of Bio- and Geopolymer Pyrolysis Products

Chairman: R. Helleur, Memorial University, St. John's, Canada.

9. N. Simmleit, Fresenius Inst., Wiesbaden, F.R.G.: Time-resolved Py–FI–MS of bio- and geopolymers.
10. A. Tas, TNO-CIVO, Zeist, The Netherlands: DCI–pyrolysis MS and MS/MS in polysaccharide research: specificity tuning by optimization of ionization conditions.

Wednesday evening

Comparisons of Thermal Analysis Methods

Chairman: R. Winans, Argonne Nat. Lab., Argonne, U.S.A.

11. T. Szekely, Research Laboratory for Inorganic Chemistry, Budapest, Hungary: Common theoretical fundamentals of thermal analysis and analytical pyrolysis from a physico-chemical point of view.
12. P.R. Salomon, Adv. Fuel Research, Inc., Hartford, U.S.A.: Application of TG–FTIR in analytical pyrolysis.

Thursday morning

Rock-Eval and Hydrous Pyrolysis

Chairman: K.E. Peters, Chevron Oil Field Res. Comp., La Habra, U.S.A.

13. N. Ryan Gray, Exxon Prod. Res. Comp., Houston, U.S.A.: Analytical pyrolysis in petroleum exploration: the utility of Rock Eval and pyrolysis/GC techniques for source rock characterization.
14. M.D. Lewan, Amoco Prod. Comp., Tulsa, U.S.A.: Fundamental aspects and application of hydrous pyrolysis in petroleum exploration.

Thursday evening

Characterization of Coals and Coal Processes by Pyrolysis

Chairman: F. Behar, IFP, Rueil-Malmaison, France.

15. M. Nip, Industrial Quimica del Nalon S.A., Trubia, Spain, and J.C. Crelling, South Illinois Univ., Carbondale, U.S.A.: Molecular characterization of coal macerals by pyrolysis methods: consequences for coal technology.
16. R.J. Evans, Solar Research Inst., Golden, U.S.A.: Rapid spectrometric characterization of biomass feedstocks and pyrolysis products and the prediction of their energy utilization potential.

Friday morning

Chairman: K.J. Voorhees, Colorado School of Mines, Golden, U.S.A.

Four oral presentations of selected posters.

GENERAL INFORMATION

A detailed leaflet Information for Authors is available from the publisher, Elsevier Science Publishers B.V., P.O. Box 330, 1000 AH Amsterdam, The Netherlands, upon request, and will also be printed in the last issue to appear each year. The most important items are given below.

Types of contributions. The *Journal of Analytical and Applied Pyrolysis* publishes original papers, short communications, and reviews. Reviews are written by invitation of the Editors, who welcome suggestions for subjects. Short communications are usually complete descriptions of limited investigations, and should generally not exceed four printed pages.

Submission of manuscripts. Three copies should be submitted to one of the Editors whose addresses are mentioned on p. 2 of the cover. Illustrations must also be submitted in triplicate. One set should be in a form ready for reproduction; the other two may be of lower quality. The language of the journal is English.

Manuscript preparation. The manuscript must be typewritten with double spacing on consecutively numbered pages of uniform size. The title page includes the title, name(s) of author(s), and their affiliations. The author to whom correspondence should be addressed must be indicated. Research papers and reviews begin with an abstract (50–250 words) which comprises a brief factual account of the contents of the paper.

References. References should be numbered in the order in which they are cited in the text, and listed in numerical sequence on a separate sheet at the end of the article. The numbers should appear in the text at the appropriate places in square brackets, on the line. The reference list must contain the names of all authors. Abbreviations for the titles of journals follow the system used by Chemical Abstracts.

Tables. Tables should be compiled on separate sheets. They must be numbered with Arabic numerals, and have brief descriptive headings. They should be referred to in the text.

Illustrations. All illustrations are to be numbered consecutively using Arabic numerals and should be referred to in the text. Legends must be typed together on a separate sheet. Line drawings should either be drawn in Indian ink or submitted as sharp glossy prints suitable for immediate reproduction. Any lettering must be large enough to stand photographic reduction. Half-tone illustrations should be black and white prints on glossy paper and have as much contrast as possible.

Proofs. One set of proofs will be sent to the author to be checked for printer's errors.

Reprints. Fifty reprints will be supplied free of charge. Additional reprints (minimum 100) may be ordered by the authors. The order form containing price quotations will be sent to the author together with the proof.

Advertisements. Advertisement rates are available from the Advertising Manager, Elsevier Science Publishers B.V., P.O. Box 211, 1000 AE Amsterdam, The Netherlands, tel. (20) 5803714, telex 18582 ESPA NL, telefax (20) 5803342.

© ELSEVIER SCIENCE PUBLISHERS B.V. (1989)

0165-2370/89/$03.50

All rights reserved. No part of this publication may be reproduced, stored in a retrieval system, or transmitted, in any form or by any means, electronic, mechanical, photocopying, recording, or otherwise, without the prior written permission of the publisher, Elsevier Science Publishers B.V., P.O. Box 330, 1000 AH Amsterdam, The Netherlands.

Upon acceptance of an article by the journal, the author(s) will be asked to transfer copyright of the article to the publisher. The transfer will ensure the widest possible dissemination of information.

Submission of an article for publication implies the transfer of the copyright from the author(s) to the publisher and entails the author(s) irrevocable and exclusive authorization of the publisher to collect any sums or considerations for copying or reproduction payable by third parties (as mentioned in article 17 paragraph 2 of the Dutch Copyright Act of 1912 and in the Royal Decree of June 20, 1974 (S. 351) pursuant to article 16b of the Dutch Copyright Act of 1912) and/or to act in or out of Court in connection therewith.

Special regulations for readers in the U.S.A. This journal has been registered with the Copyright Clearance Center, Inc. Consent is given for copying of articles for personal or internal use, or for the personal use of specific clients.

This consent is given on the condition that the copier pays through the Center the per-copy fee stated in the code on the first page of each article for copying beyond that permitted by Sections 107 or 108 of the U.S. Copyright Law. The appropriate fee should be forwarded with a copy of the first page of the article to the Copyright Clearance Center, Inc., 27 Congress Street, Salem, MA 01970, U.S.A. If no code appears in an article, the author has not given broad consent to copy and permission to copy must be obtained directly from the author. All articles published prior to 1980 may be copied for a per-copy fee of US $2.25, also payable through the Center. This consent does not extend to other kinds of copying, such as for general distribution, resale, advertising and promotion purposes, or for creating new collective works. Special written permission must be obtained from the publisher for such copying.

No responsibility is assumed by the Publisher for any injury and/or damage to persons or property as a matter of products liability, negligence or otherwise, or from any use or operation of any methods, products, instructions or ideas contained in the material herein.

Although all advertising material is expected to conform to ethical (medical) standard, inclusion in this publication does not constitute a guarantee or endorsement of the quality or value of such product or of the claims made of it by its manufacturer.

Printed in The Netherlands

VOL. 16, NO. 1 JOURNAL OF ANALYTICAL AND APPLIED PYROLYSIS MAY 1989

CONTENTS

(Abstracts/Contents Lists published in Analytical Abstracts, Biological Abstracts, Chemical Abstracts, Current Contents/Physical, Chemical and Earth Sciences, Mass Spectrometry Bulletin, and Science Citation Index)

Overseas travel for Americans – the image and the expense
R.P. Lattimer 1

Pyrolysis–gas chromatography/mass spectrometry and pyrolysis–gas chromatography/Fourier transform infrared/flame ionization detection studies of particle size fractions of woody peat
G.D. Calvert (Columbia, SC, U.S.A.), J.S. Esterle (Lexington, KY, U.S.A.) and J.R. Durig (Columbia, SC, U.S.A.) 5

Fluidized bed pyrolysis of digested sewage sludge
W. Kaminsky and A.B. Kummer (Hamburg, F.R.G.) 27

Thermal decomposition studies of some organophosphorus compounds
J.R. Durig, D.F. Smith and D.A. Barron (Columbia, SC, U.S.A.) 37

Simultaneous determination of natural and styrene–butadiene rubber tire tread particles in atmospheric dusts by pyrolysis–gas chromatography
Y.-K. Lee, M.G. Kim and K.-J. Whang (Seoul, Korea) 49

Mechanism and kinetics of thermolysis of ethers modelling the oxygen–methylene 'bridge' bonds in coal organic matter
V.Yu. Korobkov, E.N. Grigorieva, V.I. Bykov and I.V. Kalechitz (Moscow, U.S.S.R.) 57

Slow gas-phase oxidation of diethylacetal
J.A. García Domínguez, M.J. Molera and J.M. Santiuste (Madrid, Spain) 75

Unimolecular thermal reactions of C_5 to C_8 alkynes. Low temperature matrix IR spectroscopic and mass spectrometric studies
U. Ziegler, G. Zimmermann and B. Ondruschka (Leipzig, G.D.R.) and L.E. Gusel'nikov, V.V. Volkova and L.V. Shevelkova (Moscow, U.S.S.R.) 87

Symposium report
A.P. Snyder (Aberdeen Proving Ground, MD, U.S.A.) 99

Meeting Announcement

Gordon Research Conference on Analytical Pyrolysis 101